# ประวัติของการเปลี่ยนแปลงระดับน้ำทะเลของพื้นที่ปากน้ำชุมพร อำเภอเมือง จังหวัดชุมพร

นางสาวปาริสา นิ่มเนตร

วิทยานิพนธ์นี้เป็นส่วนหนึ่งของการศึกษาตามหลักสูตรปริญญาวิทยาศาสตรมหาบัณฑิต
สาขาวิชาธรณีวิทยา ภาควิชาธรณีวิทยา
คณะวิทยาศาสตร์ จุฬาลงกรณ์มหาวิทยาลัย
ปีการศึกษา 2555
ลิขสิทธิ์ของจุฬาลงกรณ์มหาวิทยาลัย

บทคัดย่อและแฟ้มข้อมูลฉบับเต็มของวิทยานิพนธ์ตั้งแต่ปีการศึกษา 2554 ที่ให้บริการในคลังปัญญาจุฬาฯ (CUIR)
เป็นแฟ้มข้อมูลของนิสิตเจ้าของวิทยานิพนธ์ที่ส่งผ่านทางบัณฑิตวิทยาลัย
The abstract and full text of theses from the academic year 2011 in Chulalongkorn University Intellectual Repository(CUIR)
are the thesis authors' files submitted through the Graduate School.

# HISTORY OF SEA-LEVEL CHANGE OF PAK NAM CHUMPHON AREA, AMPHOE MUANG, CHANGWAT CHUMPHON

Miss Parisa Nimnate

A Thesis Submitted in Partial Fulfillment of the Requirements

for the Degree of Master of Science Program in Geology

Department of Geology

Faculty of Science

Chulalongkorn University

Academic Year 2012

Copyright of Chulalongkorn University

| | |
|---|---|
| Thesis Title | HISTORY OF SEA-LEVEL CHANGE OF PAK NAM CHUMPHON AREA, AMPHOE MUANG, CHANGWAT CHUMPHON |
| By | Miss Parisa Nimnate |
| Field of Study | Geology |
| Thesis Advisor | Associate Professor Montri Choowong, Ph.D. |
| Thesis Co-advisor | Vichai Chutakositkanon, Ph.D. |

---

Accepted by the Faculty of Science, Chulalongkorn University in Partial Fulfillment of the Requirements for the Master's Degree

.....Dean of the Faculty of Science

(Professor Supot Hannongbua, Dr. rer. nat.)

THESIS COMMITTEE

.....Chairman

(Assistant Professor Thasinee Charoentitirat, Ph.D.)

.....Thesis Advisor

(Associate Professor Montri Choowong, Ph.D.)

.....Thesis Co-advisor

(Vichai Chutakositkanon, Ph.D.)

.....Examiner

(Santi Pailoplee, Ph.D.)

.....External Examiner

(Prinya Putthapiban, Ph.D.)

ปาริสา นิ่มเนตร: ประวัติของการเปลี่ยนแปลงระดับน้ำทะเลของพื้นที่ปากน้ำชุมพร อำเภอเมือง จังหวัดชุมพ ร. (HISTORY OF SEA-LEVEL CHANGE OF PAK NAM CHUMPHON AREA, AMPHOE MUANG, CHANGWAT CHUMPHON) อ.ที่ปรึกษาวิทยานิพนธ์หลัก: รศ.ดร.มนตรี ชูวงษ์, อ.ที่ปรึกษาวิทยานิพนธ์ร่วม: ดร.วิชัย จูฑะโกสิทธิ์กานนท์, 154 หน้า.

การศึกษาธรณีสัณฐานชายฝั่งทะเลในบริเวณปากน้ำชุมพรในวิทยานิพนธ์นี้มีวัตถุประสงค์เพื่อวิเคราะห์ประวัติของการเปลี่ยนแปลงระดับน้ำทะเล แผนที่ธรณีสัณฐานชายฝั่งได้จากการแปลความหมายจากภาพถ่ายทางอากาศเป็นหลักซึ่งสามารถจำแนกชนิดของธรณีสัณฐานชายฝั่งออกได้เป็น 7 หน่วย ได้แก่ หาดทรายเก่า ลากูนเก่า ชายหาดปัจจุบัน ที่ราบน้ำทะเลขึ้นถึงเก่า ที่สูงและภูเขาที่ราบน้ำทะเลขึ้นถึงบริเวณระหว่างระดับน้ำขึ้นสูงสุดกับน้ำลงต่ำสุดและที่ราบน้ำทะเลขึ้นถึง ในการศึกษานี้ได้นำตะกอนจากหาดทรายเก่าไปหาอายุด้วยวิธีเรืองแสงด้วยความร้อนเพื่ออธิบายการเปลี่ยนแปลงของระดับน้ำทะเลในอดีต

หาดทรายเก่าสามารถแบ่งออกเป็น 3 แนว ได้แก่ แนวหาดทรายด้านใน แนวหาดทรายกลาง และแนวหาดทรายด้านนอก ซึ่งมีทิศทางการวางตัวเกือบขนานกับแนวชายฝั่งทะเลปัจจุบัน ทิศทางกระแสน้ำชายฝั่งในอดีตสามารถคาดการณ์ได้จากทิศทางการสะสมตัวของหาดทราย แนวหาดทรายด้านในมีการสะสมตัวของตะกอนไปทางทิศเหนือส่วนแนวหาดทรายกลาง และแนวหาดทรายด้านนอกมีทิศทางการสะสมตัวไปทางใต้ ขนาดตะกอนของหาดทรายเก่าที่พบมีขนาดทรายกลางถึงทรายละเอียด ตะกอนในลากูนเก่าพบเป็นขนาดโคลนปนทรายแล ะโคลน บางตำแหน่งพบเศษชั้นส่วนของพีต หาดทรายเก่าด้านในมีองค์ประกอบเป็นเฟลด์สปาร์และเฟอร์โรแมกนีเซียนมากกว่าแนวหาดทรายกลางและแนวหาดทรายด้านนอก ความ กลมมนโดยเฉลี่ยของตะกอนแนวหาดทรายคือมีความกลมมนน้อยมีความเป็นทรงกลมสูง พบซากดึกดำบรรพ์ทางทะเลจำพวกเศษเปลือกหอยในหลุมเจาะตัวอย่างบริเวณหาดทรายเก่าซึ่งสามารถบ่งบอกสภาพแวดล้อมในอดีตได้ว่าบริเวณนี้เกิดจากการสะสมตัวบริเวณที่ราบน้ำทะเลขึ้นถึง หรือสะสมตัวในบริเวณป่าชายเลน อายุของหาดทรายเก่าที่พบในพื้นที่จากการกำหนดอายุโดยวิธีการเรืองแสงความร้อนแสดงถึงประวัติการเกิดธรณีสัณฐานชายฝั่งว่าอยู่ตั้งแต่ช่วงตอนปลายสมัยไพลสโตซีนถึงตอนต้นสมัยโฮโลซีน

| | | |
|---|---|---|
| ภาควิชา | ธรณีวิทยา | ลายมือชื่อนิสิต |
| สาขาวิชา | ธรณีวิทยา | ลายมือชื่อ อ.ที่ปรึกษาวิทยานิพนธ์หลัก |
| ปีการศึกษา | 255 5 | ลายมือชื่อ อ.ที่ปรึกษาวิทยานิพนธ์ร่วม |

# # 5372285023 : MAJOR GEOLOGY
KEYWORDS : SEA-LEVEL CHANGE / HOLOCENE / BEACH RIDGE/ GEOMORPHOLOGY

PARISA NIMNATE: HISTORY OF SEA-LEVEL CHANGE OF PAK NAM CHUMPHON AREA, AMPHOE MUANG, CHANGWAT CHUMPHON. ADVISOR: ASSOC. PROF. MONTRI CHOOWONG, Ph.D., CO-ADVISOR: VICHAI CHUTAKOSITKANON, Ph.D., 154 pp.

The study of coastal geomorphology at Pak Nam Chumphon area in this research is aimed to explain the historical of sea-level change in relation to coastal landform evolution. The coastal geomorphological map was constructed based on the aerial-photo interpretation. As a result, coastal landforms can be classified into 7 units as old sandy beach, old lagoon, young sandy beach, old tidal flat, upland and mountain, intertidal flat and tidal flat. The formation of beach ridges units presented in the area together with their thermoluminescence datings can be used in the construction of historical of sea-level change.

The beach ridges can be divided into 3 parts as inner beach ridges, middle beach ridges and outer beach ridges. Beach ridges orientate nearly parallel to the shoreline but they reflect the difference in paleo-longshore current direction. Longshore current direction during the formation of inner ridge series was likely to northward direction ,but middle and outer ridges formed was likely in southward direction. Grain sizes from all beach ridge are fine to medium sand in general, whereas in swale (old lagoon), grain size is often characterized as sandy mud with peat fragments in some localities. Beach ridges show similarity in composition of quartz except the inner ridge its minor composition includes feldspar and ferromagnesian in greater number than those found in the middle and outer ridges. All of beach ridge sediments show high sphericity. Marine fossils indicate former tidal deposit, intertidal or mangrove environments. Based on TL dating of beach ridge sand, the three beach ridges in the study area are of the late Pleistocene to early Holocene.

Department : Geology Student's Signature .....

Field of Study : Geology Advisor's Signature .....

Academic Year : 2012 Co-advisor's Signature .....

# ACKNOWLEDGEMENTS

Great acknowledgement goes to Associate Professor Dr. Montri Choowong, my thesis Advisor and Dr. Vichai Chutakositkanon, co-advisor, Department of Geology, Faculty of Science, Chulalongkorn University for their valuable supervision, encouragement and inspiration on scientific thinking. Thanks also go to Assistant Professor Dr. Thasinee Charoentitirat, Chairman of thesis committee for suggestion. Dr. Santi Pailoplee is thanked for his valuable advises, helpful and comment both technically and nontechnically of thermoluminescnece dating. Grateful acknowledge to Dr. Prinya Putthapiban, external examiner for wonderful guidance throughout thesis examination.

The author would like to extend the acknowledgement to Dr. Krit Won-in and Master's degree students of the Department of Earth Science, Kasetsart University, Miss Teeraporn Chuenpee, Miss Rapeeporn Sakulnee, Miss Yuratikarn Jantaravikorn and Miss Raweewan Suwanpimon for their advice on laboratory experiments on TL dating and experiences on theories and technical knowledge. Special recognition and thanks for friendship to Master's degree students of the Department of Geology, Chulalongkorn University Mr. Thanakrit Thongkhao, Mr. Pawee Klongvessa, Mr. Chaiwit Petchsongkram bachelor's degree students of the Department of Geoscience, Mahidol University, Mr. Watthanachai Nimnate and Mr. Prinya Nimnate (My brothers) for field assistance. Special thanks go to Mr. Sumet Phantuwongraj, Mrs. Jiraprapa Niumparn, Miss Rukchanok Srabua and Mr.Kaitkajorn Nuchprasert for the suggestion on sediment laboratory and Mr. Peerasit Surakiatchai for the help and advice in classification of shell. Also, the author wishes to acknowledge to Office of Atomic Energy for Peace (OAEP), Thailand for measurement radioactive elements and the section of artificial irradiation.

It is not easy to mention all persons who have contributed to my research study. I, personally, have already expressed my gratitude to everyone that has direct and indirect assistance with this research. Finally, I have to thanks my parents for their moral support and encouragement and Mr. Sasinon Subsangthip who invariably help me directly and indirectly.

# CONTENTS


Page

ABSTRACT IN THAI ..... iv

ABSTRACT IN ENGLISH ..... v

ACKNOWLEDGEMENTS ..... vi

CONTENTS ..... vii

LIST OF TABLES ..... ix

LIST OF FIGURES ..... x

LIST OF PLATES ..... xviii

CHAPTER I INTRODUCTION .....

1.1 Background .....

1.2 Objective ..... 2

1.3 Scope and Output ..... 2

1.4 The Study Area ..... 3

1.5 Literature Reviews ..... 6

CHAPTER II METHODOLOGY ..... 11

2.1 Data Collection in Office Work Study ..... 11

2.2 Fieldwork ..... 13

2.3 Laboratory Work ..... 16

2.4 Data analysis, Interpretation and Conclusion ..... 45

CHAPTER III RESULTS OF THE STUDY ..... 46

3.1 Geomorphological description ..... 46

3.2 Sedimentological description ..... 50

3.3 Physical properties of sediments ..... 58

3.4 Age determination by thermoluminescence dating. ..... 74

3.5 Fossil evidence ..... 76

CHAPTER IV DISCUSSIONS ..... 90

4.1 Boundary of paleo-shoreline from aerial photograph interpretation ..... 90

4.2 Sedimentological characteristics from each of beach ridge plain ..... 91

4.3 Fossil evidence ..... 93

4.4 Age determination ..... 94

4.5 Paleo-sea level changes ..... 94

4.6 Model of coastal geomorphological evolution ..... 101

CHAPTER V CONCLUSION ..... 105

REFERENCES ..... 108

APPENDICES ..... 118

BIOGRAPHY ..... 154

# LIST OF TABLES

Page

Table 3.1 Result of grain size analysis of former sand sediment in Inner Ridge Series……. 60

Table 3.2 Result of grain size analysis of former sand sediment in Middle Ridge Serie……. 61

Table 3.3 Result of grain size analysis of former sand sediment in Outer Ridge Serie……. 63

Table 3.4 Result of grain size analysis of recent beach sand sediment……... 64

Table 3.5 Summary of sieve parameter in the study area as inner ridge, middle ridge, outer ridge and recent beach**…**……. 64

Table 3.6 Composition of sediment from inner, middle and outer beach ridge series…… 72

Table 3.7 Result of thermoluminescense dating of inner beachridges…… 74

Table 3.8 Result of thermoluminescense dating of middle beachridges……. 74

Table 3.9 Result of thermoluminescense dating of outter beachridges……... 75

Table 3.10 Result of thermoluminescense dating of recent beachridges……... 75

# LIST OF FIGURES

Page


| | | |
|---|---|---|
| Figure 1.1 | Topographic map showing the study area……... | 5 |
| Figure 1.2 | Geologic map of Changwat Chumphon……... | 6 |
| Figure 2.1 | Diagram showing the methodology of this research……... | 11 |
| Figure 2.2 | Mozaic of aerial photographs with approximately 1:50,000 scale covering the study area…… | 13 |
| Figure 2.3 | Field measurement for sampling sediments. (top left) hand auger ; Edelman auger and sand bucket (sampling sand) , (top right) gouge auger (sampling mud). (bottom left) description of samples and (bottom right) samples were kept from each 20 centimeter depth in zip-lock plastic bag. | 15 |
| Figure 2.4 | Photos showing how to collect sample for Optically Stimulated Luminescence dating. Sample is prevented from sunlight for paleo-dose and annual dose in zip-lock plastic bag…….. | 16 |
| Figure 2.5 | Photographs showing the preparation of sample before dry in the oven…. | 19 |
| Figure 2.6 | Photographs show drying sample in oven at temperature $80^{o}$ C about 5-6 hours for release water in samples…….. | 19 |

Page


| | | |
|---|---|---|
| Figure 2.7 | A) Grinding sediment make individual grain.<br>B) Mix sediment and then split the sample 2 times (4 piles).<br>C) Prepare sieve meshes at equivalent sieve mesh no.5, 10, 18, 35, 60, 120 and 230 (A.S.T.M) or in ϕ (phi) scale at -2.00, -1.00, 0.00, 1.00, 2.00, 3.00, and 4.00 respectively.<br>D) Pouring sediment in each sieve mesh weight samples in each beaker and note in weight table……..... | 20 |
| Figure 2.8 | Photographs show sieve mesh and sieve shaker and weight measurement used in this study…….. | 20 |
| Figure 2.9 | Record weight retained of sample from sieve analysis. ……. | 22 |
| Figure 2.10 | Calculating moment measures in 1phi interval midpoint…… | 22 |
| Figure 2.11 | Chart for comparison of Mean, Standard deviation, Skewness and Kurtosis in moment method……. | 23 |
| Figure 2.12 | Photograph showing standard binocular microscope for estimating sphericity and roundness…….. | 24 |
| Figure 2.13 | Comparison chart for estimating percentage composition…..……... | 25 |
| Figure 2.14 | Comparison chart for estimating roundness of sediment…… | 25 |

Page

Figure 2.15 Hypothetical thermoluminescence level versus time. An event permitting the sediment to be exposed to sunlight reduces the captured electron causes thermoluminescence signal to a residual level (Io)……. 27

Figure 2.16 Schematic charts of regeneration technique for measurement of the TL intensity; N is natural sample, Io is residual intensity from sample, H is 320$^{o}$C heated sample and samples is known dosage that irradiated sample……..……... 29

Figure 2.17 Simplified flow chart illustrating laboratory analysis use in this research study. The pink blog is the annual dose procedure and the yellow blog is the equivalent dose procedure……. 30

Figure 2.18. Water content sample preparation……... 31

Figure 2.19 Annual dose sample preparation……. 32

Figure 2.20 Gamma ray spectrometer at Akita University, Japan. This equipment is used for measure uranium, thorium and potassium contents……... 34

Figure 2.21 Thermoluminescence Detector for measure electrons from traps, as a result of laboratory heating, produces a luminescent signal that is proportional to the absorbed dose (Equivalent dose) of radiation energy... 35

Figure 2.22 Bring sample in to Aluminium froid and baked it at 320 °C around 5 hours for reset electron to zero…… 37

Page

Figure 2.23 Sample for Equivalent dose can separate in to 4 part; bleaching , irradiation at 50Gy, 200Gy 400Gy and 800Gy by Gammacell ,Plateau test and natural (prevented from light)…… 37

Figure 2.24 Sample for irradiation by Gammacell (Source $^{60}Co$) at 50Gy, 200Gy 400Gy and 800Gy at Office of Atoms for Peace. After that baked it at 120 °C (1 day) for reduce noise…….. 38

Figure 2.25 Thermoluminescence Detector (TLD) at Earth Science Department, Faculty of Science, Kasetsart University cooperated with Akita University, Japan; that is used for TL glow curve measurement…… 38

Figure 2.26 Glow curve of sample no. T1-PN8, old beach sand in middle ridge. The graph shows a graph relationship between TL intensity versus temperature. The graph measured from thermoluminescence detector (TLD) at Earth Science Department, Kasetsart University……. 39

Figure 2.27 Plateau test of sample no T1-PN8, old beach sand in middle ridge. showing a relationship between natural/artificial ratios from glow-curves versus temperature ($^{o}C$)…… 40

Figure 2.28 Growth curve of old beach sand sample no. T1-PN8 from middle ridge, using regeneration technique. The curve showing relationship between TL ratio (artificial glow curves/ natural glow curve) versus temperature ($^{o}C$). N is natural signal, $I_0$ is bleached sample and H (+50Gy, +200Gy, +400GY, +800Gy) is heated sample at 320 $^{o}C$ for 5 hours and irradiated sample by Gammacell…….. 41

Page


| | | |
|---|---|---|
| Figure 2.29 | Drawing of parts of Gastropod…….…….. | 42 |
| Figure 2.30 | Drawing of parts of Bivalve…… | 43 |
| Figure 2.31 | Positions of the shell fossil found in the study area (6 locations: T1-PN12, T2-PN10, T2-PN11, T3-PN1, T3-PN2 and T3-PN5)……. | 44 |
| Figure 3.1 | Coastal geomorphological map of Pak Nam Chumphon, Amphoe Muang, Changwat Chumphon. Dots in red and blue color showing locations of coring…….. | 46 |
| Figure 3.2 | Locations of old sandy beach (beach ridge) and old lagoon (disturbed swale) in inner ridge series described in geomorphological map and the photograph showing the present conditions of both landforms in thefield…….…… | 51 |
| Figure 3.3 | The lithological log of inner most old beach sand at station T1-PN1…… | 52 |
| Figure 3.4 | Young sandy beach at Ban Kho Son where it is gentle slope to seaward .. | 53 |
| Figure 3.5 | The lithological log of young sandy beach at station T1-PN13……. | 54 |
| Figure 3.6 | Location where the old tidal flat locates in the geomorphological map. The present condition of old tidal flat and general composition of tidal flat containing mainly of gray-dark gray mud with both complete shell and fragments…….…… | 55 |

Page


| | | |
|---|---|---|
| Figure 3.7 | The lithological log of old tidal flat at station T1-PN11…… | 56 |
| Figure 3.8 | Location of old lagoon in coastal geomorphological map that commonly locate between old sandy beaches. Present condition of the old lagoon area in the field……...……. | 57 |
| Figure 3.9 | The lithological log of old lagoon at station T1-PN2.……. | 58 |
| Figure 3.10 | Scatter plot of mean size versus standard deviation (sorting). It is narrow range of grain size (very fine to coarse sand)……. | 67 |
| Figure 3.11 | Scatter plot of mean size versus skewness. Almost samples are classified as coarse to fine skewed……... | 67 |
| Figure 3.12 | Scatter plot of mean size versus kurtosis. Almost sediment samples are classified as leptokurtic…… | 68 |
| Figure 3.13 | Scatter plot of standard deviation (sorting) versus skewness. Almost sediment samples are classified as coarse to fine skewed and moderately to moderately well sorted……. | 68 |
| Figure 3.14 | Scatter plot of standard deviation (sorting) versus kurtosis. Almost sediment samples are classified as leptokurtic to mesokurtic. Some of sand sediments in outer ridge and inner ridge (red oval dash line) showed extreme kurtosis value and good sorting. That indicated in neritic sediments, extreme kurtosis values are common because the sand mode achieves good sorting in the high energy environment of the beach…….. | 69 |

Page

Figure 3.15 Scatter plot of skewness versus kurtosis. Almost sediment samples are classified as fine to coarse skewed and mesokurtic to leptokurtic kurtosis. Half of all sediment samples are characteristically leptokurtic and positive skewed sediments. They indicated that sediments are transported near the sort of the sand in red oval dash line. Beach sands are normal or negative skewness and leptokurtic, dune sand have positive skewness and mesokurtic, Aeolian flat sand have positive skewed and leptokurtic. The beach sand is more poorly sorted than to other types. Beach sands generally have negative skewness ……. 70

Figure 3.16 Graph of sediment composition in inner, middle and outer beach ridge series. Major composition is quartz. In inner ridge, minor compositions are feldspar and ferromagnesian more than those recognized in the middle and outer ridges…… 73

Figure 3.17 Show borehole location of TL dating and age in study area…….. 75

Figure 4.1 Coastal geomorphological map interpreted from aerial photographs. The westernmost boundary of paleo shoreline recognized from aerial photograph……..…. 91

Figure 4.2 The estimated eustatic sea-level change from the Last Glacial Maximum to the present day……. 96

Figure 4.3 Land surface of the southern Arabian (Persian) Gulf elevation, for the last 53 ka, superimposed on sea level…….. 96

Figure 4.4 Sea-level curve for the Sunda Shelf derived from shoreline facies…… 97

Page

Figure 4.5 Sea-level changes for last 150 ka derived from isotope record using temperature and sea-level isotope from Huon Peninsula sea-level data….. 97

Figure 4.6 Sea-level curves from Thailand and neighbouring countries. They show rapid transgression from the early Pleistocene to the mid-Holocene highstand, at about 3-4 m above present MSL. Fluctuations were reported locally from Thailand and Penninsular Malaysia during sea-level regression after the mid-Holocene highstand……..…….. 99

Figure 4.7 Holocene sea-level envelope for Thailand……..…… 100

Figure 4.8 Model of coastal geomorphological evolution in Pak Nam Chumphon…….. 103

Figure 4.9 Tentative paleo-longshore of beachridges in Pak Nam Chumphon…… 104

# LIST OF PLATES

Page


Plate 1 Figs.1 (a,b) *Celypeomorus coralia* Figs. 2 (a,b) *.Polinices(Polinices) mammilla* Figs. 3 (a,b) *Natica trigina* Figs. 4 (a,b) *Nassarius pullus* Figs. 5 (a,b) *Nassarius siquijorensis* Figs. 6 (a,b) *Peristernia incarnate*, all scale bar are 1 cm.……..... 86

Plate 2 Figs. 1 (a,b,c,d), scale bar 5 cm. Figs. 2 (a,b), scale bar 1 cm. Figs. 3 (a,b) , scale bar 1 cm Figs. 4 (a,b) ), scale bar 1 cm Ostreidae…….…….……... 87

Plate 3 Figs. 1 (a,b) *Anadara oblonga* Figs. 2 (a,b) *Tegillarca granosa* Figs. 3 (a,b) *Scapbarca* sp. Figs. 4 (a,b) *Mytilus* sp. Figs. 5 (a,b) *Didimacar tenebrica* Figs. 6 (a,b) *Striarca lacteal* Figs. 7 (a,b) *Carditella (Carditellona)* pulebella Figs. 8 (a,b,c,d) *Batbytormus radiates* Figs. 9 (a,b) *Mactra* sp. Figs. 10 (a,b) *Solen* sp. Figs. 11 (a,b) *Psammotreta (Tellinimactra) edentula* Figs. 12 (a,b) *Semele carnicolor* Figs. 13 (a,b) *Anomalocardia (Anomalodiscus) squamosa* Figs. 14 (a,b) *Placamen cholorotica***,** all scale bar are 1 cm.……. 88

Plate 4 Figs. 1 (a,b) *Paphia (Papbia) undulate* Figs. 2 (a,b) Figs. 3 (a,b) *Dosinia sp.* Figs. 4 (a,b) *Dosinia Scopoli* Figs. 5 (a,b) *Donax sp.* Figs. 6 (a,b) *Capsella sp* Figs. 7 *Tellina timorensis* Figs. 8 (a,b) *Leptomya* sp. Figs. 9 *Antalis sp.* Figs. 10 Echinoidea, all scale bar are 1 cm.…… 89

# CHAPTER I

# INTRODUCTION

## 1.1 Background

Changwat Chumphon, one of the southern provinces of Thailand, is geographically, composed of the highland in the west and the coastline in the east. Chumphon itself is bounded in the north by Prachuap Khiri Khan, in the south by Surat Thani and the west by Ranong. To the northwest it also borders the Burmese province of Tanintharyi. Changwat Chumphon is far approximately 460 km from Bangkok and is narrow and long in N-S trend along with Ta Nao Sri mountain range and owns about 200 km long of the coastal zone in the Gulf of Thailand. Forty percent of Chumphon area is covered by forest, alluvial plain that appropriate for plant growth. Fluvial system consists of Tha Ta Pao River in Amphoe Muang, Sawi River in Amphoe Sawi and Langsuan River. All of them flow almost eastward into the Gulf of Thailand and supply terrestrial sediments to the Chumphon coastal zone. Coastal area of Chumphon preserves the spectacular geomorphological landform as beach ridges because of the rising and falling of sea-level in the past (Middle Holocene). Also the study in evolution of coastal geomorphology and its related to sea-level change is possible.

Several researchers explained the history of mid-Holocene sea-level changes in the Gulf of Thailand. A sea-level curve in the Gulf was firstly established by Sinsakul et al. (1985). Later on, new data of radiocarbon dating suggest that sea level rose rapidly from -12.75 m below MSL until reach maximum highstand at about +3.5 m above present MSL at around 6,500 to 4,000 years ago studied by Choowong et al. (2004). However, no data of sea-level history have been reported from this research area.

## 1.2 Objective

This research will mainly be concerned with the study of sea level change history that was evidenced by sedimentological clues. The evolution of coastal landform will be explained from the progradation of beach ridge plains possibly deposited at the same time during the mid to late Holocene marine regression (Choowong et al., 2004) As a result, the better understanding in the history of sea-level change and the episodic evolution of the coastal landforms in the study area will be explained. Additionally, the western coastal area of the Gulf of Thailand, particularly at Chumphon exhibits various geomorphological differences which these geomorphological features may own its individual depositional style that may be reflected by the difference in directions of longshore current. Therefore, the prime objectives of this research are as follows:

1. To examine the coastal evolution of Pak Nam Chumphon area, Amphoe Muang, Changwat Chumphon, especially from the sedimentological evidences, geomorphology and age determination.
2. To discuss the history of sea-level change and the evolution of coastal morphology.

## 1.3 Scope and Output

The scope of the research is limited with the analysis in the coastal geomorphology and coastal stratigraphy only where they can be inferred as evidences of the Holocene shoreline. All data contributes to the linkage of coastal geomorphology and its change during the maximum transgression until the regression to the present mean sea level. The total study area covers around 90 $km^2$.

The output of this research is expected to comprehend of sea level change that contributes to illustrate coastal geomorphological evolution in Pak Nam Chumphon area, Amphoe Muang, Changwat Chumphon.

## 1.4 The Study Area

This section describes the environmental setting of Pak Nam Chumphon, Amphoe Muang, Changwat Chumphon. The description will start with general topography, geology and finally climate conditions.

### 1.4.1 General topography

Pak Nam Chumphon, Amphoe Muang, Changwat Chumphon is the coastal area in Chumphon province which is located in the southern part of Thailand along the Gulf of Thailand. The area is located at $10^{o}20'$ N and $99^{o}08'$ E to $10^{o}30'$ N and $99^{o}19'$ E. It appears in the reference topographic map at a scale of 1:50,000 series L7018 WGS 84 number 4829IV (Changwat Chumphon) (Figure 1.1).

### 1.4.2 Geology

Geology of Changwat Chumphon consists of sedimentary, metamorphic and igneous rocks which can be described as follows (Figure 1.2):

Sedimentary and metamorphic rocks

1.4.2.1. Permo-carboniferous Rocks

The Permo-carboniferous rocks in Changwat Chumphon are composed of pebbly mudstones, shales siltstones, cherts, greywackes, gray, greenish gray, brown orthoquartzites found fossil as brachiopods, bryozoas, coral and crinoids. In the western and northern area, these rocks are exposed at Lamae, Lang Suan, Thung Tako, Sawi, Phato, Tha sae, Pathio and Muang Chumphon District.

1.4.2.2. Permian Rocks

The Permian rocks in Ratchaburi group consist of limestones, dolomitic limestones intercalated with chert nodules and chert layers. Fossils found in this rock are fusulinids, brachiopods, corals and bryozoas in Sawi and Pathio District.

1.4.2.3. Jurassic Rocks

Arkosic sandstones, mudstones and siltstones are characterized by red-brown color show cross bedding in upper part of stratigraphy and fresh and brackish bivalvia were found in lower part. In coastal area and islands, these rocks are exposed at La Mea, Lang Suan and Muang Chumphon District as Ma Prao island, Samed island, Leam Ko Kwang, Leam Thung Sai , Leam Tan, Kai island. 1.4.2.4. Quaternary Sediments

Quaternary colluvial deposit consists of colluvium and in situ sediments such as gravels, sands, silts, laterites and rock fragments. Quaternary marine sediment is composed of sands, sands and gravels in barrier beaches, sand bars and sand dune, and its orientation is controlled by the present and paleo longshore current. Sediments are controlled by tidal as clays, silts and fine sands in tidal flats, salt marshes, swamps mangrove forests and estuary. There are found in coastal area from north to south of Changwat Chumphon. Fluvial sediments are composted of gravels, sands, silts and clays that deposit in channels, levees and floodplains.

Igneous rock

1.4.2.5 Cretaceous granite is composed of biotite-hornblende granite and muscovite granite. It usually has a fined- to medium-grained and show equigranular texture. Granodiorite shows porphyritic texture. There form mountain range in north-south trend in Sawi, Phathio, Tha sae District.

**1.4.3 Climate**

Climate of Chumphon is mainly rainy from June to January. Summer starts on February until May with monsoon. In November 1989, the typhoon Gay hit the province and 529 people were killed, 160,000 became homeless and 7,130 $km^2$ (2,753 sq. mi) of farm land was destroyed. Gay was one of tropical storms on historical record which reached Thailand with typhoon wind strength.

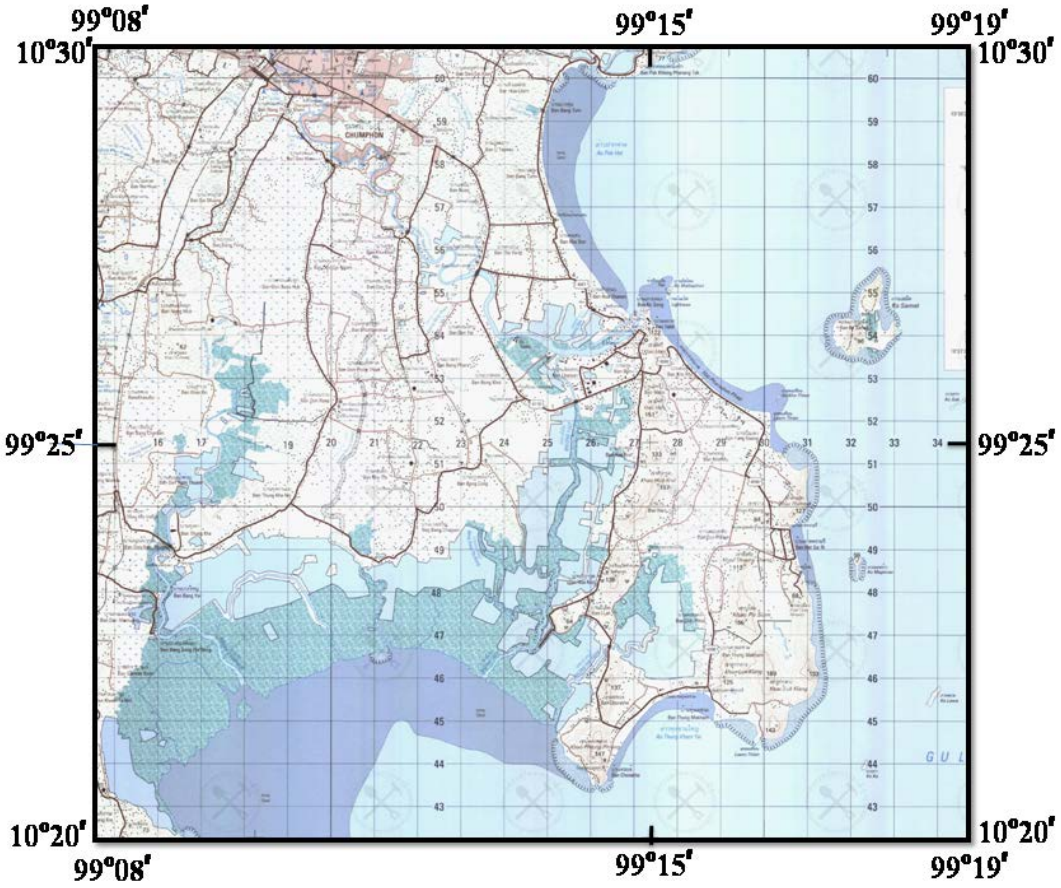


**Figure 1.1** Topographic map showing the study area map sheet 4829 IV (Royal Thai Survey Department, 2000).

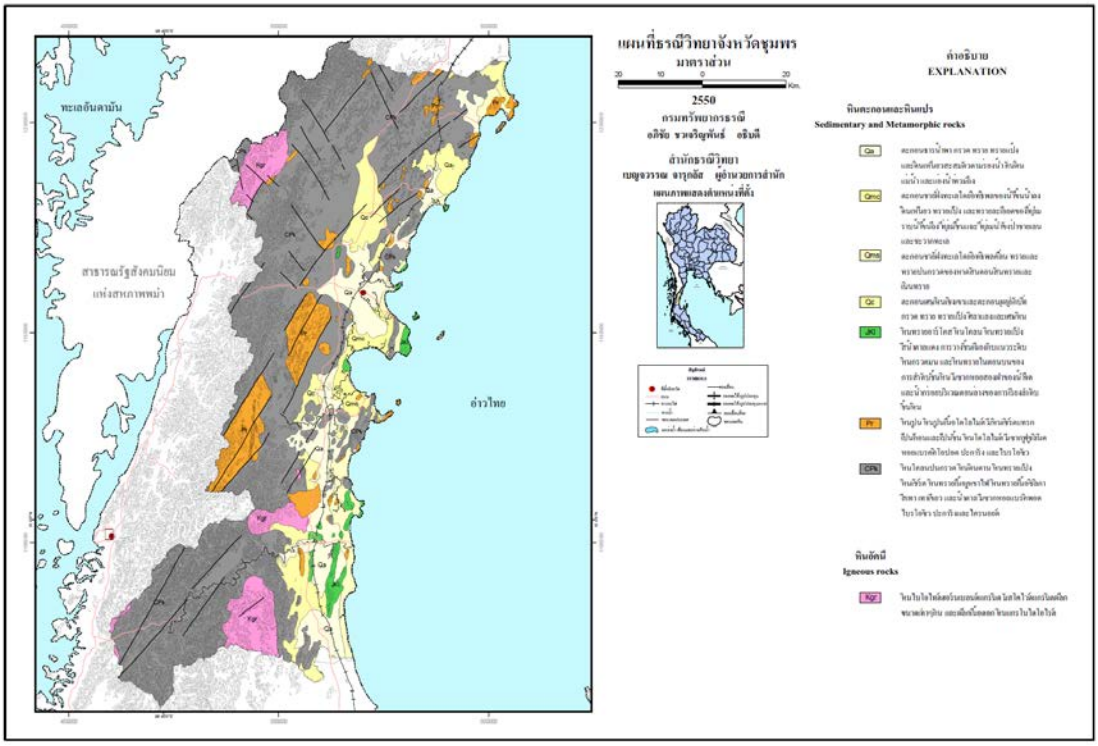


**Figure 1.2** Geologic map of Changwat Chumphon (Thongpinyochai, 1996).

### 1.5 Literature Reviews

In literature review section, the previous studies relating to this research will be described, for example, the works on sea level change in Thailand and vicinity, the dating methodology for determining age of beach deposits and so on.

Aitken (1985) studied TL dating in both theoretical and practical terms, particularly with a strong background in physics. He proposed application of TL dating for archaeological objects including Quaternary sediments and introduced some phenomena about residual signal of sediments after 6-10 hours bleaching by natural light.

Sinsakul et al. (1985) concluded the fluctuations of the sea level occurred twice, producing the two levels of highstand. The first level was at +5.0 m that formed about 6,000 years BP and the second was +3 m about 4,000 years BP. The rebound phase of marine transgression was around 4,700 years BP before stable at the present MSL. In Southeast Asian countries, the

sea rose up to nearly 5.0 m above the present MSL for the Peninsular Malaysia and 3.0 m for Singapore and the sea began to fall to the present MSL.

Dheeradilok (1995) studies Quaternary stratigraphic sequence, depositional process and coastal morphology of the Thailand coast response to climate and eustatic sea level change. The landscape of the coastal Lower Central Plain of Thailand, developed during the Holocene marine transgression and regression and subsequence coastal progradation at about 11,000 to 3,000 BP, as fluvial and coastal process adjusted to the rising and subsequent relatively stable sea level. The Holocene marine Bangkok Clay Formation which covers most of the Lower Central Plain accumulated at this time.

Hesp et al. (1998) presented the Holocene sea level curve for Singapore. Radiocarbon dating of a variety of shell, wood, and coral material is utilized to derive a curve. Most of the dated material comes from estuarine environment. The tentative result indicate that the Holocene Post-Glacial Marine Transgression (PGMT) reached the present mean sea level around 6,500 to 7,000 years BP, rose to nearly 3 m above the present, and began to fall to the present MSL around 3,000 or less years ago.

Chaimanee (2001) studied coastal evolution of the Greater Surat Thani city area. Paleo-geography and facies relationship of Quaternary sediments in the Surat Thani basin was proposed basing on $C_{14}$ dating. The depositional environment during the Quaternary is mainly non-marine or fluvial environment with some marine incursion. During the Late Pleistocene glaciations, this was believed to cause a sea level drop all over the world. In Southeast Asia, especially in the Gulf of Thailand, the sea level dropped more than 50 meter leading to the Sunda shelf emerged as a continent. At the end of the Late Pleistocene, the climate became wet and warm. The melting of ice mass resulted in a sea level rise all over the world. The rise of sea level had an impact of sea water inundating throughout the coastal plain of Thailand.

Robba et al. (2002) studied bivalves recovered from the Holocene Bangkok clay in the lower Central Plain of Bangkok along with those obtained from modern shallow bottom in Phetchaburi coastal area. The bivalve assemblage of the Holocene Bangkok Clay appear to parallel the recent ones recovered at the sea, from intertidal and shallow infralittoral, predominantly muddy substrates. Arcoidae, Galcommatoidae, Tellinoidea and Veneroidea are most diverse group.

Choowong (2002a) studied sea-level changes occur on all space and timescales, from local to global scales. The argument regarding sea-level changes in the Gulf of Thailand (GOT) have arisen from this work and literatures. Some literatures concluded that sea-level changes in the GOT were only a result of global changing in ocean volume caused by glacial melting during the last Post-Glacial period, but some argued that isostasy has played an additional role in creating different history of sea-level changes in the Gulf. Subsidence of the land may be one additional cause that results in recent groundwater extraction. This recent human activity depletes the aquifer underneath urban and industrial areas because of the rapid withdrawal of underground water. Due to the resulting of subsidence, the sea has transgressed on to the coastal plains and the Lower Central Plain. It is reasonable to assume that the GOT should not only be attributed to eustatic changes but also to isostatic adjustment.

Choowong (2002b) studied an assessment of evidence of sea-level changes in explaining the evolution of the coastal plain from the Gulf of Thailand. The evolution of coastal plain responded to a relative change in sea level in particular during a rapid rising of the sea in the early Holocene. Evidence of sea-level change includes geological and biological features. Geological indicators are sea notches, sea caves and arches, platforms and benches with weathered feature such as honeycomb structure, former tidal flats and salt marshes, and relict barrier. Biological indicators include palynology, fossil crabs, shell fragment and peat.

Choowong et al. (2004) studied the detailed coastal evolution in particular the investigation of biological clues in Holocene coastal deposits from Sam Roi Yod National Park.

Biological evidences such as fossil shells and pollen have been used as evidence of palaeo-environmental changes and the palaeo-shoreline, in particular, the Lower Central Plain and the western coast of the GOT. Most researchers concluded from pollen evidence that, on the lower Central Plain, the palaeo-shoreline at the highstand level extends as far as 70 km inland from the present coastline at an elevation of 5 meter above the present mean sea level, whereas, in the western and eastern coasts of the GOT, the other evidence of highstand palaeo-shoreline, such as marine notches has been located as far as 10 km. Marine crabs were preserved within tidal and estuarine deposit. Marine crabs deposited in former tidal flat at about 6,000 years ago, found at 13 m beneath the present surface.

Pailoplee (2004) studied Thermoluminescence (TL) dating of sediments in conjunction with accelerator-mass-spectrometry (AMS) radiocarbon dating of organic materials from Quaternary samples from Ban Bom Luang trench, northern Thailand and Thung Tuk archaeological site, southern Thailand. These two sites permit detailed comparisons of thermoluminescence and radiocarbon chronologies. Both techniques produce self-consistent chronologies for the colluvial deposits (Ban Bom Luang trench) and beach sand deposits with the ancient remain (Thung Tuk archaeological site). In case of TL dating, the focuses are placed on problems connected with equivalent dose (ED) estimation. The dated results obtained by using two techniques: regeneration and total bleach techniques were compared with AMS radiocarbon dating. The obtained results show that the ED values are strongly dependent on the applied technique. Most of TL ages obtained by the regeneration technique were confirmed by AMS radiocarbon ages while total bleach technique seems to be discrepancy.

Silapanth (2005) studied the relationships among geomorphology, sedimentology and archeology evidences from Cha-am coastline. A result reveals that the change of landscape here has been occurring since the middle Holocene. The propragation of the land in eastward direction can be referred relatively to the mid Holocene marine regression. Base on the archeological sites and remains, the Dharavati habitation site at Thungsetthi had been located on a beach ridge and

barriers close to Permain limestone hill and surrounded by palaeo-channels connecting to palaeo-shoreline. The morphological changes of the coastal area have been occurring until the present time. The investigation on coastal stratigraphy supports evidence about boundary of palaeo-shoreline. Furthermore, these palaeo-landforms especially beach ridges and sand barriers also present that the people at Thungsetthi and other Dharavati sites in adjacent area selected the innermost sand barrier for their settlement and communication route since this sand barrier was stable and higher than where were close to the shoreline at that time.

Surakiatchai (2005) studied gastropod and bivalve fossils from the Khao Sam Roi Yod National Park, Prachuap Khiri Khan Province, Thailand and correlated paleoenvironment by molluscan fossils. The analysis and correlation between the dominant molluscan fossil (Cerithidea cigulata, Natica trigina, Nassarius pullus, Placamen choloticum and Marcia hiantina) and recent mollusca show the similarity in their shapes and size. It can be assumed the environment in the past that was intertidal or mangrove, except Wat Ban Khao Daeng area which is recent coastline.

Vongvisessomjai (2010) studied the effect of global warming in Thailand. The analysis of the meteorological data of the Thai Meteorological Department in six decades showed that rainfall data in all part over Thailand showed decreasing trends. It can be concluded that rainfall in Thailand showed little change. The analysis of sea level data of the Hydrographic Department in six decades showed no increasing trend. The sea levels at Samut Prakan and Samut Sakorn showed some rising trends due to land subsidence from pumping of groundwater. Coastal erosion in Thailand is mainly attributed to a decrease in the sediment supplied from rivers to the sea. The land subsidence due to pumping of groundwater in Samut Prakan and Samut Sakhon, however not global warming, was the cause in the rise of the sea level.

# CHAPTER II

# METHODOLOGY

The thesis approach is divided into three steps, including 1) data collection in office work: study for literature review, aerial photo interpretation and GIS analysis, 2) fieldwork: identification of coastal geomorphology, description of sedimentary profile, sediment sampling and beach profile measurement, 3) laboratory work: laboratory analysis for sediment samples, fossil identification and age determination.

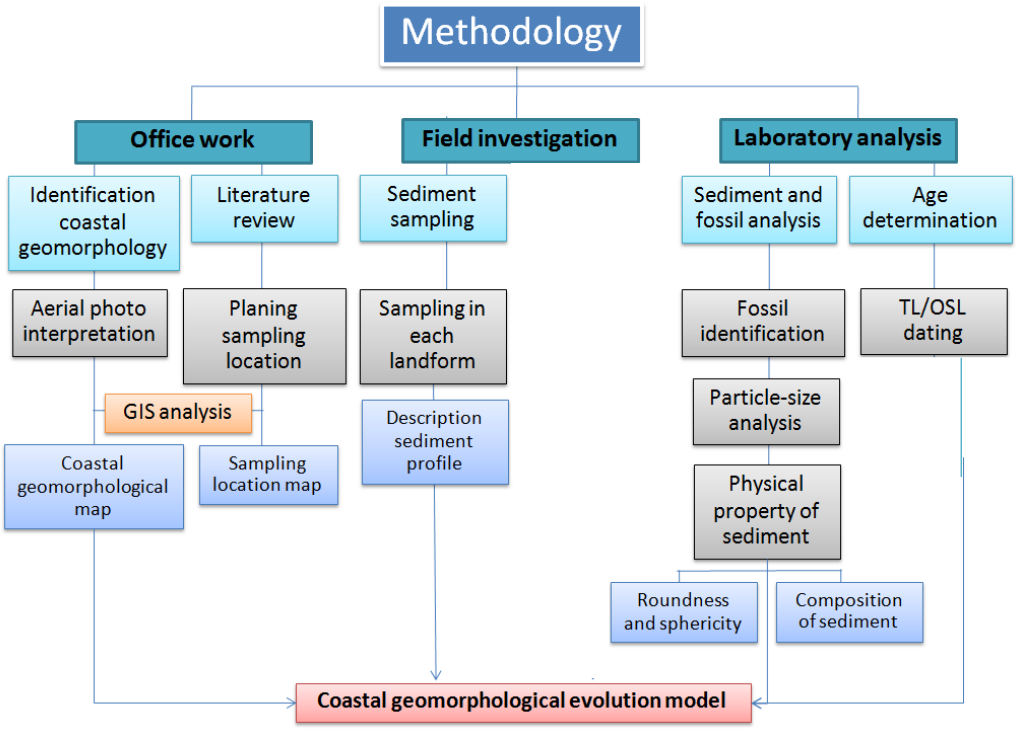


**Figure 2.1** Diagram showing the methodology of this research.

## 2.1 Data collection in office work study

Literature reviews on previous geological and oceanographical reports both in the study area and adjacent were carried out. Most of literatures have been done regarding the

reconstruction of paleo-shoreline in the Central Plain of Thailand since 1980s (Dheeradilok, 1995; Sinsakul et al., 2002; Choowong, 2002a; Choowong, 2002b; Choowong et al., 2004; Choowong, 2010 and 2011). A few researches have mentioned the relationship of the climate change during the Quaternary age in Thailand (Choowong, 2002a, b). At Pak Nam, Changwat Chumphon there has been mentioned that the Holocene sea level transgression has reached about 10 kilometers inland (Choowong, 2002b).

The interpretation of aerial photograph is one practical way to recognize the orientation of beach ridge plain at Pak Nam Chumphon. Not only the recent geomorphology, the aerial photograph interpretation can be applied, but also the relict landforms far away inland that can be recognized clearly from the 1998 air-photos can be taken. The aerial photographs interpretation provides the detailed data of coastal geomorphology of the study area, including three different beach ridge plains. The aerial photographs applied to this study are approximately 1:50,000 scales officially produced by the Royal Thai Survey Department in 1998 covering Amphoe Muang, Changwat Chumphon. The aerial photographs include the area number 0066, 0067 ,0068 ,0069, 0070, 0118, 0119, 0120, 0121 and 0122 (Figure 2.2). After aerial photograph interpretation, the coastal geomorphological map was done with the classification of each landform. All maps were done by ArcMap program. Then, sampling locations along the transect line perpendicular to present shoreline were assigned for the detail field investigation.

**Figure 2.2** Mozaic of aerial photographs with approximately 1:50,000 scale covering the study area (modified from Thai Survey Department, 1998).

## 2.2 Fieldwork

Geomorphological field check was carried out with one special aim to examine the accuracy of aerial photographs interpretation. Some relict landforms observed from aerial photographs were also examined by ground survey as well as coring. Sediment samples were taken from different landforms in the three different beach ridge plains. The major detail field investigation can be divided into 2 steps as 1) the measurement of beach profile and 2) sediment sampling.

### 2.2.1 Sediment sampling

Sediment sequences can record the history of the earth and its changing environment, in particular, the study of sea-level change. The sequences provide information required, the type of analysis that can be performed on the core including grain size, sedimentary structures, identification of shells and minerals, radiometric dating (Larson et al, 1997). Therefore, the careful sampling is principal thing that should take into account. In this research, sediment samplings were collected from each morphological feature appears in the study area as the former beach, former lagoon, and former tidal flat and modern beach. Vertical variation in sediment samples were collected from each reference point along beach profile by hand auger. The auger was carried out in ridge and swale where exact locations were pointed out earlier from aerial photographs and satellite image. Drilling the sample by hand auger was done as deep as possible along with the study of stratigraphy and lithology of each borehole. Samples were picked from each 20 centimeter core throughout the entire length of drilling and installed it in zip-lock plastic bag (Figure 2.3). Samples for Thermoluminescense (TL) and optionally, Optically Stimulated Luminescence (OSL) were kept from excavation pit (60x60x60 centimeters$^3$). After that, sample in the uppermost undisturbed sediment was collected into PVC tube to prevent from sunlight for calculating equivalent dose. Sample for annual dose was kept from the same layer of the equivalent dose, with weight approximately 1 kilogram (Figure 2.4).

**Figure 2.3** Field measurement for sampling sediments. (top left) hand auger; Edelman auger and sand bucket (sampling sand), (top right) gouge auger (sampling mud). (bottom left) description of samples and (bottom right) samples were kept from each 20 centimeter depth in zip-lock plastic bag.

**Figure 2.4** Photos showing how to collect sample for TL and Optically Stimulated Luminescence dating. Sample is prevented from sunlight for paleo-dose and annual dose in zip-lock plastic bag.

During fieldwork, the beach profile measurement and sediment sampling were concentrated from the inner sandy beach to the middle and outer series. Those sand sediment samplings were collected, not only for physical texture classification, but also to the next step that is age determination. As assumption mentioned in the first chapter, age determination from those old sandy beach sediments may be related to the history of eustatic sea-level changes in the early Holocene. Additionally, the changing in beach morphology and shoreline change at present may provide the clue for the comparison in rate of deposition as well.

## 2.3 Laboratory Work

### 2.3.1 Description of sediment

Description of sediment was carried out by observing the difference of sediment layers in term of their physical characteristics. The description is followed Silapanth (2005) as follows:

Layer observation - The description of different sedimentary layers is carried out in representative strata.

Color - The description in color of sediment sample from each layer.

Texture - Field determination of sediment texture is made by hand that major and minor sediment composition will be noted together for the identification of sedimentary types such as sand, silt and clay.

Layer contact - The deposition of the unconsolidated sediments was discontinuous accumulated. The record of depositional layer contact can indicate the continuity of the deposition. The general description in layer contact can be divided into sharp contact, gradual contact and unclear contact.

### 2.3.2 Grain-size analysis

The coastal zone is composed of many dynamic morphologic features that frequently change their forms and sediment distribution. Although a beach can display a large range of sizes and shapes, each beach is expected to characterize by particular texture and composition representing the available sediments. Textural trends alongshore and cross-shore are indicative of the depositional energy and the stability or instability of the foreshore and near shore zones (Larson et al, 1997).

Grain size is the most fundamental property of sediment particle, affecting their transport and depositional. Grain size analysis, therefore, provides important clue to the sediment provenance, transport history and depositional condition (Simon, 2001).

Sediment from each landform was collected during fieldwork. Representative sample was prepared for the analysis of sedimentary properties in laboratory. For this research, 115 samples in 22 boreholes of the old sandy beach, young sandy beach were analyzed, aiming to characterize sediment that showed in each landform. Grain-size analysis of surface sediments in this research was modified after Friedman and Sanders (1987). Grain size distribution and the other statistic values of sediments were calculated by moment method followed Bogg (1987) and comparison of moment parameter followed Simon (2001).

The moment method was used worldwide to calculate the statistic parameters in differentiating the type of sediment deposition. In this research, dry sieving and weight measurement were done by sieve mesh, sieve shaker and weight measurement (Figures 2.5 to 2.8) The method of Grain-size analysis was divided into 3 parts as followed (Phantuwongraj, 2006):

**A) Sieve experiment**

- Dry sample in oven at temperature $80^{o}$ C about 5-6 hours for release water in samples which make grain of sediment sticking together.
- Mix sediment and then split the sample 2 times (4 piles).
- Weight a pile of sample which was spitted typically several hundred grams depend on grain size such as 500 gram for coarse grain, 200 gram for medium grain, and 100 gram is fine to very fine grain.
- Prepare sieve meshes at equivalent sieve mesh no.5, 10, 18, 35, 60, 120 and 230 (A.S.T.M) or in $\phi$ (phi) scale at -2.00, -1.00, 0.00, 1.00, 2.00, 3.00, and 4.00 respectively.
- Fill sample into sieve meshes which were prepared and put sieve meshes on sieve shaker.
- About 10 minutes later, contain beakers which prepared for each sieve mesh, with sieved samples by divide samples in each mesh into each beaker.

- Weight samples in each beaker and note in weight Table.

**Figure 2.5** Photographs showing the preparation of sample before dry in the oven.

**Figure 2.6** Photographs showing drying sample in oven at temperature $80^{o}$ C about 5-6 hours for release water in samples.

**Figure 2.7** A) Grinding sediment make individual grain.

B) Mix sediment and then split the sample 2 times (4 piles).

C) Prepare sieve meshes at equivalent sieve mesh no.5, 10, 18, 35, 60, 120 and 230 (A.S.T.M) or in ϕ (phi) scale at -2.00, -1.00, 0.00, 1.00, 2.00, 3.00, and 4.00 respectively.

D) Pouring sediment in each sieve mesh weight samples in each beaker and note in weight Table

**Figure 2.8** Photographs showing sieve mesh and sieve shaker and weight measurement used in this study.

**B) Calculation of statistic parameter**

According to a large number of samples, the method of moments was selected. Method of calculations from a great number of parameters was modified from Phantuwongraj (2006).

Calculate all weight data into weight retained percentage and cumulative weight percentage (Figure 2.9) Then enter the sample weight in each size class (column 3 in Figure 2.10) Then multiply the weight in each size class (f in column 3) by the midpoint size (m in column 2) for 1 phi class interval and enter product (f x m) in column 4. Mean value (Equation 1) is calculated by divide $\Sigma$(f x m) (sum of value in column 4) by the n (total weight% in column 3 in Figure 2.10) Subtracts the mean from the midpoint size (m in column 5) and enter this value in column 5. Take the m - $\overline{X}$ deviation in column 5 to the $2^{nd}$,$3^{rd}$ and $4^{th}$ power and enter these values in column 6, 8 and 10 respectively. Next multiply the weight% (f in column 3) by the values in column 6, 8 and 10 and enter these values in column 7, 9, and 11 respectively. Then sum column 9, 10 and 11. Divide the summed value from column 9 by the 100 ($\Sigma$ W from column 3) and square root of this value (Equation 2). This is the $2^{nd}$ moment which is also called the standard deviation. To get the $3^{rd}$ moment of Skewness (in Eqn 3) is calculated by dividing the summed value from column 9 by the $100\sigma^3$. The last moment is Kurtosis, and calculated by dividing the summed value from column 11 by the $100\sigma^4$.

After obtain value of each moment as Mean, Standard Deviation, Skewness and Kurtosis, the comparison of these values from Chart for comparison of Mean, Standard Deviation, Skewness and Kurtosis in moment method was done followed Simon (2001) as shown in Figure 2.11. To understand the geological significance of the four size parameters, it is necessary to plot them again each other in turn as scatter diagrams (base on log-normal distribution with phi size value) after Folk and Ward (1957) and Simon (2001). All 6 two-variable scatter plots are composed of Mean versus Standard deviation, Mean versus Skewness, Mean versus Kurtosis,

Standard deviation versus Skewness, Standard deviation versus Kurtosis and Skewness versus Kurtosis.

| Sample Number | Sample Weight | Screen Mesh Number | Particle Size | Phi Size (ϕ) | Weight REtained | Weight Percent | Cumulative Weight Percent | Remark |
|---|---|---|---|---|---|---|---|---|
| T1-PN1-11 | 200 | | 16 mm | -4.0 | | | | |
| | | | 8 mm | -3.0 | | | | |
| | | #5 | 4 mm | -2.0 | | | | |
| | | #10 | 2 mm | -1.0 | | | | |
| | | #18 | 1 mm | 0.0 | | | | |
| | | #35 | 0.50 mm | 1.0 | | | | |
| | | #60 | 0.25 mm | 2.0 | | | | |
| | | #120 | 0.125 mm | 3.0 | | | | |
| | | #230 | 0.0625 mm | 4.0 | | | | |
| | | tray | | | | | | |
| | | Total | | | | | | |
| | | Sieve loss | | | | | | |

**Figure 2.9** Record weight retained of sample from sieve analysis. (Modified from Phantuwongraj, 2006).

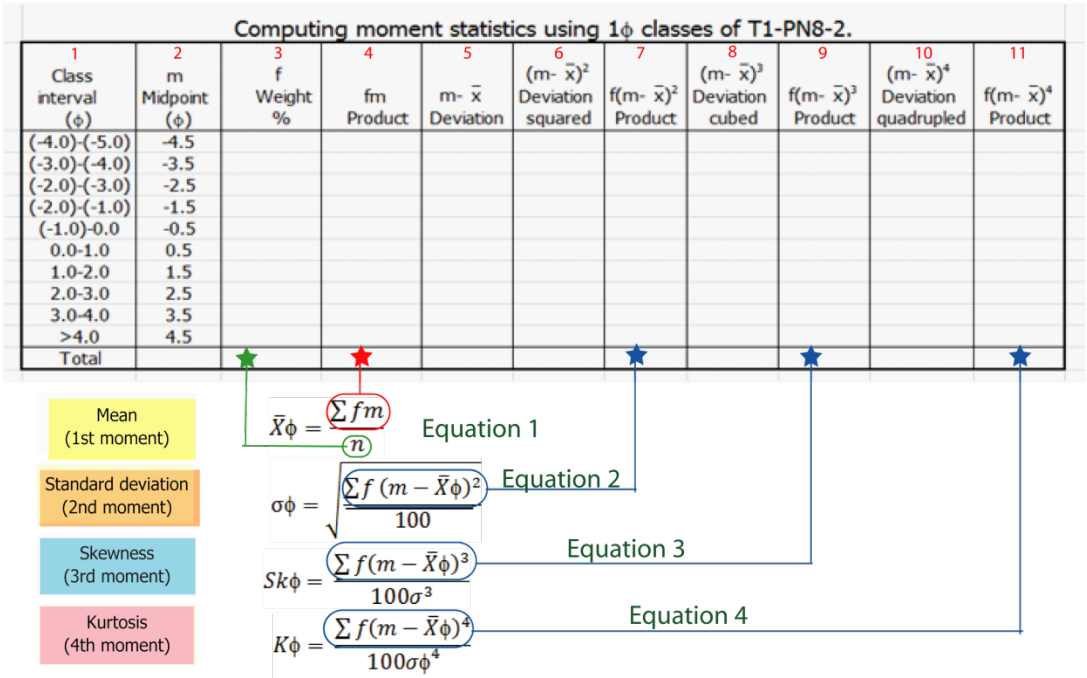


**Figure 2.10** Calculating moment measures in 1phi interval midpoint (Modified from Boggs, 1987).

| Mean | Standard deviation | Skewness | Kurtosis |
|---|---|---|---|
| $\bar{x}_\phi = \frac{\Sigma f m_\phi}{100}$ | $\sigma_\phi = \sqrt{\frac{\Sigma f (m_\phi - \bar{x}_\phi)^2}{100}}$ | $Sk_\phi = \frac{\Sigma f (m_\phi - \bar{x}_\phi)^3}{100 {\sigma_\phi}^3}$ | $K_\phi = \frac{\Sigma f (m_\phi - \bar{x}_\phi)^4}{100 \sigma_\phi^4}$ |

| Sorting ($\sigma_\phi$) | | Skewness ($Sk_\phi$) | | Kurtosis ($K_\phi$) | |
|---|---|---|---|---|---|
| Very well sorted | <0·35 | Very fine skewed | $>^{+}1{\cdot}30$ | Very platykurtic | <1·70 |
| Well sorted | 0·35–0·50 | Fine skewed | $^{+}0{\cdot}43$ to $^{+}1{\cdot}30$ | Platykurtic | 1·70–2·55 |
| Moderately well sorted | 0·50–0·70 | Symmetrical | $^{-}0{\cdot}43$ to $^{+}0{\cdot}43$ | Mesokurtic | 2·55–3·70 |
| Moderately sorted | 0·70–1·00 | Coarse skewed | $^{-}0{\cdot}43$ to $^{-}1{\cdot}30$ | Leptokurtic | 3·70–7·40 |
| Poorly sorted | 1·00–2·00 | Very coarse skewed | $<^{-}1{\cdot}30$ | Very leptokurtic | >7·40 |
| Very poorly sorted | 2·00–4·00 | | | | |
| Extremely poorly sorted | >4·00 | | | | |

**Figure 2.11** Chart for comparison of Mean, Standard deviation, Skewness and Kurtosis in moment method (Simon, 2001).

Analysis in sediment compositions, the composition of sediment was classified using binocular microscope as quartz, feldspar, rock fragment, Mica and ferromagnesian (Figure 2.12). The percentage was estimated also in binocular comparing to the standard chart of sediment's percentage composition (Figure 2.13). Sphericity and roundness defined meaning from Friedman and Sander (1978). Roundness is an attribute of a particle that is related to the sharpness or curvature of edges and of corner. Sphericity is geometrically independent of sphericity. The common method of describing roundness is by comparison to standard images (e.g., Krumbein, 1941; Pettijohn, 1957). However, roundness of sediment is measured in this research based on the comparison chart suggested by Powers (1953) (Figure 2.14).

**Figure 2.12** Photograph showing standard binocular microscope for estimating sphericity and roundness.

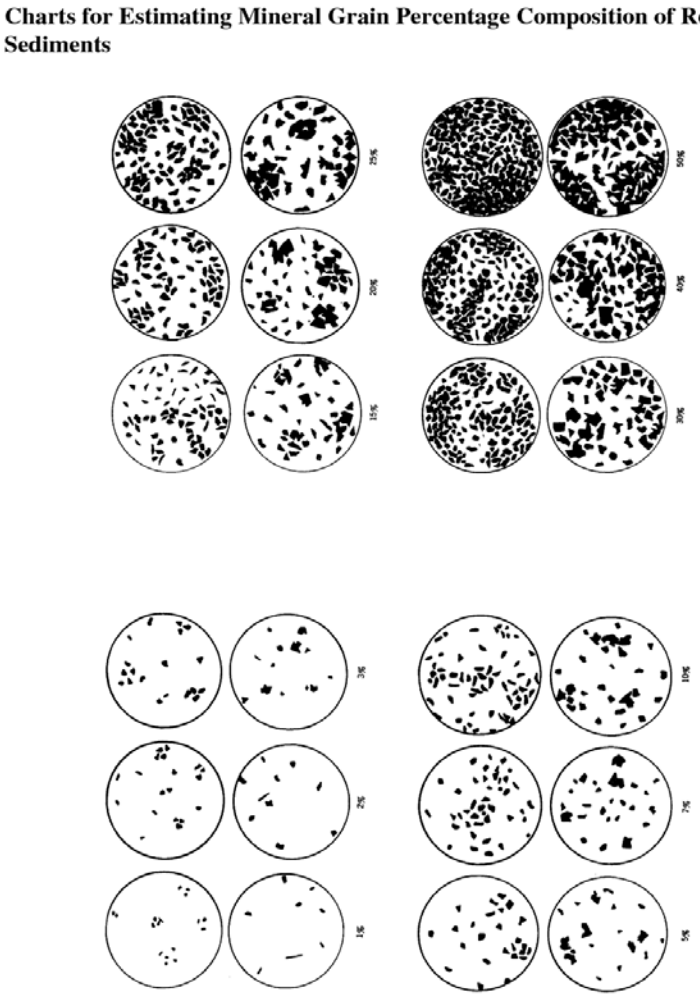


**Figure 2.13** Comparison chart for estimating percentage composition (After Compton, 1962).

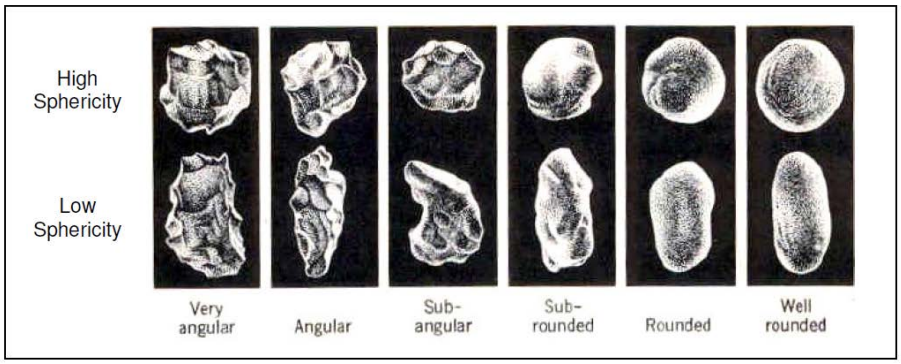


**Figure 2.14** Comparison chart for estimating roundness of sediment (modified from Power, 1953).

### 2.3.3 Age determination by thermoluminescence dating.

In Thermoluminescence (TL) dating, this method detected the amount of light that is emitted by minerals such as quartz and feldspar as a response to rapid heating in the laboratory is registered with the aid of a photomultiplier tube and photon counter used as a measure of time. During burial in sediment, free electron is activated by ionizing radiation from environment particularly by uranium, thorium and potassium radiation. Some excited electrons are able to diffuse through the lattice and gets trapped at various lattice defects. The release of these electrons from these traps, as a result of laboratory heating, produces a luminescent signal that is proportional to the absorbed dose (Equivalent dose) of radiation energy. The age reflecting the time since the sediment grains were last exposed to sunlight (Wintle and Hunley, 1980). However, the resetting of the TL signal by sunlight is less efficient than by heat. Because sunlight does not completely evict the electron from traps that produce TL signal (Wintle and Huntley, 1980; Huntley et al., 1985). Themoluminescence dating process shows in Figure 2.15. By measuring the natural TL signal and the sensitivity of the mineral sample (i.e. the amount of thermoluminescence light emitted per unit of absorb dose), the equivalent dose is evaluate. From an additional determination of the dose rate the sediment grains have been exposed to during their burial, a TL age can be determined (Munyikwa et al., 2000). This application can now give credible ages from a few tens of years to 500 ka (Huntley and Prescott, 2001).

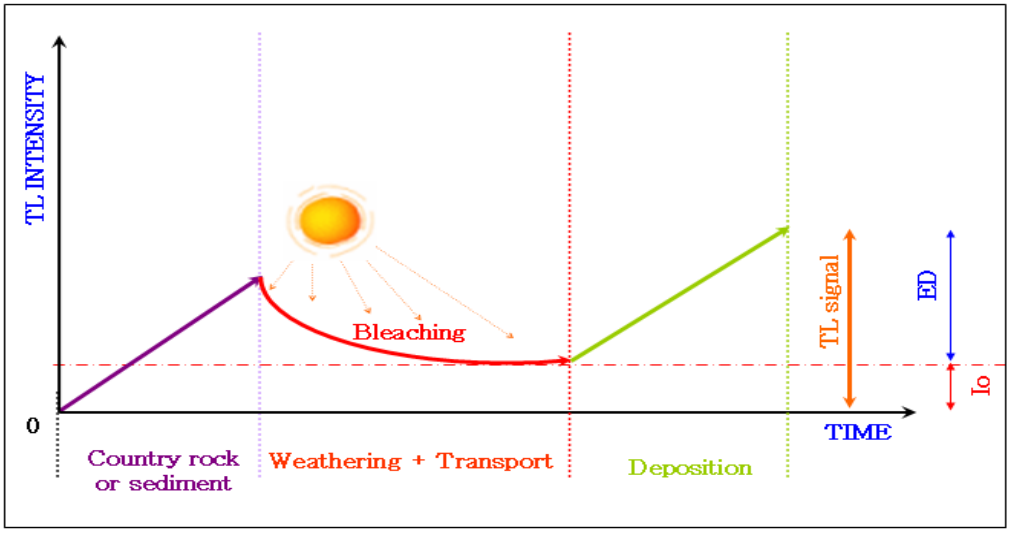


**Figure 2.15** Hypothetical thermoluminescence level versus time. An event permitting the sediment to be exposed to sunlight reduces the captured electron causes thermoluminescence signal to a residual level (Io). (modified from Won-in, 2003).

This method was applied for dating ancient beach ridge sediments based on the hypothesis that each beach ridge formed in a specific time span and may be related to the next ridge. Thus, thermoluminescence dating involves the determination of two major parameters: the equivalent dose (palaeo dose) and the annual dose. Calculating age of sediment from relative equation of age determination is based on the following equation and relation (Aitken, 1985; Pailoplee, 2004; National Center of Excellence For Environmental And Hazardous Waste Management, 2006).

$$\textbf{Age of material} = \frac{\textbf{Equivalent dose (ED)}}{\textbf{Annual dose (AD)}}$$

Where

- Equivalent dose (ED): The total accumulated dose that received by irradiation from natural radioactivity and preserve this record through time. In the case of sediments, residual intensity ($I_o$) from the bleaching experiment is considered herein.

- Annual dose (AD): Irradiation dose per year from natural radioactivity. Annual dose is calculated from the chemical data of radiogenic elements (uranium, thorium, and potassium) and comic ray evaluation.

Thus, TL dating involves the determination of 2 major parameters; equivalent dose and the annual dose.

**Regeneration technique**

In this study choose regeneration technique, the simplest approach to the evaluation of equivalent dose is by the straight-forward procedure of measuring the natural TL intensity from a natural sample (N) and comparing it with the artificial TL intensity from the same sample that know certain dosage (artificial irradiate sample). The artificial irradiate sample was preheat in 320 °C and 5 hours duration which were enough to reset existing TL signals to zero level (Takashima et al., 1989). The preheated samples (H) were exposed to artificial irradiation from radioisotope source, which can control the certain dosage (e.g. 50Gy, 200Gy, 400Gy and 800Gy). The preheat sample (H) adds artificial irradiate shows as H+50Gy, H+200Gy, H+400Gy and H+800Gy. After irradiation, the unstable signals of the samples must be excluded by heating at 120 °C for 24 hours (Figure 2.16). The equivalent dose is read from a starting point of horizontal line drawn at the level of the natural thermoluminescence Pailoplee (2004).

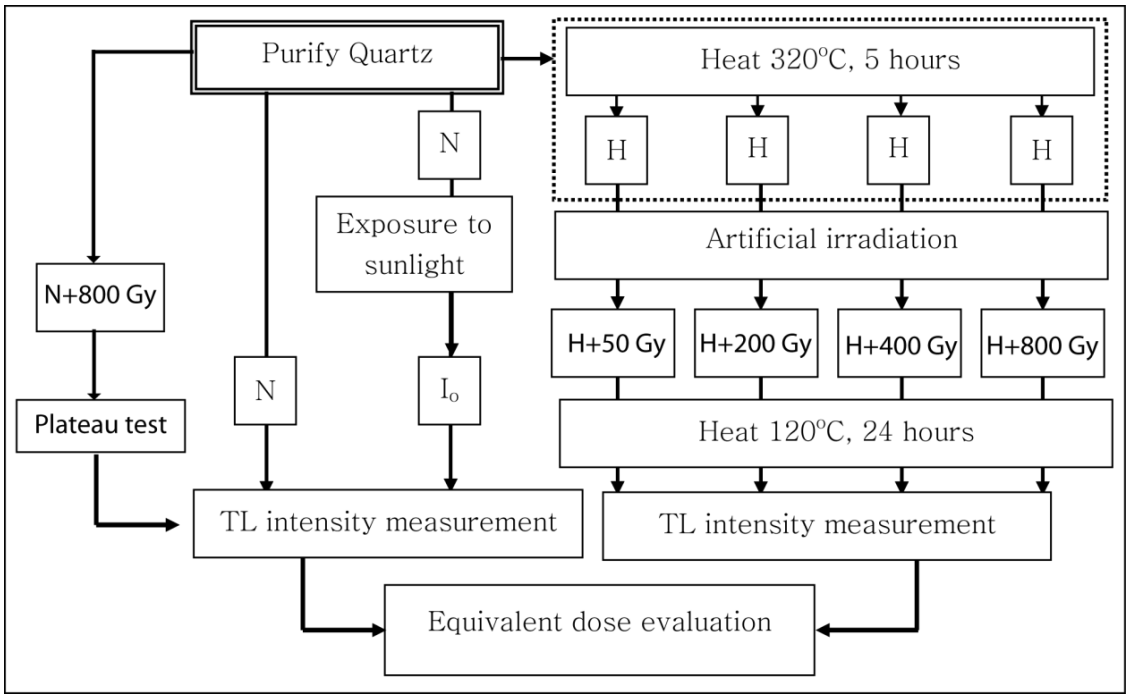


**Figure 2.16** Schematic charts of regeneration technique for measurement of the TL intensity; N is natural sample, Io is residual intensity from sample, H is 320°C heated sample and samples is known dosage that irradiated sample (modified from Pailoplee, 2004).

#### 2.3.3.1 Thermoluminescence dating procedure

TL laboratory procedure proposed by Pailoplee (2004) is applied for this research study. The methodology of analysis is composed of 3 main procedures, including equivalent dose evaluation and annual dose evaluation (Figure 2.17).

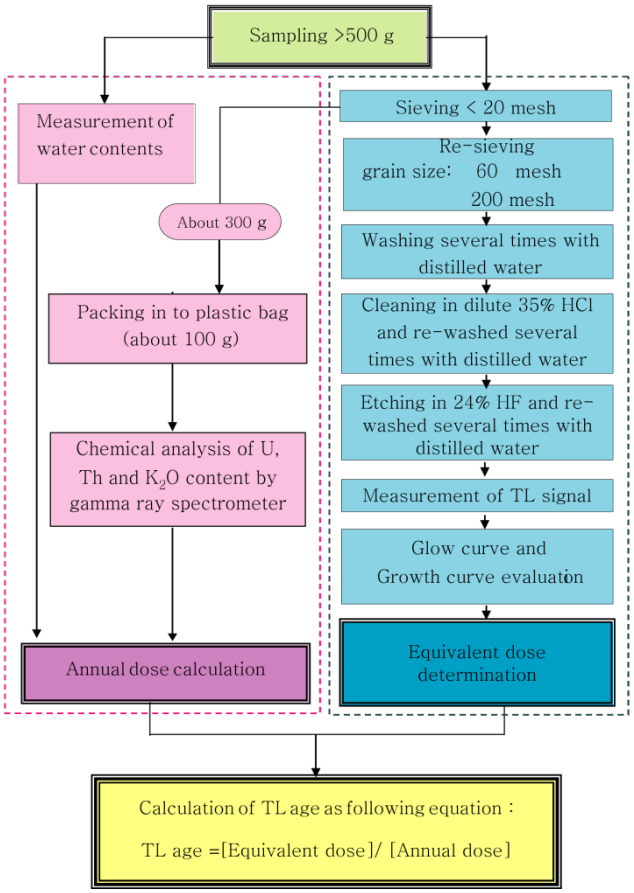


**Figure 2.17** Simplified flow chart illustrating laboratory analysis use in this research study. The pink blog is the annual dose procedure and the yellow blog is the equivalent dose procedure (modified from Pailoplee, 2004).

#### 2.3.3.1.1 Annual Dose Evaluation

Water content is quantity of surface moisture that contained around sediment grain. The calculation is done from different weight of sediment after dry in oven at temperature 80°C about 5-6 hours (Figure 2.18). Water content is also measured for all samples being dated because it is the one significant parameter for annual dose determination. The formula of water content calculation is;

(weight of a wet sample- weight of a dried sample) X 100 ---------- (Eq.2.1)
weight of a dried sample

Annual dose sample is prepared by bring sample in to tray and baked in oven for eliminate surface moisture in samples at temperature 80°C about 5-6 hours. Each sediment sample was shattered by using a pestle or hand and the material passed through sieves to isolate the grain size fraction in 2 parts. Sediments which grain size pass through a 20 mesh (<841µm) were collected about 300 g was separated to keep in plastic containers and tightly sealed for annual dose determination (Figure 2.19).

**Figure 2.18** Water content sample preparation.

**Figure 2.19** Annual dose sample preparation.

Annual dose calculation can be done by many types of equipment such as gamma spectroscopy, neutron activation analysis (NAA), flame photometer and atomic absorption of Vana (2012). However, this thesis chooses gamma spectroscopy that is suitable for solid sample.

Generally sediments are exposed continuously to ionizing radiation which originates from their radioactive contents, plus a small fraction from cosmic rays (Aitken, 1985). There are essentially 3 radioactive elements which contribute to the natural dose rate (annual dose) i.e. uranium (U), thorium (Th) and potassium ($K_2O$). The decay of uranium and thorium results in $\alpha$, $\beta$ and $\gamma$ radiation whereas potassium emits $\beta$ and $\gamma$. Normally, the natural dose rate in most sediments is of the order of mGy/year (Pailoplee, 2004).

For age determination, it is necessary to evaluate the natural dose rate accurately. Several components are needed for an accurate annual dose is

1. Measurement of U, Th and K contents,

2. Calculation of environmental water content in field at time of sample collection, and

3. Cosmic ray component evaluation.

The annual dose to the sample is computed from the concentrations of K, U and Th by the method described by Bell (1979) and Aitken (1985).

Annual dose (AD) = $D_\alpha+D_\beta+D_\gamma+D_c$ _____ (Eq. 2.2)

Where $\alpha$= Alpha irradiation content,

$\beta$= Beta irradiation content,

$\gamma$= Gamma irradiation content, and

C = Cosmic ray irradiation content.

A) Measurement of Uranium, Thorium and Potassium Contents

U, Th and $K_2O$ contents used gamma ray spectrometer. The first step is to select equal grains of samples being dated by sieving with 20 mesh sample. The samples are contained in the plastic vessel. A plastic vessel put on 75 mm Nal sincirator unit with a multi-channel analyzer unit. Chemical analyses were performed by gamma ray spectrometry at Akita University, Japan (Figure 2.20). The detector employed was a 76∅ x 76 mm NaI (T1) scintillator connected to a multichannel analyzer (Takashima and Watanabe, 1994). Standard samples employed were NBS samples for U and Th, and $K_2O_3$ chemical reagent for K. Each sample was measured for two days (Kalchgruber et al., 2002). The estimated standard errors were less than 10% for U and Th, and less than 3% for K using the fixed count error calculation method (Takashima and Watanabe, 1994).

**Figure 2.20** Gamma ray spectrometer at Akita University, Japan. This equipment is used for measure uranium, thorium and potassium contents.

B) Annual Dose Calculation

Annual dose is calculated from chemical data of U, Th and K2O contents with the equation proposed by Bell (1979) and Aitken (1985).

AD = [0.15(2.783U + 0.783Th)/(1+1.50(W/100))]+[(0.1148BU + 0.0514BTh + 0.2069BK)/(1+1.14(W/100))] + [(0.1462U + 0.0286Th +0.6893K)K/(1+1.25(W/100))]+0.15 ---------- (Eq. 2.3)

Where AD = Annual dose (mGy/year),

U = Concentration of uranium in ppm,

Th = Concentration of thorium in ppm,

K = Concentration of potassium oxide (%),

B = Beta coefficient in quartz grains, and

W = Water content (%).

#### 2.3.3.1.2 Equivalent Dose Evaluation

Age of equivalent dose measure of TL intensities on 3 sample portions: 1) natural sample portion, 2) artificial irradiation sample portion and 3) residual sample portion. The TL emissions of quartz were measured by using the Thermoluminescence Detector (Figure 2.25) at Kasetsart University, Thailand. Approximately 20 mg of sample was filled in aluminum pan and placed on a Nicrome heater plate. The sample is heated on heater plate under nitrogen condition to 450 °C. Filter system applied in this research study is a blue filter. The light emission is amplified and measured by photomultiplier and record simultaneously with the temperature of the sample (Figure 2.21). The graph shows a relationship between TL intensity and temperature which is called "glow curve" (Aitken, 1985). The term glow curve is given to plot intensities of emitted light versus temperature (Figure 2.26). The light is recorded and it can plot to a establish TL growth curve which relates TL output and the absorbed radiation dose (Figure 2.28). Calculation of equivalent dose can be done by interpolating natural signal intensity and residual signal intensity with a growth curve from artificial irradiated signal intensity. The result is assumed to be proportional to the equivalent dose of Eq.2.1.

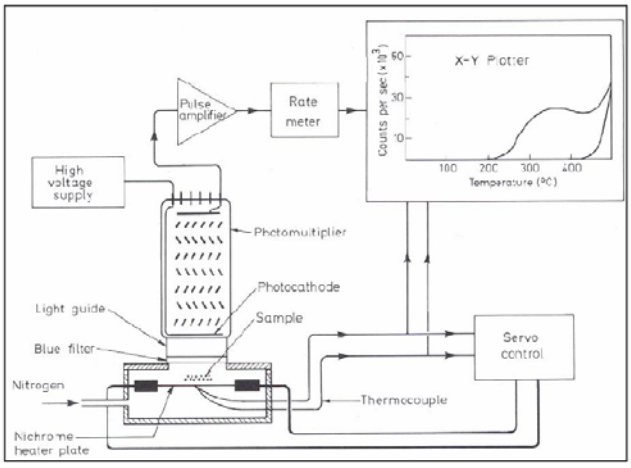


**Figure 2.21** Thermoluminescence Detector for measure electrons from traps, as a result of laboratory heating, produces a luminescent signal that is proportional to the absorbed dose (Equivalent dose) of radiation energy.

All samples for equivalent dose were prepared by sieved between 60 mesh (149 μm) and 200 mesh (149 μm). After that, chemical treatment was done as step follows;

a) Washing several time with distilled water for remove some organic materials and clay particles.
b) Cleaning sample by dilute 50 % HCl at 50-60 °C in a period of 15-30 minutes and re-washed several times with distilled water for eliminating carbonates and deep-rooted organic material.
c) Etching the sample in 24% HF at 50-60 °C for 15-30 minutes and re-washed it several times with distilled water. HF was used to dissolve the plagioclase. After that dry in oven (1 day).

Purifying quartz for measuring radioactivity quantity is then carried out (Huntley, 1985; Pailoplee, 2004; and National Center Of Excellence For Environmental And Hazardous Waste Management, 2006.) The purifying quartz sample is subdivided into 3 parts:

- Part1: Natural quartz sample used for evaluated natural sensitivities of previously acquired TL signal.

- Part2: Sample was bleached with natural sunlight for 12 hours to effectively remove residue TL signal.

- Part3: Samples are irradiated (in unit Grey) known as 50 Grey, 200 Grey 400 Grey and 800 Grey and natural sample is irradiated for 800 Grey for plateau test. Before irradiation, Bring sample in to aluminium sheet and baked it at 320 °C around 5 hours for reset electron to zero (Figure 2.22, Figure 2.23). After that baked it at 120 °C (1 day) for reduce noise. This step used to find out the characteristic of quartz effective with artificial irradiation that amount of radioactive.

The gamma ray source for artificial irradiation is from Office of Atomic Energy for Peace (OAEP), Bangkok (Figure 2.24).

**Figure 2.22** Sample is brought into Aluminium froid and baked it at 320 °C around 5 hours for reset electron to zero.

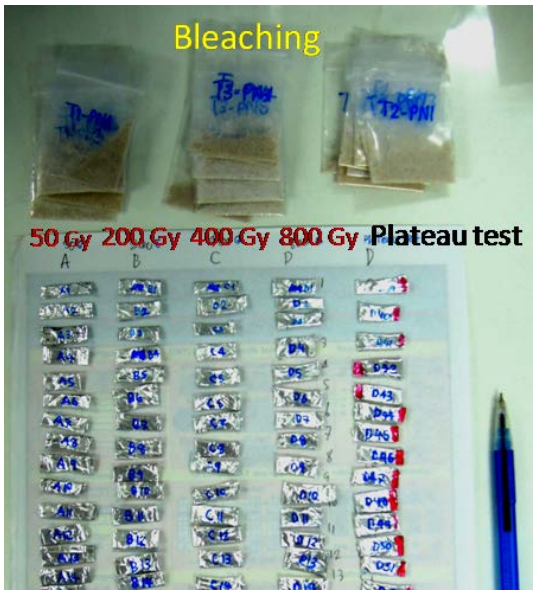


**Figure 2.23** Sample for Equivalent dose can separate in to 4 part; bleaching, irradiation at 50Gy, 200Gy 400Gy and 800Gy by Gamma cell, Plateau test and natural (prevented from light).

**Figure 2.24** Sample for irradiation by Gamma cell (Source $^{60}$Co) at 50Gy, 200Gy 400Gy and 800Gy at Office of Atoms for Peace. After that baked it at 120 °C (1 day) for reduce noise.

**Figure 2.25** Thermoluminescence Detector (TLD) at Earth Science Department, Faculty of Science, Kasetsart University cooperated with Akita University, Japan; that is used for TL glow curve measurement.

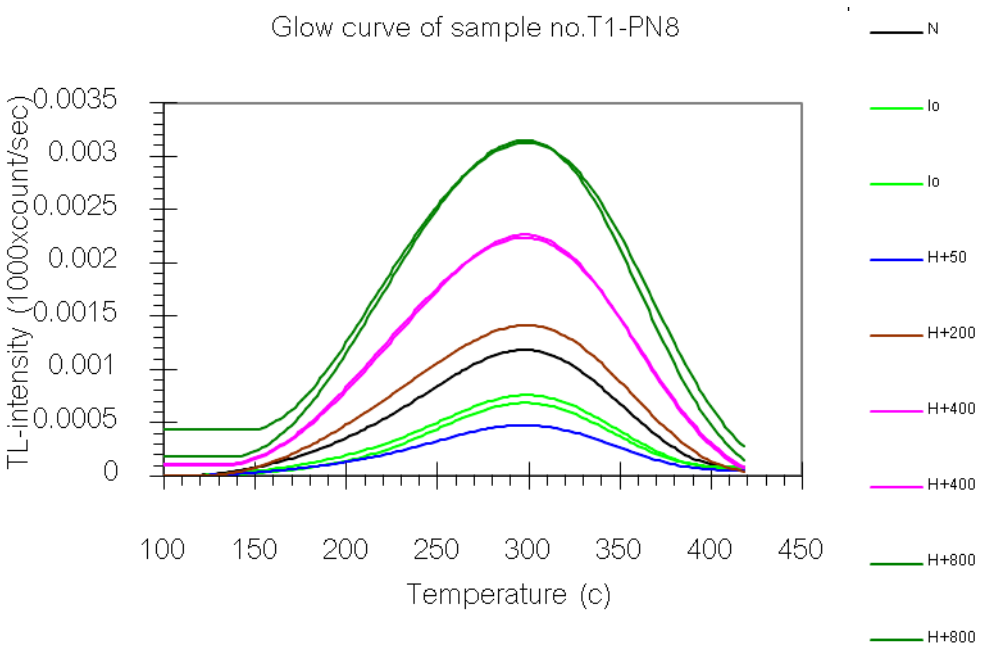


**Figure 2.26** Glow curve of sample no. T1-PN8, old beach sand in middle ridge. The graph shows a graph relationship between TL intensity versus temperature. The graph measured from thermoluminescence detector (TLD) at Earth Science Department, Kasetsart University.

Although the glow curve shown in Figure 2.26 is smooth continuum, it is really composed of stable and unstable signal. The TL signal in a stable region of glow curve should be considered by the plateau test method (Aitken, 1985) (Figure 2.27). This procedure makes by compare the shape of the natural glow-curve (i.e. the glow-curve observed from a sample which has not received any artificial irradiation in the laboratory) with the artificial glow-curve observed at 800 Grey as a result of artificial irradiation. Thus a constant ratio between natural and artificial glow curves gives an indication that, throughout this plateau region, there has been negligible leakage of electrons over the centuries (Pailoplee, 2004).

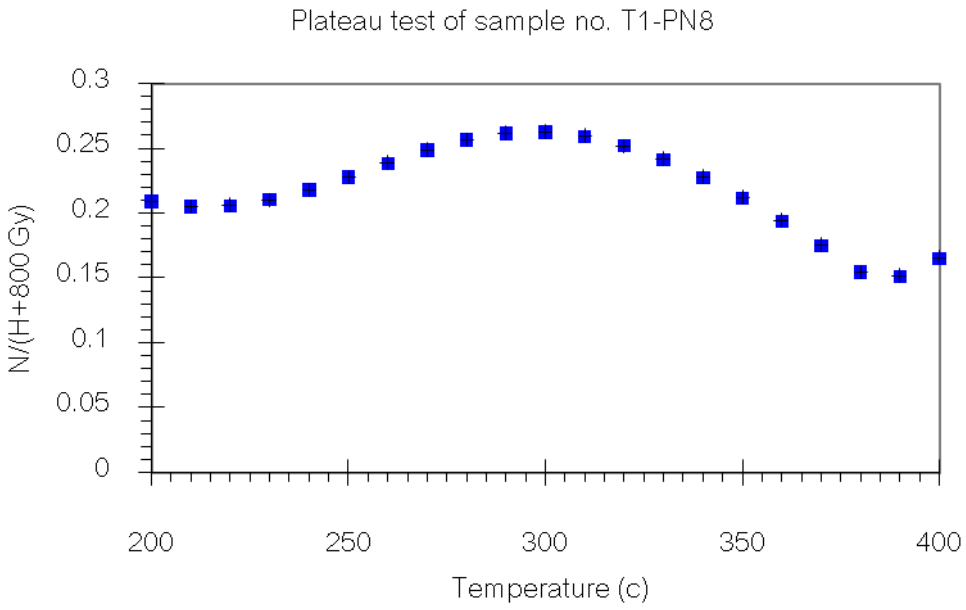


**Figure 2.27** Plateau test of sample no T1-PN8, old beach sand in middle ridge showing a relationship between natural/artificial ratios from glow-curves versus temperature ($^{o}$C).

The next step is for the construction of growth curve. This can be done by the increases of TL output with known amounts of additional radiation that induced the sample. The graph showing this relationship is called “growth curve” (Figure 2.28). In this is used the regeneration technique (Takashima and Honda, 1989).

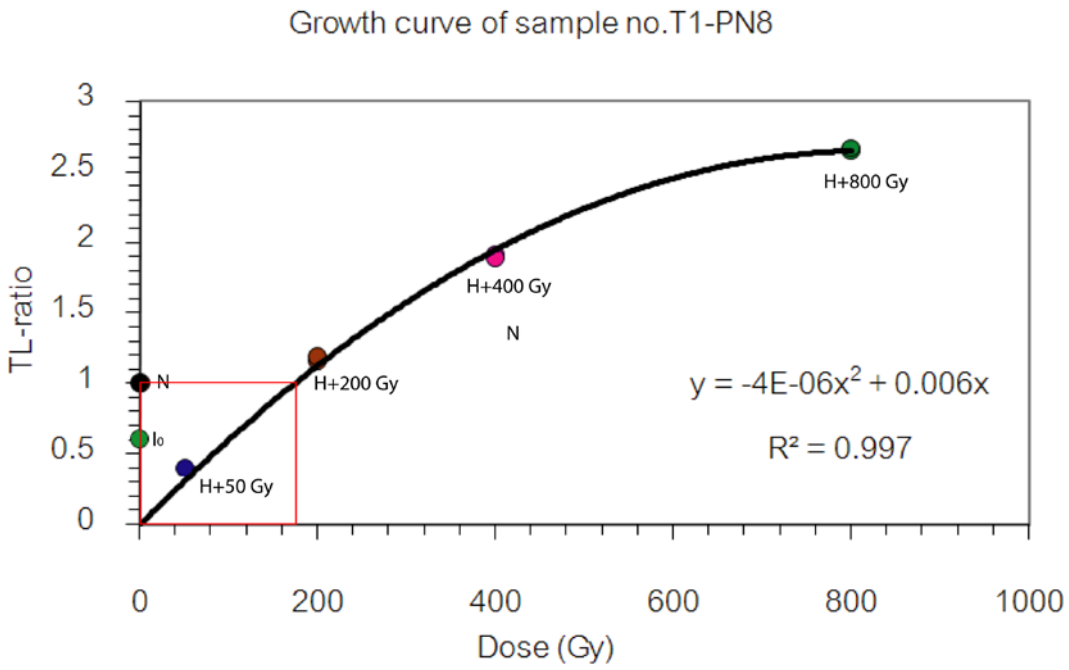


**Figure 2.28** Growth curve of old beach sand sample no. T1-PN8 from middle ridge, using regeneration technique. The curve showing relationship between TL ratio (artificial glow curves/ natural glow curve) versus temperature ($^{o}$C). N is natural signal, $I_0$ is bleached sample and H (+50Gy, +200Gy, +400GY, +800Gy) is heated sample at 320 $^{o}$C for 5 hours and irradiated sample by Gamma cell.

### 2.3.4 Fossil identification

Fossil identification was done from the shell samples collected from fieldwork. Cleaning is a first step. Systematically classification the characteristic of shells are different for each species by comparison with previous thesis or research. Taking photographs of shell samples will be done.

The name of Mollusca was first use by the French zoologist Cuvier in 1978 to describe squids and cuttlefish, animal whose shell is reduce and internal, or entirely absent. Molluscs are found in nearly all habitats. In the sea they occur from the deepest ocean trenchs to the intertidal

zone. They may be found in freshwater as well as on land where they occupy a wide range of habitats (Surakiatchai, 2005).

Shell fossils were found in the field is mostly belonged to the Phylum Mollusca. The Phylum Mollusca is second in numerical size only to the insect. This phylum can be divided in to 6 classes as Gastropoda, Bivalvia, Cephalopoda, Scaphopoda, Polyplacophora and Monoplacophora. Only 3 classes were found as Class Gastropoda, Class Bivalvia and class scaphopoda.

Mollusks are adapted to live almost anywhere except in barren, lifeless zone where food is non-existent or inaccessible. Thus, sandy areas are havens for mollusks with long siphons and bodies adapted for burrowing, such as a majority of bivalves, many gastropods, and most tusk shells (Wye et al., 1996).

#### 2.3.4.1 Gastropod

The gastropods are a large and diverse class that lives in almost every conceivable environment, from high tide levels to the dark depths of the ocean floor. But the majority, and certainly the most colorful and attractive, inhabit varying substrates in shallow waters relatively close to the shore, where all manner of marine life is to be found in great variety and abundance (Abbott et al., 1989).

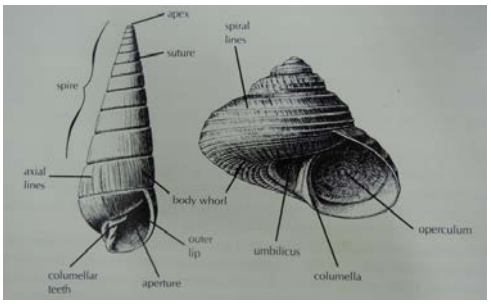


**Figure 2.29** Drawing of parts of Gastropod (Wye et al., 1996).

### 2.3.4.2 Bivalve

The bivalve animal, following a different growth pattern, rarely infers with any part of its shell once it has been formed. Bivalves have two-piece shells, each piece being called a valve. Two valves, equal or unequal in shape and size, are jointed together by a flexible, chitinous ligament and they close effectively because the upper, inner edge of each has a hinge embellish with interlocking teeth and pit. The small teeth immediately below the umbones (embryonic valves) are the cardinals, the longer ones on each side of them, the lateral.

Also visible on the inside of each valve are marks left by certain muscle. The adductor muscles leave prominent adductor scars in the valves. In some bivalves, such as oysters and scallops, there is only one adductor scar in each valve, but many more have two in each valve usually have a clearly visible pallial line connecting them. In most bivalves the pallial line has a distinct embayment, known as the pallial sinus, indicating the former present siphons.

Often it is possible to identify a bivalve by its external characteristics alone, for these are many and varied. It is often necessary to distinguish one valve from the others. With very few exceptions bivalve have an upper or dorsal margin and lower ventral margin. The umbones are situated on the dorsal margin and usually incline toward the anterior end of the shell (Wye et al., 1996).

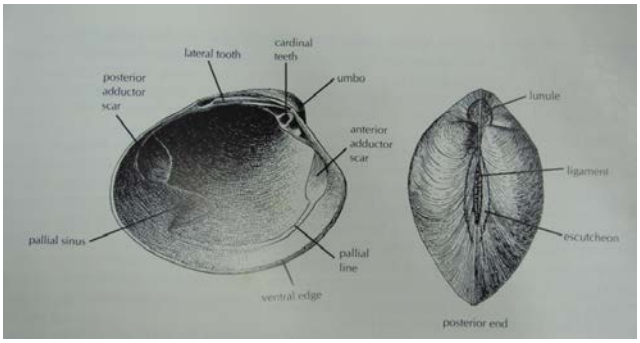


**Figure 2.30** Drawing of parts of Bivalve (Wye et al., 1996).

Shells and other fossils found in the area including 6 positions as T1-PN12 this point located at grid reference 524591, 1155372. Fossils were found in grey muddy sand at 150 cm depth. T2-PN10 is located at grid reference 523548, 115138. Fossils were found in greenish grey sand approximately depth at 140-180 cm. T2-PN11 located at grid reference 523548, 115138. Fossils were found in grey muddy sand approximately depth at 150 cm. T3-PN1 located at grid reference 520733, 1148838. Fossils were found in grey sand approximately depth at 170-180 cm.T3-PN2 located at grid reference 519807, 1149851.and fossil were found in grey sand approximately depth at 350-360 cm. T3-PN5 located at grid reference 522560, 1150423.

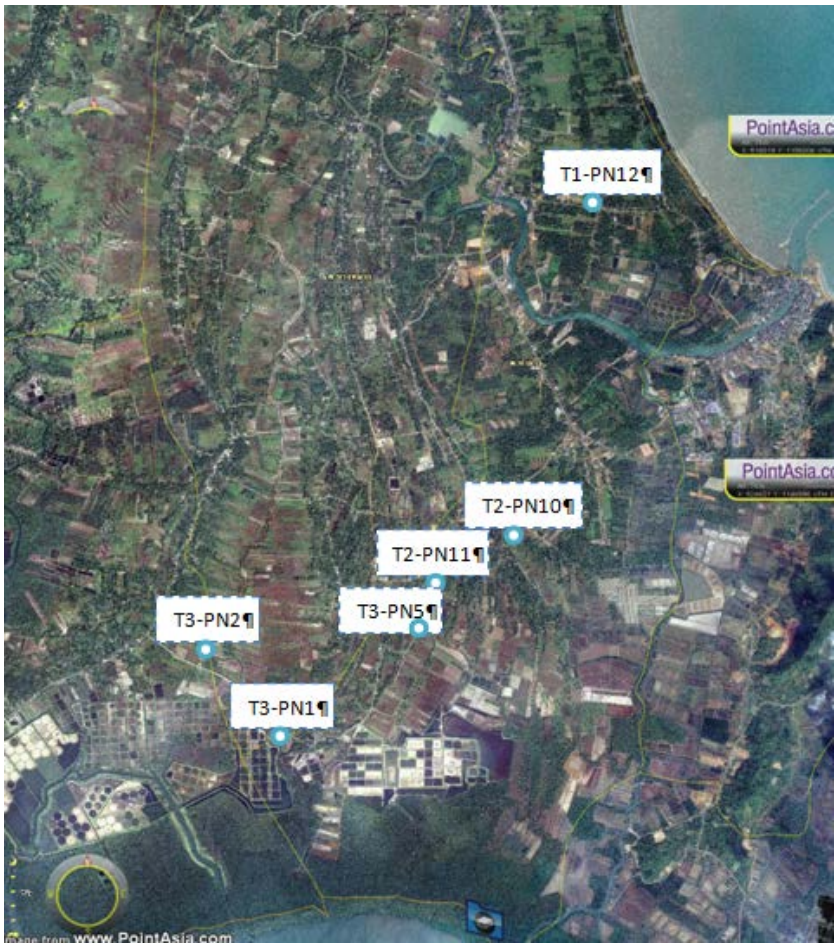


**Figure 2.31** Positions of the shell fossil found in the study area (6 locations: T1-PN12, T2-PN10, T2-PN11, T3-PN1, T3-PN2 and T3-PN5) (map is modified from www.pointasia.com).

### 2.4 Data analysis, Interpretation and Conclusion

The analysis and discussion will rely on the fact evidence from field and laboratory works. However, the first analysis will be focused on the checking of the geological and morphological mapping. Classification of fauna in beach ridge sand together with detail analysis in sedimentology will help to better understanding of paleo-environment analysis of the study area. After that, the correlation and comparison of the geological and morphological data will be done carefully in order to create a paleo-environmental model and come up with the final research conclusion.

# CHAPTER III

# RESULTS OF THE STUDY

This chapter provides results of the study including the geomorphological description, sedimentological description, age determination from series of beach ridges and identification of fossils found in both swale and in beach profiles. Results were divided into three parts, starting with aerial photograph interpretation. As mentioned in previous chapter, the interpretation of aerial photograph is aimed at classifying series of beach ridge plains and divided them based on the difference in orientation of ridges and the preferable direction of paleo-longshore currents in different period of depositional times. Then later in this chapter, sedimentological description will be shown especially the characteristics of sediments from each of coastal geomorphology in the study area. Results of grain size distribution and the analysis in sediment compositions, and other significant sediment properties, such as roundness and sphericity were analyzed and described. In the final part of this chapter, age determination from TL techniques from each beach ridge will be ascribed. Finally, identified fossils found in sediment profiles of beach ridge and swale will be shown in order to confirm the depositional environment where they were living. All results will help to model the evolution of coastal plain in relation to the sea level change.

## 3.1 Geomorphological description

The geomorphological landforms in this area were firstly classified by using aerial photographs, and then, the correction of interpretation was checked in the field. The geomorphological map of recent surface landform shows the discontinuity of some landforms because after they deposited, some changes have occurred probably due to the effect of sea level variations. However, some relict landforms indicating the former beach ridges were preserved and can be classified and mapped into the detailed geomorphological map. Coastal

geomorphological units were divided into 7 units as (1) old sandy beach, (2) old lagoon, (3) young sandy beach, (4) old tidal flat, (5) upland and mountain, (6) intertidal flat and (7) tidal flat. Each of these units can be described as follows.

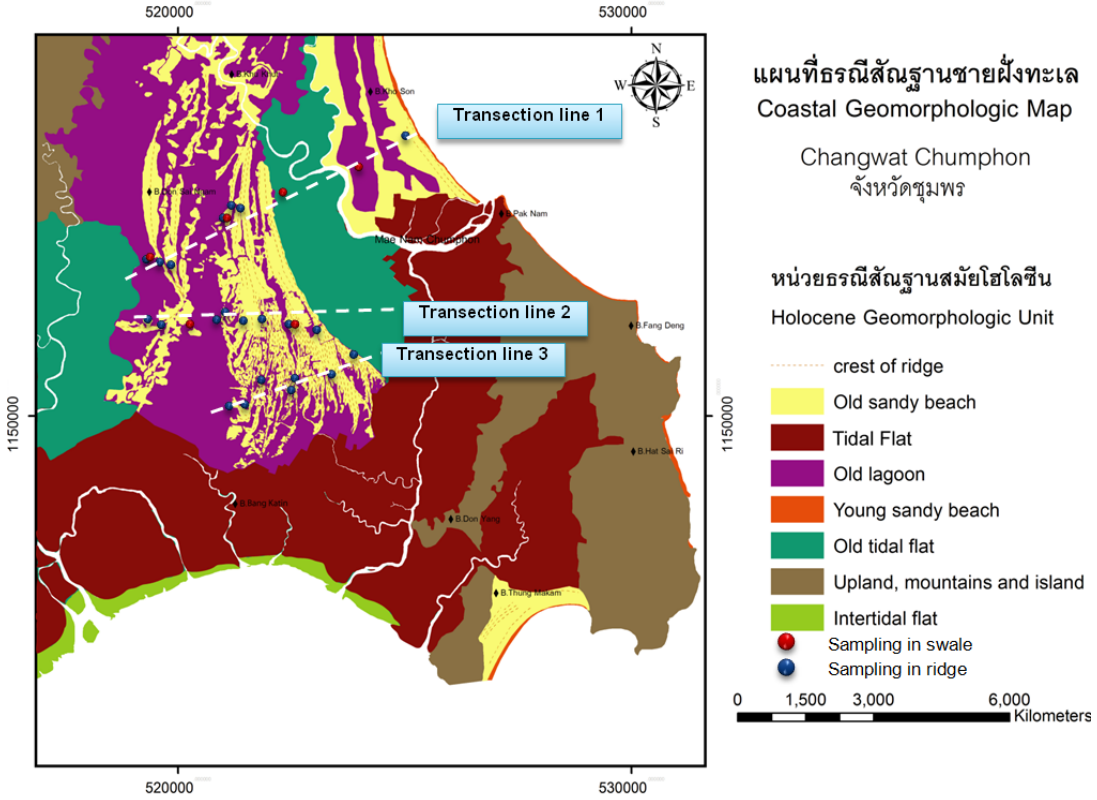


**Figure 3.1** Coastal geomorphological map of Pak Nam Chumphon, Amphoe Muang, Changwat Chumphon. Dots in red and blue color showing locations of coring.

### 3.1.1 Classification of landforms

As seen in Figure 3.1, the geomorphological landforms can be divided into 7 units as follows.

#### 3.1.1.1 Old sandy beach

Old sandy beach is a relict feature that always of interest to the study of sea level changes because it commonly preserves the evidence of marine transgression. Age of each old beach ridge

can also be related to sea level incursion and regression at the time when it translated into the land and prograded to seaward direction, respectively. As seen in aerial photographs, the old sandy beach unit shows dark gray color with the curvature as a continue ridge line, and it branches to many lines within one series of beach ridge. It commonly shows irregular topography. At least 3 clear series of beach ridges were classified using the difference in direction of orientations reflecting the difference in paleo-longshore current directions. Inner series of beach ridges shows the direction of longshore current in northward direction. Inner series of this beach ridge plain consists of four beach ridge. On the other hand, the middle and outer beach ridge series show the paleo-longshore current direction to the south. Both middle and outer series of beach ridge plain contain a plenty of small beach ridges. Areas between beach ridges are mostly classified as dry and wet swale and old lagoon.

#### 3.1.1.2 Old lagoon

Old lagoon can be seen in light gray color and mostly displays as flat topography. Some lagoons are disturbed and changed by aquaculture area (shrimp farm) and water-distribution canal. It is commonly located between old sandy beaches. In the field, this landform is composed of mud and shell fragments (both complete and incomplete shell). Almost of old lagoon is disturbed by agriculture as palm forest. Swale is covered with sand sediment in cultivating step. Nevertheless, it is favorable opportunity to see sediment profile excavated by local people in places where hand auger drilling is not possible. Oyster fossils and the other fossils were recognized from the cultivated area.

#### 3.1.1.3 Young sandy beach

Young sandy beach is white color appeared in aerial photograph with long and narrow ridge line at the present shoreline. Its geomorphology is contributed by sandstone headland as Khao Matsi. Younger sandy beaches in the study area are located at Ao Pak Hat, Hat Pharadon

Phap, Had Sai Ree and Ao Thung Kham Yai. Young sandy beach is characterized as gentle slope. Some beaches are composed of laterite and lateritic granules.

#### 3.1.1.4 Old tidal flat

Old tidal flat can be seen in gray color and flat topography in aerial photograph. This old tidal flat area has been affected by sea water because the elevation is within the present tidal range.

#### 3.1.1.5 Mountains

The mountainous area is composed mainly of the Jurassic pebbly sandstone, and siltstone hills in the eastern part of the study area. These mountains are oriented in NE-SW and can be inferred to the Lam Thab Formation (DMR, 2001).

#### 3.1.1.6 Intertidal flat

Inter tidal flat can be seen in light gray color. Inter tidal flat areas are composed on the coastal wetlands that form when mud is dominated by tides or rivers. Intertidal flat may be viewed geologically as exposed layers of bay mud, resulting from deposition of estuarine silts, clays and marine animal detritus. It is submerged and exposed approximately twice daily.

#### 3.1.1.7 Tidal flat

The tidal flat can be seen clearly from the aerial photograph as dark gray areas nearby the recent shoreline. Tidal flat is a part of small recent estuary system in this study that also contains inlet/outlets. It submerged and exposed to the air by changing tidal levels. In addition to the alternating submergence and exposure, the varying influences of fresh river water and salty marine waters because physical conditions to vary more widely than in any other marine environment.

## 3.2 Sedimentological description

The sedimentological study in Pak Nam Chumphon area has been done from 28 samples collected in several locations in different landforms. Samples are picked up mainly from old sandy beach, old lagoon, young sandy beach and old tidal flat. Old sandy beach and old lagoon are special dominated in this study area, thus, coring by hand auger has been carried out. The average depth of the drilling is approximately 300 cm. Limitation was arisen in place where drilling has reached groundwater level. The basic description of each sediment samples has been recorded during the fieldwork. Systematic description started with lithological log from coring samples as follows.

### 3.2.1 Lithological description from coring

The lithological description aims to record the characteristic of sediment layer from the oldest in bottom to the youngest at the top. Grain size distribution of sediment in each layer was analyzed by sieve analysis technique. Lithological description from coring were aimed to differentiate landforms within the study area as old sandy beach, young sandy beach, old tidal flat and old lagoon. The whole lithological description form the other locations can be seen in appendices.

#### 3.2.1.1 Inner most beach ridge (old sandy beach) in station T1-PN1.

The location of T1-PN1 at the most inner part of beach ridge plain was found at UTM grid of 519617 E 1153469 N on map sheet number 4829 IV (Amphoe Muang Chumphon). The total depth of the core is 400 cm. It can be classified as 8 lithological layers as shown in Figure 3.3.

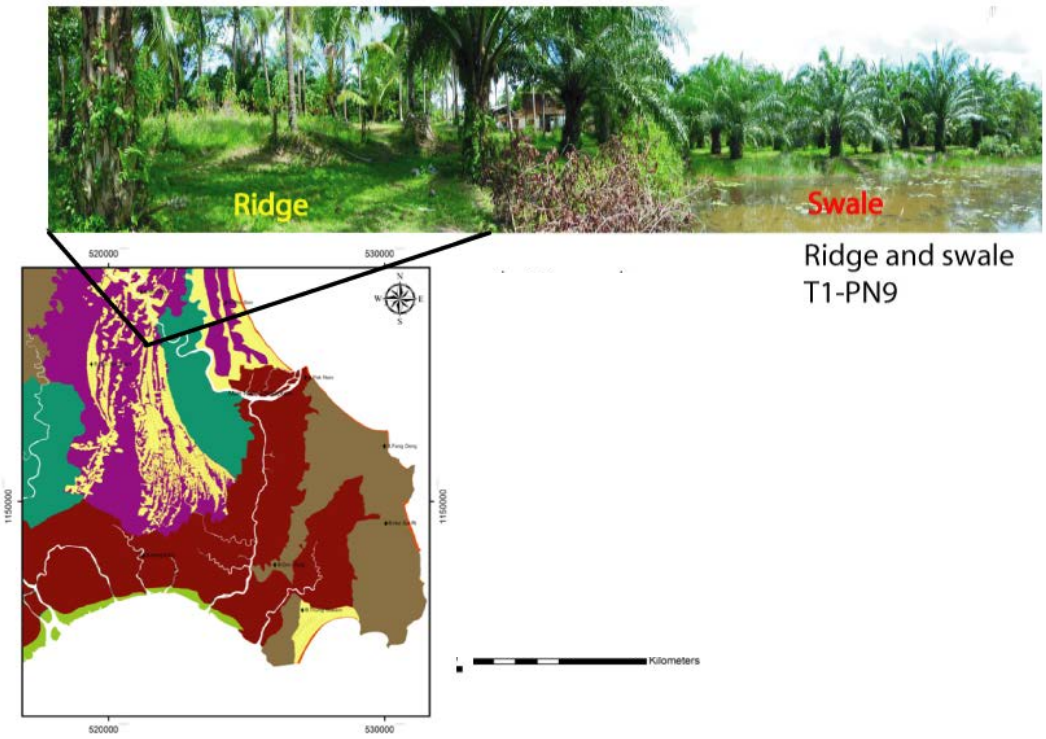


**Figure 3.2** Locations of old sandy beach (beach ridge) and old lagoon (swale) in inner ridge series described in geomorphological map (below) and the photograph showing the present conditions of both landforms in the field (above).

| Lithology | Layer contact | Thickness (cm) | Description |
|---|---|---|---|
| 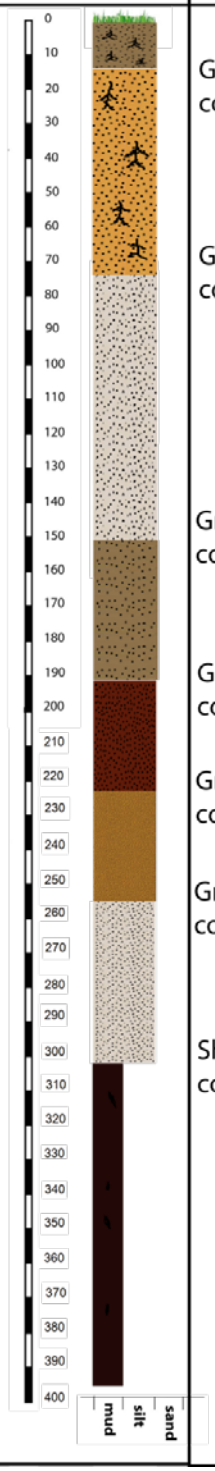 | Gradational contact | 13 | Organic sand ; fine sand; brownish black; rootlets. |
| | | 61 | Fine sand; brown; granules; rootlets. |
| | Gradational contact | | |
| | | 76 | Fine sand; light brown. |
| | Gradational contact | | |
| | | 40 | Fine sand; brown. |
| | Gradational contact | | |
| | | 33 | Fine sand; reddish brown. |
| | Gradational contact | | |
| | | 34 | Fine sand; brown. |
| | Gradational contact | | |
| | | 45 | Fine sand; light brown. |
| | Sharp contact | | |
| | | 95 | Mud; black; chacoal fragment. |



**Figure 3.3** The lithological log of inner most old beach sand at station T1-PN1.

### 3.2.1.2 Young sandy beach in station T1-PN13 at Ban Kho Son.

The location of T1-PN13 at young sandy beach was found at UTM grid of 525529 E 1156257 N on map sheet number 4829 IV (Amphoe Muang Chumphon). The recent beach is at Aao Pak Had as shown in Figure 3.4. The total depth of the core is 180 cm. It can be classified as 3 layers and shell fragments were also recognized as shown in Figure 3.5.

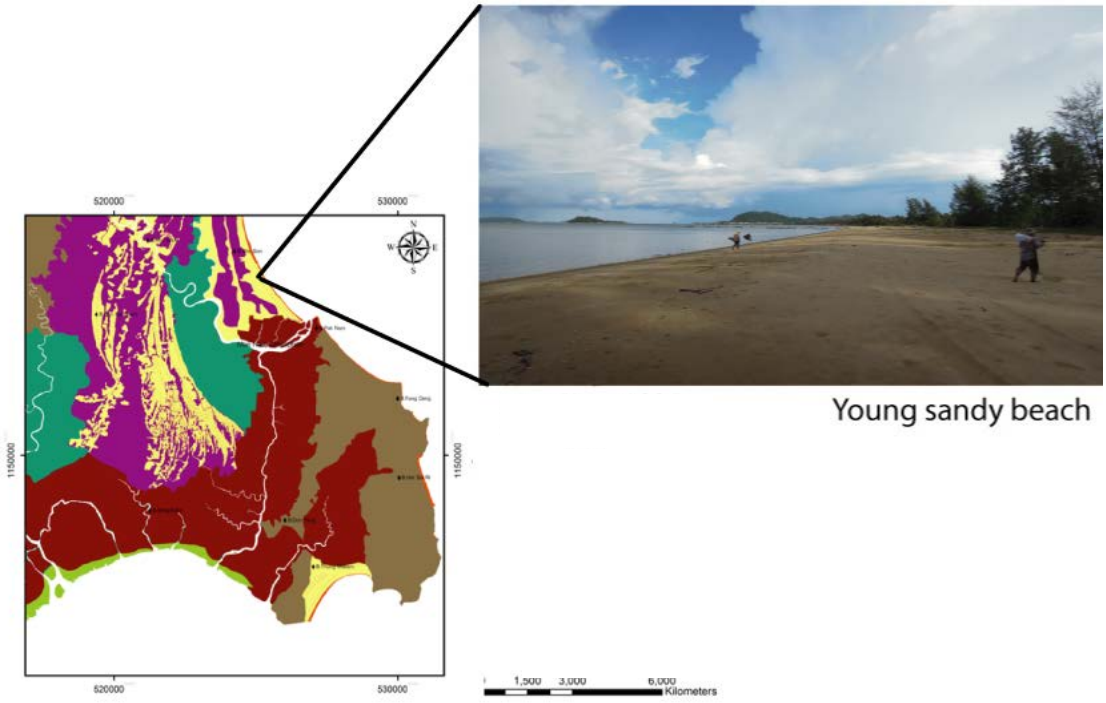


**Figure 3.4** Young sandy beach at Ban Kho Son where it is gentle slope to seaward.

| Lithology | Layer contact | Thickness (cm) | Description |
|---|---|---|---|
| 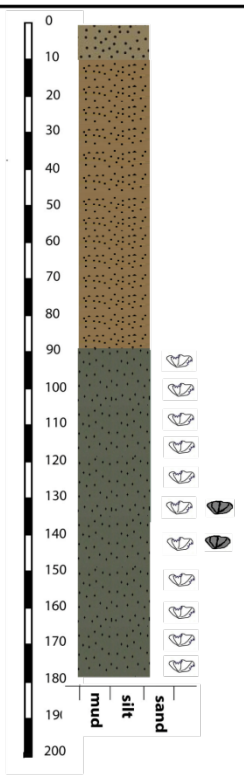  | Gradational contact<br><br>Gradational contact | 10<br><br>80<br><br>80 | Fine sand; light brown.<br><br>Fine sand; brown.<br><br>Fine sand; grey to greenish gray with shell fragments. |

**Figure 3.5** The lithological log of young sandy beach at station T1-PN13.

### 3.2.1.3 Old tidal flat in station T1-PN11 at Klong Bang Phara.

The location of T1-PN11 at old tidal flat is located at UTM grid of 522744 E 1154770 N on map sheet number 4829 IV (Amphoe Muang Chumphon). Old tidal flat in this station is drilled at Klong Bang Phara that connects to Chumphon River in the north of the study area shown in Figure 3.6. The total depth of the core is the 270 cm. It can be divided into 4 layers and shell fragments, shell as bivalve and gastropod were found and shown in Figure 3.7. Peats are also recognized that possibly indicates the stability and growth of marshes at or near sea level (Larson, Morang and Gorman, 1997).

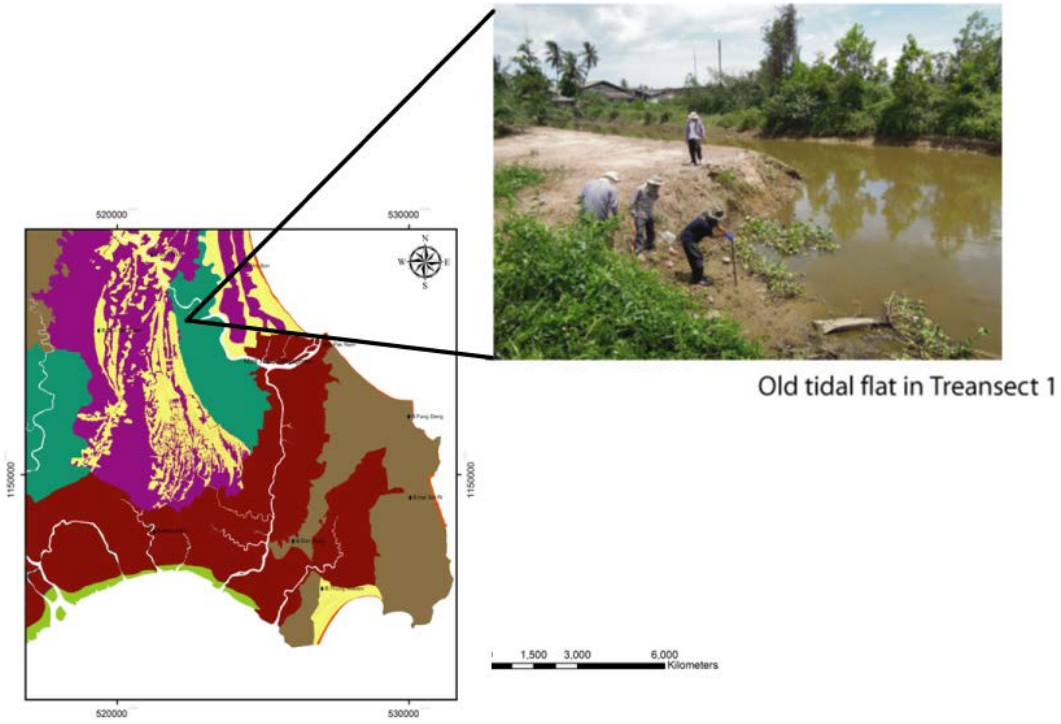


**Figure 3.6** Location where the old tidal flat locates in the geomorphological map (left). The present condition of old tidal flat (top right picture) and general composition of tidal flat containing mainly of gray-dark gray mud with both complete shell and fragments (bottom right picture).

| Lithology | Layer contact | Thickness (cm) | Description |
|---|---|---|---|
| 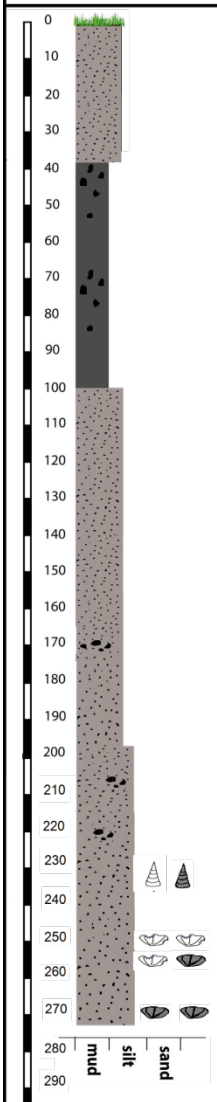 | Sharp contact | 38 | Muddy sand; greyish black with greenish grey mottle. |
| | Gradational contact | 62 | Mud; brownish black with peat fragment approximately 70%. |
| | | 100 | Muddy sand; brownish black with some peat fragment. |
| | Gradational contact | 70 | Sandy mud; brownish black to grey; with some peat fragment; shell fragment size 2-3 mm. and complete shell (bivalve and gastropod. |

**Figure 3.7** The lithological log of old tidal flat at station T1-PN11.

### 3.2.1.4 Old lagoon (swale) in station T1-PN2

The location of T1-PN2 at old lagoon is found at UTM grid of 519649 E 1153504 N on map sheet number 4829 IV (Amphoe Muang Chumphon). The total depth of the core is the 190 cm. It can be divided into 2 layers. The upper part of the profile was recorded to have disturbed by local people and partly borrowed by animal as shown in Figure 3.9.

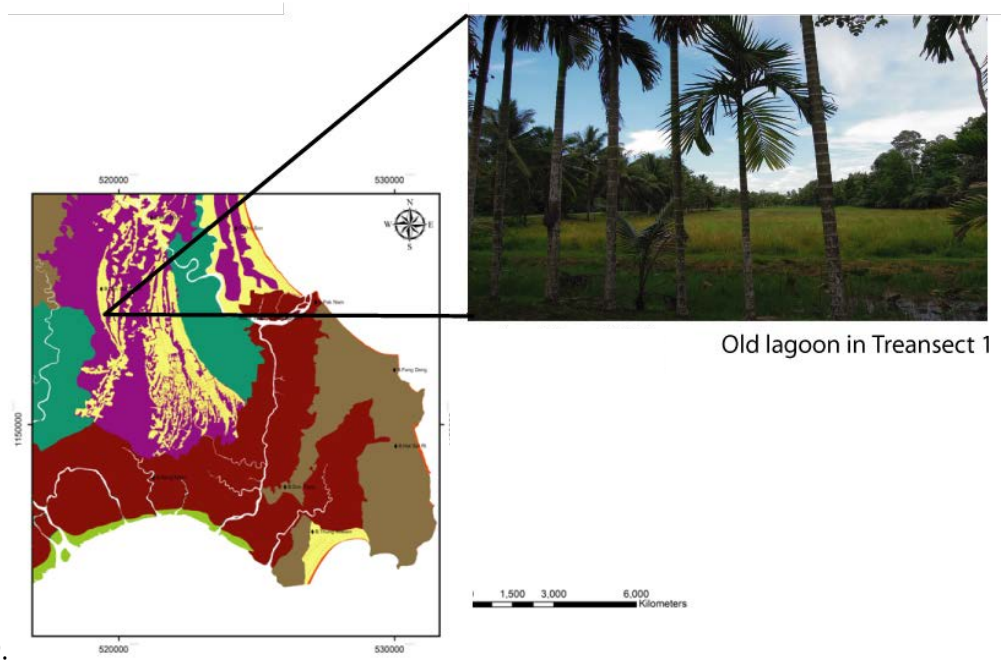


3.9.

**Figure 3.8** Location of old lagoon in coastal geomorphological map (left) that commonly locate between old sandy beaches. Present condition of the old lagoon area in the field (picture in top right).

| Lithology | Layer contact | Thickness (cm) | Description |
|---|---|---|---|
| 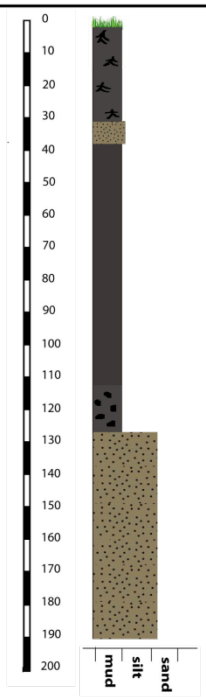  | disturbed 50-60 cm. | 126 | Mud; brownish grey to grey; contaminated with sandy mud . in the bottom of layer found peat fragment. |
| | Gradational contact | 64 | Fine sand; grey. |

**Figure 3.9** The lithological log of old lagoon at station T1-PN2.

## 3.3 Physical properties of sediments

### 3.3.1 Grain size analysis

As described in chapter 2, the standard sieves at 1phi ($\phi$) unit interval was applied to this study. Phi defines negative logarithm of the grain dimension in millimeters to the base 2. The equation for the relationship of millimeters to phi scale (Larson et al., 1997) is described as following equation:

$$(\phi) = -\log_2 (d)$$

Where $d_{mm}$ = particle diameter in millimeters

Standard grain size distribution statistic (Larson et al., 1997) includes as follows:

- Mean grain size or average grain size
- Standard deviation or the spread of the distribution about the mean – define concept of sorting
- Skewness or measure of symmetry of the distribution around mean
- Kurtosis or measure of the peakness of the frequency distribution

Each of those above statistical parameters will help to provide information on the grain-size distribution and its depositional environment. Textural attributes of sediment parameter as mean, standard deviation, skewness and kurtosis are widely used to reconstruct the depositional environments of sediments. In this research, plotting of those statistic parameters can be separated into 4 groups based on different geographical position of landforms as inner ridge series, middle ridge series, outer ridge series and recent beach as shown in Tables 3.1, 3.2, 3.3 and 3.4.

At the inner ridge series, mean grain size is characterized as very fine to medium sand with moderately to moderately well sorted, coarse to fine skewed and very leptokurtic to very leptokurtic.

At the middle ridge series, mean grain size is described as medium sand moderately sorted, symmetrical to fine skewed and very leptokurtic.

At the outer ridge series, mean grain sized is classified as fine sand moderately to moderately well sorted, coarse to symmetrical skewed and very mesokurtic to leptokurtic.

Recent beach is dominated by fine sand with moderately to moderately well sorted, coarse to symmetrical skewed and leptokurtic. Results from sieve analysis with all statistic parameters are shown Table 3.5.

**Table 3.1** Result of grain size analysis of former sand sediment in inner ridge series.

| BH | Mean (1st moment) | Standard deviation (2nd moment) | Skewness (3rd moment) | Kurtosis (4th moment) | Mean Grain size | Sorting | Skewness | Kurtosis |
|---|---|---|---|---|---|---|---|---|
| T1-PN1-1 | 2.41 | 1.24 | -2.76 | 14.55 | Fine sand | Poorly sorted | Very coarse skewed | Very leptokurtic |
| T1-PN1-2 | 2.54 | 0.65 | 0.07 | 10.86 | Fine sand | Moderately well sorted | Symmetrical | Very leptokurtic |
| T1-PN1-3 | 2.45 | 0.51 | 0.02 | 10.53 | Fine sand | Moderately well sorted | Symmetrical | Very leptokurtic |
| T1-PN1-5 | 2.52 | 0.31 | 1.92 | 21.17 | Fine sand | Very well sorted | Very fine skewed | Very leptokurtic |
| T1-PN1-7 | 2.49 | 0.37 | 0.86 | 14.37 | Fine sand | well sorted | Symmetrical | Very leptokurtic |
| T1-PN1-9 | 2.44 | 0.54 | -4.79 | 52.05 | Fine sand | Moderately well sorted | Very coarse skewed | Very leptokurtic |
| T1-PN1-11 | 2.42 | 0.51 | -1.18 | 10.45 | Fine sand | Moderately well sorted | Very coarse skewed | Very leptokurtic |
| T1-PN1-14 | 2.40 | 0.47 | -0.44 | 7.27 | Fine sand | well sorted | Coarse skewed | Leptokurtic |
| | | | | | | | | |
| T1-PN3-1 | 2.31 | 0.75 | 0.04 | 5.57 | Fine sand | Moderately sorted | Symmetrical | Leptokurtic |
| T1-PN3-2 | 2.31 | 0.70 | -0.04 | 5.72 | Fine sand | Moderately well sorted | Symmetrical | Leptokurtic |
| T1-PN3-3 | 2.27 | 0.66 | -0.24 | 6.10 | Fine sand | Moderately well sorted | Symmetrical | Leptokurtic |
| T1-PN3-6 | 2.30 | 0.58 | -0.34 | 6.48 | Fine sand | Moderately well sorted | Symmetrical | Leptokurtic |
| T1-PN3-9 | 2.25 | 0.76 | -0.58 | 5.17 | Fine sand | Moderately sorted | Coarse skewed | Leptokurtic |
| T1-PN3-11 | 2.28 | 0.58 | -0.91 | 6.17 | Fine sand | Moderately well sorted | Coarse skewed | Leptokurtic |
| | | | | | | | | |
| T1-PN5-1 | 1.90 | 0.84 | 0.62 | 6.60 | Medium Sand | Moderately sorted | Fine skewed | Leptokurtic |
| T1-PN5-4 | 1.85 | 0.71 | 1.12 | 5.76 | Medium Sand | Moderately sorted | Fine skewed | Leptokurtic |
| T1-PN5-6 | 1.80 | 0.66 | 1.25 | 6.43 | Medium Sand | Moderately well sorted | Fine skewed | Leptokurtic |
| T1-PN5-8 | 1.73 | 0.61 | 0.59 | 5.76 | Medium Sand | Moderately well sorted | Fine skewed | Leptokurtic |
| T1-PN5-11 | 1.65 | 0.68 | 0.84 | 6.32 | Medium Sand | Moderately well sorted | Fine skewed | Leptokurtic |
| T1-PN5-13 | 1.58 | 0.73 | 0.10 | 4.79 | Medium Sand | Moderately sorted | Symmetrical | Leptokurtic |
| T1-PN5-15 | 1.88 | 0.82 | -0.29 | 3.88 | Medium Sand | Moderately sorted | Symmetrical | Leptokurtic |
| | | | | | | | | |
| T2-PN2-1 | 2.23 | 0.83 | 0.55 | 4.29 | Fine sand | Moderately sorted | Fine skewed | Leptokurtic |
| T2-PN2-3 | 2.17 | 0.72 | -0.77 | 7.01 | Fine sand | Moderately sorted | Coarse skewed | Leptokurtic |
| T2-PN2-6 | 2.19 | 0.79 | -0.73 | 7.05 | Coarse sand | Moderately sorted | Coarse skewed | Leptokurtic |
| T2-PN2-7 | 1.95 | 1.05 | -1.67 | 8.53 | Medium Sand | Poorly sorted | Very coarse skewed | Very leptokurtic |
| T2-PN2-8 | 0.02 | 2.40 | -0.30 | 2.04 | Fine sand | Very poorly sorted | Symmetrical | Platykurtic |
| | | | | | | | | |
| T2-PN3-1 | 2.53 | 0.92 | 0.13 | 3.37 | Fine sand | Moderately sorted | Symmetrical | Mesokurtic |
| T2-PN3-3 | 2.39 | 0.86 | 0.03 | 3.39 | Fine sand | Moderately sorted | Symmetrical | Mesokurtic |
| T2-PN3-5 | 2.30 | 0.81 | -0.02 | 4.22 | Fine sand | Moderately sorted | Symmetrical | Leptokurtic |
| T2-PN3-7 | 2.84 | 0.63 | 0.37 | 4.08 | Fine sand | Moderately well sorted | Symmetrical | Leptokurtic |
| T2-PN3-8 | 3.22 | 0.61 | -1.01 | 5.89 | Very fine sand | Moderately well sorted | Coarse skewed | Leptokurtic |
| T2-PN3-9 | 2.41 | 1.00 | -1.42 | 9.17 | Fine sand | Moderately sorted | Very coarse skewed | Very leptokurtic |

**Table 3.2** Result of grain size analysis of former sand sediment in middle ridge series.

| BH | Mean (1st moment) | andard deviati (2nd moment) | Skewness (3rd moment) | Kurtosis (4th moment) | Mean Grain size | Sorting | Skewness | Kurtosis |
|---|---|---|---|---|---|---|---|---|
| T1-PN6-1 | 2.27 | 0.66 | -0.24 | 6.09 | Fine sand | Moderately well sorted | Symmetrical | Leptokurtic |
| T1-PN6-3 | 1.71 | 0.86 | 0.61 | 4.43 | Medium Sand | Moderately sorted | Fine skewed | Leptokurtic |
| T1-PN6-4 | 1.70 | 0.81 | 0.03 | 4.09 | Medium Sand | Moderately sorted | Symmetrical | Leptokurtic |
| T1-PN6-7 | 1.66 | 0.76 | 0.20 | 3.96 | Medium Sand | Moderately sorted | Symmetrical | Leptokurtic |
| | | | | | | | | |
| T1-PN8-2 | 2.19 | 0.85 | 0.37 | 3.91 | Fine sand | Moderately sorted | Symmetrical | Leptokurtic |
| T1-PN8-5 | 1.97 | 0.78 | 0.10 | 3.83 | Medium Sand | Moderately sorted | Symmetrical | Leptokurtic |
| T1-PN8-9 | 2.16 | 0.89 | -0.13 | 4.12 | Fine sand | Moderately sorted | Symmetrical | Leptokurtic |
| | | | | | | | | |
| T1-PN9-1 | 2.09 | 0.86 | 0.56 | 4.27 | Fine sand | Moderately sorted | Fine skewed | Leptokurtic |
| T1-PN9-4 | 1.99 | 0.79 | 0.42 | 4.38 | Medium Sand | Moderately sorted | Symmetrical | Leptokurtic |
| T1-PN9-8 | 1.63 | 1.02 | -0.15 | 3.45 | Medium Sand | Poorly sorted | Symmetrical | Mesokurtic |
| T1-PN9-10 | 2.40 | 0.76 | 0.08 | 5.55 | Fine sand | Moderately sorted | Symmetrical | Leptokurtic |
| | | | | | | | | |
| T2-PN4-1 | 1.70 | 0.93 | 0.62 | 4.04 | Medium Sand | Moderately sorted | Fine skewed | Leptokurtic |
| T2-PN4-2 | 1.65 | 0.85 | 0.51 | 4.11 | Medium Sand | Moderately sorted | Fine skewed | Leptokurtic |
| T2-PN4-4 | 1.66 | 0.81 | 0.44 | 4.23 | Medium Sand | Moderately sorted | Fine skewed | Leptokurtic |
| T2-PN4-5 | 1.64 | 0.83 | 0.35 | 4.07 | Medium Sand | Moderately sorted | Symmetrical | Leptokurtic |
| T2-PN4-6 | 1.52 | 0.80 | 0.56 | 4.90 | Medium Sand | Moderately sorted | Fine skewed | Leptokurtic |
| | | | | | | | | |
| T2-PN5-1 | 1.59 | 0.85 | 0.18 | 3.97 | Medium Sand | Moderately sorted | Symmetrical | Leptokurtic |
| T2-PN5-4 | 1.28 | 0.83 | 0.45 | 4.70 | Medium Sand | Moderately sorted | Fine skewed | Leptokurtic |
| T2-PN5-7 | 1.49 | 0.64 | 0.91 | 7.28 | Medium Sand | Moderately well sorted | Fine skewed | Leptokurtic |
| T2-PN5-8 | 1.59 | 0.85 | 0.18 | 3.97 | Medium Sand | Moderately sorted | Symmetrical | Leptokurtic |
| | | | | | | | | |
| T2-PN6-1 | 1.71 | 0.79 | 0.56 | 4.90 | Medium Sand | Moderately sorted | Fine skewed | Leptokurtic |
| T2-PN6-3 | 1.67 | 0.74 | 0.61 | 5.22 | Medium Sand | Moderately sorted | Fine skewed | Leptokurtic |
| T2-PN6-5 | 1.73 | 0.71 | 0.43 | 4.93 | Medium Sand | Moderately sorted | Symmetrical | Leptokurtic |
| T2-PN6-7 | 1.52 | 0.83 | 0.43 | 4.46 | Medium Sand | Moderately sorted | Symmetrical | Leptokurtic |
| | | | | | | | | |
| T3-PN3-1 | 1.98 | 0.92 | 0.76 | 3.50 | Medium Sand | Moderately sorted | Fine skewed | Mesokurtic |
| T3-PN3-4 | 1.90 | 0.85 | 0.83 | 4.00 | Medium Sand | Moderately sorted | Fine skewed | Leptokurtic |
| T3-PN3-6 | 1.79 | 0.72 | 0.73 | 4.39 | Medium Sand | Moderately sorted | Fine skewed | Leptokurtic |
| T3-PN3-7 | 1.72 | 0.72 | 0.66 | 4.50 | Medium Sand | Moderately sorted | Fine skewed | Leptokurtic |
| T3-PN3-9 | 1.50 | 0.78 | 0.90 | 4.92 | Medium Sand | Moderately sorted | Fine skewed | Leptokurtic |
| T3-PN3-11 | 2.66 | 0.79 | 0.10 | 4.02 | Fine sand | Moderately sorted | Symmetrical | Leptokurtic |

| BH | Mean (1st moment) | andard deviati (2nd moment) | Skewness (3rd moment) | Kurtosis (4th moment) | Mean Grain size | Sorting | Skewness |
|---|---|---|---|---|---|---|---|
| T3-PN4-1 | 1.83 | 1.22 | -2.18 | 13.99 | Medium Sand | Poorly sorted | Very coarse skewed |
| T3-PN4-2 | 1.97 | 0.83 | 0.31 | 3.73 | Medium Sand | Moderately sorted | Symmetrical |
| T3-PN4-4 | 1.88 | 0.82 | 0.34 | 3.89 | Medium Sand | Moderately sorted | Symmetrical |
| T3-PN4-7 | 2.32 | 0.69 | -0.76 | 6.53 | Fine sand | Moderately well sorted | Coarse skewed |
| T3-PN4-10 | 2.17 | 0.85 | 0.19 | 4.60 | Fine sand | Moderately sorted | Symmetrical |
| T3-PN4-12 | 2.53 | 0.73 | 0.04 | 6.52 | Fine sand | Moderately sorted | Symmetrical |
| | | | | | | | |
| T3-PN5-1 | 2.07 | 0.76 | 0.43 | 5.05 | Fine sand | Moderately sorted | Symmetrical |
| T3-PN5-3 | 1.94 | 0.74 | 0.30 | 4.26 | Medium Sand | Moderately sorted | Symmetrical |
| T3-PN5-5 | 1.84 | 0.74 | -0.07 | 4.88 | Medium Sand | Moderately sorted | Symmetrical |
| T3-PN5-8 | 2.35 | 0.74 | -0.25 | 5.69 | Fine sand | Moderately sorted | Symmetrical |
| T3-PN5-10 | 2.29 | 0.94 | -0.18 | 4.32 | Fine sand | Moderately sorted | Symmetrical |

**Table 3.3** Result of grain size analysis of former sand sediment in outer ridge series.

| BH | Mean (1st moment) | andard deviati (2nd moment) | Skewness (3rd moment) | Kurtosis (4th moment) | Mean Grain size | Sorting | Skewness | Kurtosis |
|---|---|---|---|---|---|---|---|---|
| T1-PN1-1 | 2.41 | 1.24 | -2.76 | 14.55 | Fine sand | Poorly sorted | Very coarse skewed | Very leptokurtic |
| T1-PN1-2 | 2.54 | 0.65 | 0.07 | 10.86 | Fine sand | Moderately well sorted | Symmetrical | Very leptokurtic |
| T1-PN1-3 | 2.45 | 0.51 | 0.02 | 10.53 | Fine sand | Moderately well sorted | Symmetrical | Very leptokurtic |
| T1-PN1-5 | 2.52 | 0.31 | 1.92 | 21.17 | Fine sand | Very well sorted | Very fine skewed | Very leptokurtic |
| T1-PN1-7 | 2.49 | 0.37 | 0.86 | 14.37 | Fine sand | well sorted | Symmetrical | Very leptokurtic |
| T1-PN1-9 | 2.44 | 0.54 | -4.79 | 52.05 | Fine sand | Moderately well sorted | Very coarse skewed | Very leptokurtic |
| T1-PN1-11 | 2.42 | 0.51 | -1.18 | 10.45 | Fine sand | Moderately well sorted | Very coarse skewed | Very leptokurtic |
| T1-PN1-14 | 2.40 | 0.47 | -0.44 | 7.27 | Fine sand | well sorted | Coarse skewed | Leptokurtic |
| | | | | | | | | |
| T1-PN3-1 | 2.31 | 0.75 | 0.04 | 5.57 | Fine sand | Moderately sorted | Symmetrical | Leptokurtic |
| T1-PN3-2 | 2.31 | 0.70 | -0.04 | 5.72 | Fine sand | Moderately well sorted | Symmetrical | Leptokurtic |
| T1-PN3-3 | 2.27 | 0.66 | -0.24 | 6.10 | Fine sand | Moderately well sorted | Symmetrical | Leptokurtic |
| T1-PN3-6 | 2.30 | 0.58 | -0.34 | 6.48 | Fine sand | Moderately well sorted | Symmetrical | Leptokurtic |
| T1-PN3-9 | 2.25 | 0.76 | -0.58 | 5.17 | Fine sand | Moderately sorted | Coarse skewed | Leptokurtic |
| T1-PN3-11 | 2.28 | 0.58 | -0.91 | 6.17 | Fine sand | Moderately well sorted | Coarse skewed | Leptokurtic |
| | | | | | | | | |
| T1-PN5-1 | 1.90 | 0.84 | 0.62 | 6.60 | Medium Sand | Moderately sorted | Fine skewed | Leptokurtic |
| T1-PN5-4 | 1.85 | 0.71 | 1.12 | 5.76 | Medium Sand | Moderately sorted | Fine skewed | Leptokurtic |
| T1-PN5-6 | 1.80 | 0.66 | 1.25 | 6.43 | Medium Sand | Moderately well sorted | Fine skewed | Leptokurtic |
| T1-PN5-8 | 1.73 | 0.61 | 0.59 | 5.76 | Medium Sand | Moderately well sorted | Fine skewed | Leptokurtic |
| T1-PN5-11 | 1.65 | 0.68 | 0.84 | 6.32 | Medium Sand | Moderately well sorted | Fine skewed | Leptokurtic |
| T1-PN5-13 | 1.58 | 0.73 | 0.10 | 4.79 | Medium Sand | Moderately sorted | Symmetrical | Leptokurtic |
| T1-PN5-15 | 1.88 | 0.82 | -0.29 | 3.88 | Medium Sand | Moderately sorted | Symmetrical | Leptokurtic |
| | | | | | | | | |
| T2-PN2-1 | 2.23 | 0.83 | 0.55 | 4.29 | Fine sand | Moderately sorted | Fine skewed | Leptokurtic |
| T2-PN2-3 | 2.17 | 0.72 | -0.77 | 7.01 | Fine sand | Moderately sorted | Coarse skewed | Leptokurtic |
| T2-PN2-6 | 2.19 | 0.79 | -0.73 | 7.05 | Coarse sand | Moderately sorted | Coarse skewed | Leptokurtic |
| T2-PN2-7 | 1.95 | 1.05 | -1.67 | 8.53 | Medium Sand | Poorly sorted | Very coarse skewed | Very leptokurtic |
| T2-PN2-8 | 0.02 | 2.40 | -0.30 | 2.04 | Fine sand | Very poorly sorted | Symmetrical | Platykurtic |
| | | | | | | | | |
| T2-PN3-1 | 2.53 | 0.92 | 0.13 | 3.37 | Fine sand | Moderately sorted | Symmetrical | Mesokurtic |
| T2-PN3-3 | 2.39 | 0.86 | 0.03 | 3.39 | Fine sand | Moderately sorted | Symmetrical | Mesokurtic |
| T2-PN3-5 | 2.30 | 0.81 | -0.02 | 4.22 | Fine sand | Moderately sorted | Symmetrical | Leptokurtic |
| T2-PN3-7 | 2.84 | 0.63 | 0.37 | 4.08 | Fine sand | Moderately well sorted | Symmetrical | Leptokurtic |
| T2-PN3-8 | 3.22 | 0.61 | -1.01 | 5.89 | Very fine sand | Moderately well sorted | Coarse skewed | Leptokurtic |
| T2-PN3-9 | 2.41 | 1.00 | -1.42 | 9.17 | Fine sand | Moderately sorted | Very coarse skewed | Very leptokurtic |

| BH | Mean (1st moment) | Standard deviation (2nd moment) | Skewness (3rd moment) | Kurtosis (4th moment) | Mean Grain size | Sorting | Skewness | Kurtosis |
|---|---|---|---|---|---|---|---|---|
| T3-PN9-1 | 2.21 | 0.63 | -0.02 | 5.09 | Fine sand | Moderately well sorted | Symmetrical | Leptokurtic |
| T3-PN9-3 | 2.22 | 0.56 | -0.54 | 5.65 | Fine sand | Moderately well sorted | Coarse skewed | Leptokurtic |
| T3-PN9-4 | 1.95 | 0.74 | -0.05 | 3.81 | Medium Sand | Moderately sorted | Symmetrical | Leptokurtic |
| T3-PN9-5 | 2.02 | 0.63 | 0.28 | 4.14 | Fine sand | Moderately well sorted | Symmetrical | Leptokurtic |
| T3-PN9-8 | 2.11 | 0.68 | -0.31 | 4.47 | Fine sand | Moderately well sorted | Symmetrical | Leptokurtic |
| T3-PN9-11 | 1.99 | 0.86 | 0.51 | 3.97 | Medium Sand | Moderately sorted | Fine skewed | Leptokurtic |

**Table 3.4** Result of grain size analysis of recent beach sand sediment.

| BH | Mean (1st moment) | Standard deviation (2nd moment) | Skewness (3rd moment) | Kurtosis (4th moment) | Mean Grain size | Sorting | Skewness | Kurtosis |
|---|---|---|---|---|---|---|---|---|
| T1-PN13-1 | 2.11 | 0.57 | -0.81 | 5.58 | Fine sand | Moderately well sorte | Coarse skewed | Leptokurtic |
| T1-PN13-3 | 2.14 | 0.59 | 0.07 | 2.92 | Fine sand | Moderately well sorte | Symmetrical | Mesokurtic |
| T1-PN13-7 | 2.35 | 0.71 | -1.80 | 11.98 | Fine sand | Moderately sorted | Very coarse skewe | Very leptokurtic |

**Table 3.5** Summary of sieve parameter in the study area as inner ridge, middle ridge, outer ridge and recent beach**.**

| Alignment of ridge | Mean grain size | Sorting | Skewness | Kurtosis |
|---|---|---|---|---|
| **Inner ridges** | Fine to medium sand | Moderately to Moderately well sorted | Coarse to fine skewed | Leptokurtic to very leotokurtic |
| **Middle ridges** | Medium sand | Moderately sorted | Symmetrical to fine skewed | Leptokurtic |
| **Outer ridges** | Fine to medium sand | Moderately to Moderately well sorted | Coarse to symmetrical skewed | Mesokurtic to leptokurtic |
| **Recent Beach** | Fine sand | Moderately to Moderately well sorted | Coarse to symmetrical skewed | Leptokurtic |

Grain size analysis by dry sieving is applied in each layer of beach sediment in different location. Interpretation of grain size parameter as mean, standard deviation, skewness and kurtosis has been done. To understand the geological significance of the four size parameter, it is necessary to plot them against each other in turn as scatter diagrams (Folk and Ward, 1957).

All 6 two-variable scatter plots are Mean Size versus Standard Deviation, Mean Size versus Skewness, Mean Size versus Kurtosis, Standard Deviation versus Skewness, Standard Deviation versus Kurtosis and Skewness versus Kurtosis. All of 6 scatter plot, sand sample in inner ridge distribution is wider than the others.

Possible geological significance can be interpreted from of sorting versus skewness. Some of sand sediments in outer ridge and inner ridge showed extreme kurtosis value and good sorting (Figure 3.14) that indicated in neritic sediments. Extreme kurtosis values are common because the sand mode achieves good sorting in the high energy environment of the beach, and then, it is transported mass by storm to the neritic environment where it becomes mixed with clay and hence is finally deposited in a medium of low sorting efficiency (Folk and Ward, 1957).

Mean Size versus Standard Deviation - generally plots of this type give a great amount of information about environment. These samples have mean size between medium sand and fine sand mode. Sorting value is dense at moderately to moderately well sorted (Folk and Ward, 1957). It can be concluded that sand sediment is produced on the beach (in middle, outer ridge and recent beach.) Inner ridge be dissimilar from other its can deduce that sediment deposit from different type of source. Mean Size versus Standard Deviation plot show in Figure 3.10.

Mean Size versus Skewness –In this unimodal sediment, it compose of pure sand mode. The sand mode abundant show positive skewed. Scatter plot of mean size versus standard deviation shows in Figure 3.11.

Mean Size versus Kurtosis –This relationship is complex. Almost sediment samples are classified as leptokurtic. It is good sorting in the central part but the sorting in the tail is worsened. Scatter plot of Mean Size versus Skewness shows in Figure 3.12.

Standard Deviation versus Skewness – It is evident that if standard deviation is a function of mean size, and if skewness is also a function of mean size, then sorting and skewness will be a mathematic relation to each other. However, the exact nature of their relation was a great surprise: the two variables form a scatter trend in the form of a nearly circular ring. The reason become obvious on a moment's thought, however; symmetrical curve may be obtained unimodal sample with good sorting. These show moderate sorting and the skewness can be either positive or negative (Folk and Ward, 1957). Scatter plot of Standard Deviation versus Skewness shows in Figure 3.13.

Standard Deviation versus Kurtosis – Highest kurtosis is found in those samples with one mode dominant and the other very subordinate. These have moderate sorting. Unimodal sediments produce normal kurtosis and are best sorted. Scatter plot of Standard Deviation versus Kurtosis shows in Figure 3.14.

Skewness versus Kurtosis – A regular path is followed on the skewness versus kurtosis. Almost sediment samples are classified as fine to coarse skewed and mesokurtic to leptokurtic kurtosis. Half of all sediment samples are characteristically leptokurtic and positive skewed sediments. They indicated sediments are transported near the sort of the sand in red oval dash line (Folk and Ward, 1957). Scatter plot of Skewness versus Kurtosis shows in Figure 3.14.

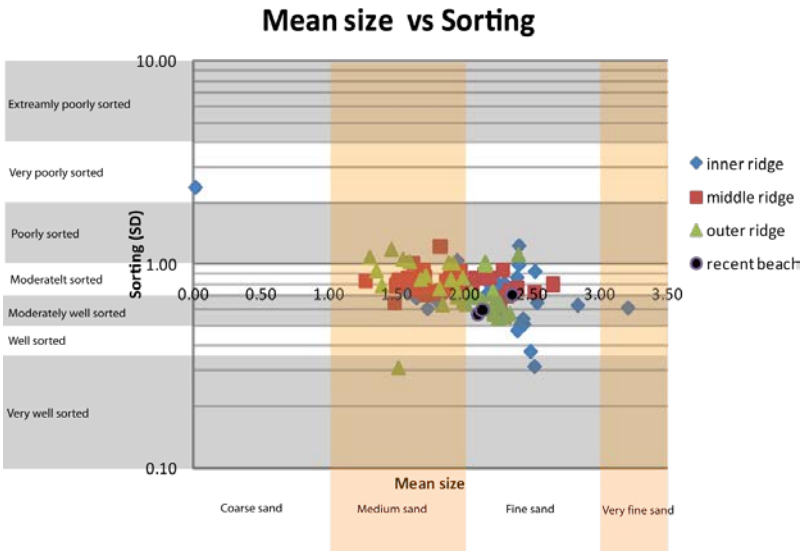


**Figure 3.10** Scatter plot of mean size versus standard deviation (sorting). It is narrow range of grain size (very fine to coarse sand). Sediments are medium to fine sand and moderately to moderately well sorted that indicate beach sediment (diagram is modified from Folk and Ward, 1957).

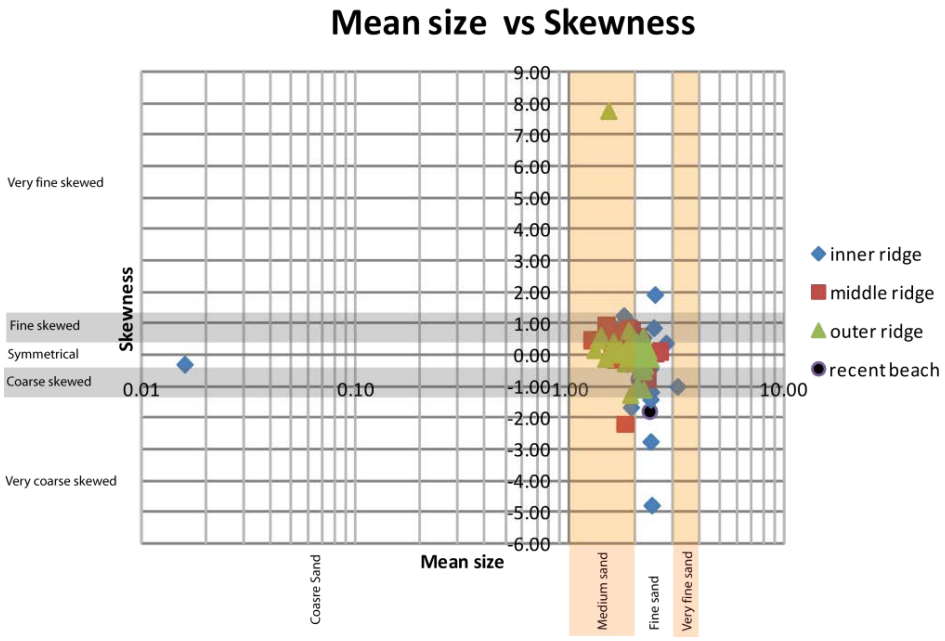


**Figure 3.11** Scatter plot of mean size versus skewness. Almost samples are classified as coarse to fine skewed (diagram is modified from Folk and Ward, 1957).

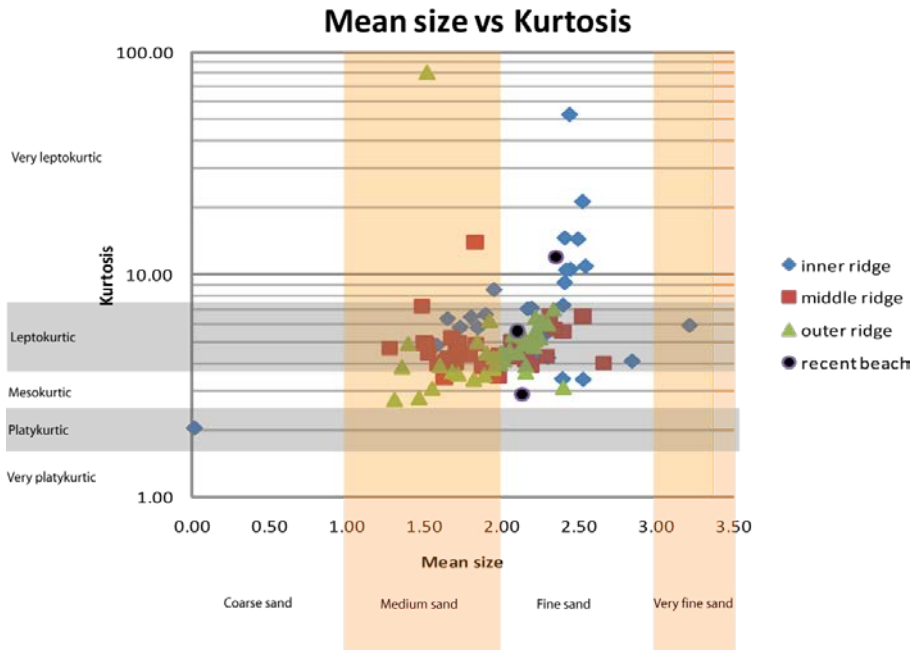


**Figure 3.12** Scatter plot of mean size versus kurtosis. Almost sediment samples are classified as leptokurtic (diagram is modified from Folk and Ward, 1957).

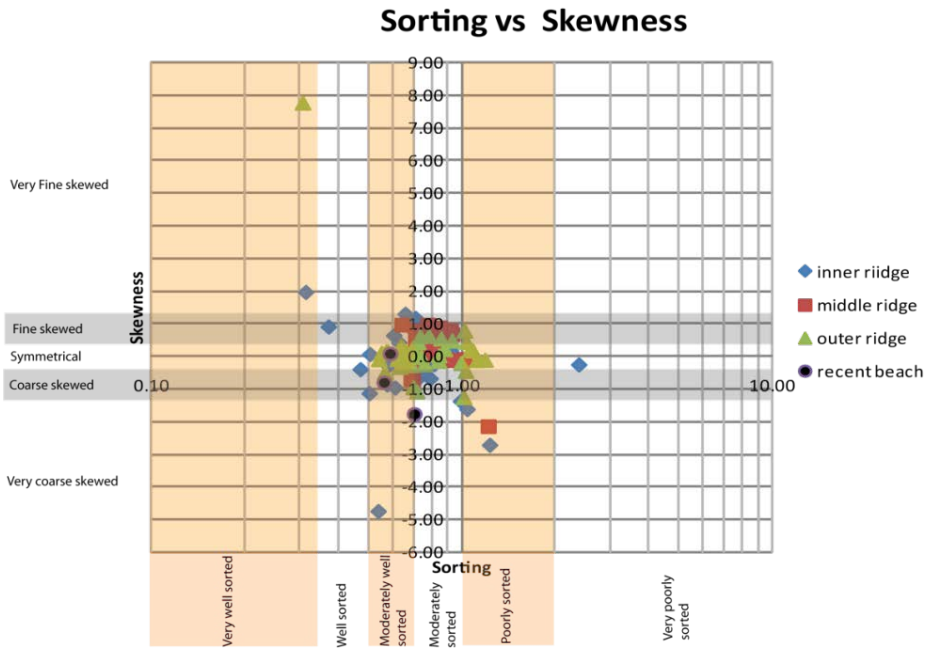


**Figure 3.13** Scatter plot of standard deviation (sorting) versus skewness. Almost sediment samples are classified as coarse to fine skewed and moderately to moderately well sorted (diagram is modified from Folk and Ward, 1957).

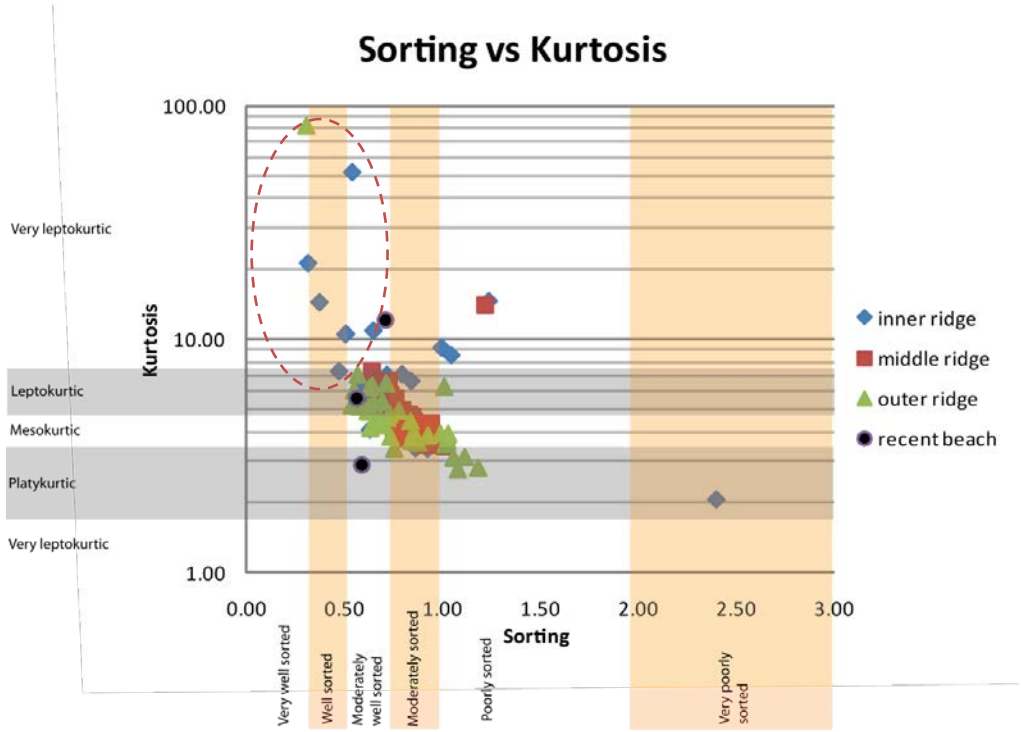


**Figure 3.14** Scatter plot of standard deviation (sorting) versus kurtosis. Almost sediment samples are classified as leptokurtic to mesokurtic. Some of sand sediments in outer ridge and inner ridge (red oval dash line) showed extreme kurtosis value and good sorting. That indicated in neritic sediments, extreme kurtosis values are common because the sand mode achieves good sorting in the high energy environment of the beach.

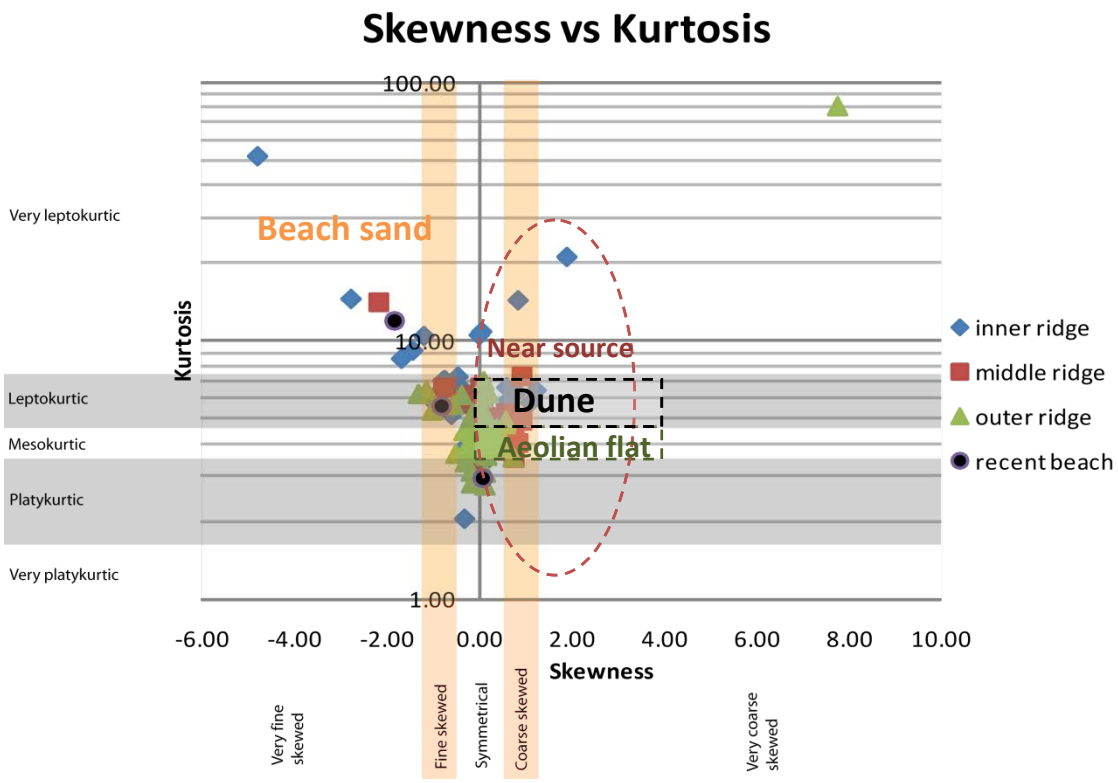


**Figure 3.15** Scatter plot of skewness versus kurtosis. Almost sediment samples are classified as fine to coarse skewed and mesokurtic to leptokurtic kurtosis. Half of all sediment samples are characteristically leptokurtic and positive skewed sediments. They indicated that sediments are transported near the sort of the sand in red oval dash line (Folk and Ward, 1957). Beach sands are normal or negative skewness and leptokurtic, dune sand have positive skewness and mesokurtic, Aeolian flat sand have positive skewed and leptokurtic. The beach sand is more poorly sorted than to other types. Beach sands generally have negative skewness (Martin, 1964).

### 3.3.2 Result of sediment compositions, roundness and sphericity.

This section describes the variation of composition of beach sediments. This result will be able to explain size fraction distribution that is determined by the composition of the source rock and weathering condition. In addition, variation of the mineralogy of sediment is controlled by source rock and weathering conditions. Resistant minerals, such as quartz and feldspars, comprise mostly in coastal deposit (Larson et al., 1997). Heavy minerals in sand can also provide useful information about the character of the source rocks (Rubey, 1933).

Average composition of old beach ridge in the Pak Nam Chumphon area is mainly composed of quartz. All beach ridge series, inner beach ridge series, middle beach ridge series and outer beach ridge series show similar composition of sand sediment, but in inner ridge minor composition are feldspar and ferromagnesian more than middle and outer ridge. Detail of sediment composition in each location exhibit in Table 3.6 and Figure 3.16. Mineral assemblage of ferromagnesian should be likely ilmenite and zircon but also contain notable amounts of leucoxene, rutile and garnet. That is reported in adjacent area at Bang Saphan to Khao Laem Yai area (Roy, 1990).

Roundness and sphericity of beach ridge sediment, sphericity value are the term of particle compactness and bladedness. In the study area, average roundness of inner ridge series is sub angular. Angular-sub angular is characterized by roundness trend of middle beach ridge series. Roundness trend from outer ridge series is sub angular. All of beach ridge sediments are high sphericity.

Based on composition of beach sand, sources of sand sediment in this coastal area may came from the mountains in the western and in the northern part of the area. Rock basements are composed of the Permo-carboniferous and Permian rocks. The weathered sediments from these rock basements were transport by active fluvial systems in the northeast of beach ridge and through coastal zone by longshore current (Thongpinyochai, 1996).

**Table 3.6** Composition of sediment from inner, middle and outer beach ridge series.

| Beach ridge | Sample number | Composition | | | | | | | |
|---|---|---|---|---|---|---|---|---|---|
| | | Quartz | Feldspar | Rock fragment | Mica | Skeleton debris | Ferromagnesian | Unknown | Other |
| Inner ridge | T1-PN1 | 95.71 | 2.20 | 0.56 | 0.00 | 0.00 | 1.53 | 0.00 | 0.00 |
| | T1-PN3 | 96.67 | 1.87 | 0.00 | 0.05 | 0.00 | 1.42 | 0.00 | 0.00 |
| | T1-PN5 | 98.00 | 1.81 | 0.00 | 0.00 | 0.00 | 0.19 | 0.00 | 0.00 |
| | T2-PN2 | 97.79 | 0.88 | 0.71 | 0.00 | 0.00 | 0.62 | 0.00 | 0.00 |
| | T2-PN3 | 98.66 | 0.03 | 0.16 | 0.02 | 0.00 | 1.12 | 0.00 | 0.00 |
| | Average | 97.37 | 1.36 | 0.29 | 0.01 | 0.00 | 0.98 | 0.00 | 0.00 |
| Middle ridge | T1-PN6 | 98.31 | 1.64 | 0.00 | 0.00 | 0.00 | 0.05 | 0.00 | 0.00 |
| | T1-PN8 | 98.02 | 1.90 | 0.00 | 0.00 | 0.00 | 0.13 | 0.00 | 0.00 |
| | T1-PN9 | 95.94 | 3.00 | 0.24 | 0.00 | 0.00 | 0.82 | 0.00 | 0.00 |
| | T2-PN4 | 99.51 | 0.03 | 0.04 | 0.01 | 0.00 | 0.42 | 0.00 | 0.00 |
| | T2-PN5 | 99.49 | 0.03 | 0.44 | 0.02 | 0.00 | 0.03 | 0.00 | 0.00 |
| | T2-PN6 | 97.18 | 2.33 | 0.34 | 0.01 | 0.00 | 0.15 | 0.00 | 0.00 |
| | T3-PN3 | 99.61 | 0.21 | 0.13 | 0.01 | 0.00 | 0.04 | 0.00 | 0.00 |
| | T3-PN4 | 99.52 | 0.04 | 0.38 | 0.04 | 0.00 | 0.03 | 0.00 | 0.00 |
| | T3-PN5 | 99.12 | 0.02 | 0.72 | 0.00 | 0.00 | 0.14 | 0.00 | 0.00 |
| | Average | 98.52 | 1.02 | 0.25 | 0.01 | 0.00 | 0.20 | 0.00 | 0.00 |
| Outer Ridge | T1-PN14 | 95.85 | 3.02 | 0.76 | 0.02 | 0.00 | 0.36 | 0.00 | 0.00 |
| | T2-PN1 | 97.65 | 1.96 | 0.02 | 0.01 | 0.00 | 0.36 | 0.00 | 0.00 |
| | T2-PN7 | 99.22 | 0.32 | 0.41 | 0.01 | 0.00 | 0.04 | 0.00 | 0.00 |
| | T2-PN9 | 98.60 | 0.12 | 0.58 | 0.00 | 0.00 | 0.70 | 0.00 | 0.00 |
| | T3-PN6 | 99.42 | 0.03 | 0.50 | 0.01 | 0.00 | 0.05 | 0.00 | 0.00 |
| | T3-PN7 | 99.89 | 0.01 | 0.06 | 0.01 | 0.00 | 0.02 | 0.00 | 0.00 |
| | T3-PN8 | 99.76 | 0.06 | 0.07 | 0.00 | 0.00 | 0.11 | 0.00 | 0.00 |
| | T3-PN9 | 99.78 | 0.02 | 0.09 | 0.00 | 0.00 | 0.10 | 0.00 | 0.00 |
| | Average | 98.77 | 0.69 | 0.31 | 0.01 | 0.00 | 0.22 | 0.00 | 0.00 |

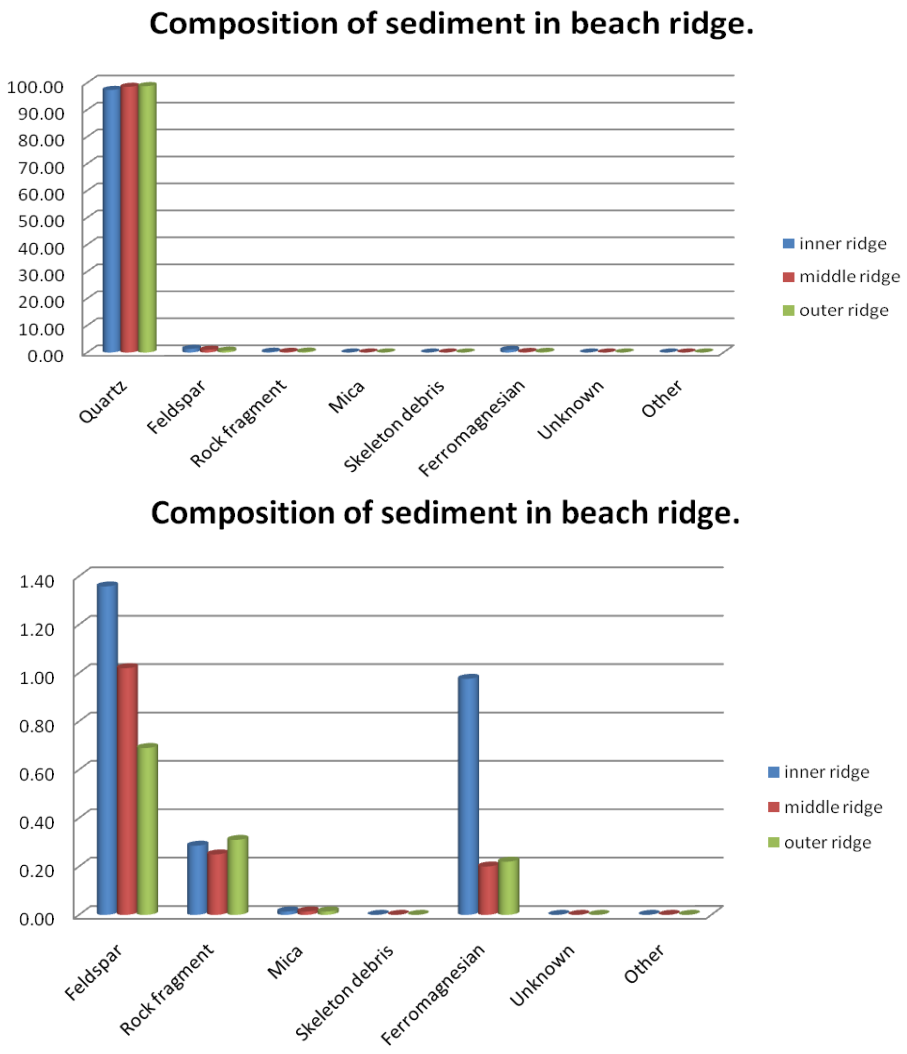


**Figure 3.16** Graph of sediment composition in inner, middle and outer beach ridge series. Major composition is quartz (above). In inner ridge, minor compositions are feldspar and ferromagnesian more than those recognized in the middle and outer ridges (below).

### 3.4 Age determination by thermoluminescence dating.

According to the main objective of this research, it is essential to age of deposition of beach ridges. The results of TL procedure from glow curve results, plateau test results, growth curve results, residual testing results and annual dose calculated from uranium, thorium and potassium content. Age determination of 23 beach ridge sand samples age as shown in Table 3.7 to 3.10 and Figure 3.17.

Inner beach ridges, the age of the deposition are in the range of 6,000-14,000 yr. Age of middle beach ridges are during 6,800-50,000 yr. Outer beach ridges, the age of the deposition are in the range of 4,000-29,000 yr and recent beach sand sediment is approximately 7,000 yr.

**Table 3.7** Result of thermoluminescence dating of inner beach ridges.

| Sample No. | U (ppm) | Th (ppm) | K (%) | W (%) | AD (Gy/ka) | N (Gy) | Io (Gy) | ED (Gy) | ED (Error) | Age (Yr) | Error (Yr) |
|---|---|---|---|---|---|---|---|---|---|---|---|
| T1-PN3 | 1.27 | 4.94 | 0.38 | 3.72 | 1.23 | 125.00 | 107.58 | 17.42 | 1.04 | 14146.29 | 900 |
| T1-PN5 | 2.69 | 13.29 | 0.15 | 2.04 | 1.97 | 148.33 | 124.12 | 24.22 | 0.86 | 12293.33 | 400 |
| T2-PN2 | 1.88 | 4.67 | 0.22 | 3.72 | 1.20 | 75.50 | 61.53 | 13.97 | 0.26 | 11640.82 | 300 |
| T2-PN3 | 2.68 | 8.84 | 0.37 | 2.34 | 1.86 | 133.97 | 122.61 | 11.36 | 0.29 | 6108.33 | 100 |

**Table 3.8** Result of thermoluminescence dating of middle beach ridges.

| Sample No. | U (ppm) | Th (ppm) | K (%) | W (%) | AD (Gy/ka) | N (Gy) | Io (Gy) | ED (Gy) | ED (Error) | Age (Yr) | Error (Yr) |
|---|---|---|---|---|---|---|---|---|---|---|---|
| T1-PN6 | 1.64 | 7.14 | 0.45 | 6.59 | 1.53 | 146.45 | 114.95 | 31.49 | 1.32 | 20518.84 | 900 |
| T1-PN8 | 1.09 | 2.86 | 0.52 | 2.62 | 1.19 | 154.25 | 90.36 | 63.89 | 0.13 | 53863.00 | 1300 |
| T1-PN9 | 2.23 | 13.55 | 0.40 | 2.62 | 2.13 | 118.98 | 104.44 | 14.54 | 0.25 | 6834.23 | 100 |
| T2-PN4 | 1.35 | 4.96 | 0.48 | 7.06 | 1.34 | 111.11 | 95.09 | 16.02 | 0.07 | 11947.73 | 200 |
| T2-PN6 | 1.02 | 5.33 | 0.41 | 2.68 | 1.24 | 133.97 | 95.28 | 38.69 | 0.47 | 31095.67 | 800 |
| T3-PN3 | 1.42 | 4.21 | 0.52 | 2.23 | 1.37 | 105.57 | 77.59 | 27.98 | 0.46 | 20423.03 | 500 |

**Table3.9** Result of thermoluminescence dating of outer beach ridges.

| Sample No. | U (ppm) | Th (ppm) | K (%) | W (%) | AD (Gy/ka) | N (Gy) | Io (Gy) | ED (Gy) | ED (Error) | Age (Yr) | Error (Yr) |
|---|---|---|---|---|---|---|---|---|---|---|---|
| T1-PN14 | 2.71 | 13.22 | 0.54 | 2.12 | 2.36 | 136.68 | 85.22 | 51.46 | 0.26 | 21777.71 | 200 |
| T2-PN1 | 6.34 | 34.88 | 0.32 | 8.69 | 4.44 | 87.83 | 68.36 | 19.48 | 0.44 | 4387.62 | 100 |
| T2-PN7 | 1.31 | 5.32 | 0.35 | 3.36 | 1.24 | 139.62 | 103.27 | 36.35 | 0.39 | 29363.61 | 700 |
| T2-PN9 | 2.31 | 10.71 | 0.23 | 7.15 | 1.72 | 118.98 | 104.74 | 14.23 | 0.26 | 8277.61 | 200 |
| T3-PN6 | 1.29 | 4.75 | 0.38 | 4.46 | 1.23 | 133.97 | 91.86 | 42.11 | 0.40 | 34361.90 | 900 |
| T3-PN8 | 1.02 | 3.65 | 0.31 | 2.90 | 1.01 | 100.00 | 83.13 | 16.87 | 0.20 | 16639.34 | 500 |
| T3-PN9 | 1.46 | 6.68 | 0.31 | 5.33 | 1.32 | 131.48 | 112.76 | 18.72 | 0.35 | 14134.76 | 400 |

**Table 3.10** Result of thermoluminescence dating of recent beach ridge.

| Sample No. | U (ppm) | Th (ppm) | K (%) | W (%) | AD (Gy/ka) | N (Gy) | Io (Gy) | ED (Gy) | ED (Error) | Age (Yr) | Error (Yr) |
|---|---|---|---|---|---|---|---|---|---|---|---|
| T1-PN13 | 1.45 | 5.15 | 0.39 | 10.61 | 1.27 | 120.85 | 111.63 | 9.22 | 0.07 | 7264.43 | 100 |

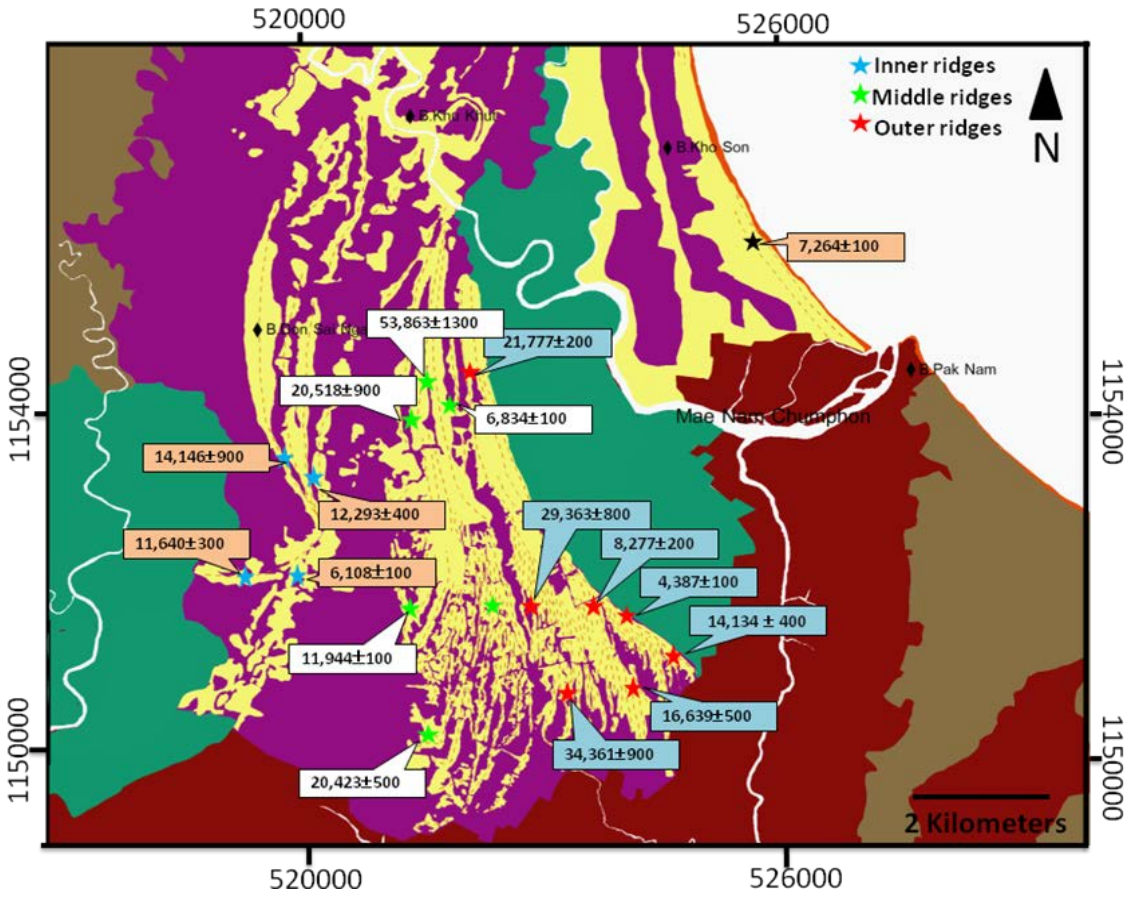


**Figure 3.17** Borehole locations with TL dating age from the study area.

## 3.5 Fossil evidence

### 3.5.1 Systematic description

**Class** Gastropoda

**Subclass** Prosobranchia

**Order** Mesogastropoda

**Family** Cerithida

**Genus** *Celypeomorus Jousseaume*, 1888

*Celypeomorus coralia* (Kiener,1834)

Pl.1 Figs. 1 (a,b)

**Distribution:** Kii Peninsular, Japan and southward to tropical West Pacific, and northeastern Indian Ocean.

**Habitat**: On mud in intertidal estuarine mangrove swamp.

**Superfamily** Naticoidea Forbes,1838

**Family** Naticidae Forbes,1838

**Subfamily** Polinicinae Gray, 1847

**Genus** *Polinices Montfort*, 1810

**Subgenus** *Polinices* (Polinices) Montfort, 1810

*Polinices(Polinices) mammilla* (Linnaeus,1758)

Pl.1 Figs. 2 (a,b)

**Distribution**: China, Australia, Japan, Indo-West Pacific and Thailand.

**Habitat**: Sand flat in low tide.

**Subfamily** Naticinea Forbes, 1838

**Genus** *Natica Scopoli*, 1777

*Natica trigina* (RÖdind, 1798)

Pl.1 Figs. 3 (a,b)

**Distribution**: India, Japan, Malaysia, Singapore and Thailand.

**Habitat**: Muddy sand to mud flats in mangrove forest, intertidal and shallow subtidal to 30 m.

**Fossil records**: Late Miocene to Quaternary of Indonesia; Quaternary inThailand.

**Superfamily** Buccinoidea

**Family** Nassariidae Iradale, 1916

**Subfamily** Nassariinae Iradale, 1916

**Genus** *Nassarius Dumeril*, 1860

*Nassarius pullus* (Linnaeus,1758)

Pl.1 Figs. 4 (a,b)

**Distribution**: Indo-West Pacific, Mauritius, New Caledonia, Japan, Malaysia, Singapore and Thailand.

**Habitat**: Sands, rocks, corals, rocky and mud flats in mangroves to intertidal and subtidal.

**Fossil records**: Pliocene of Indonesia; Quaternary of the Red Sea area.

*Nassarius siquijorensis (*Adam,1852)

Pl.1 Figs. 5 (a,b)

**Distribution**: Indo-Pacific, New Caledonia, Red Sea, Japan, Tolo Channel, Hong Kong and Thailand.

**Habitat**: Fine sandy and muddy in sublittoral and upper bathyal zone.

**Fossil records**: Late Middle Miocene to Quaternary of Indonesia; Holocene of Thailand.

**Superfamily** Muricordia

**Family** Fasciolariidae

**Subfamily** Peristerniinae

**Genus** *Peristernia*

*Peristernia incarnate*

Pl.1 Figs. 6 (a,b)

**Distribution**: Western Australia

**Habitat**: Shallow water species, living under rock or coral

**Class** Bivalvia

**Subclass** Heterodonta

**Order** Ostreoida

**Suborder** Ostreina

**Superfamily** Ostreoidea

**Family** Ostreidae

Pl.2 Figs. 1 (a,b,c,d)

Pl.2 Figs. 2 (a,b)

Pl.2 Figs. 3 (a,b)

Pl.2 Figs. 4 (a,b)

**Subclass** Pteriomorpha Beurlen, 1944

**Order** Arcoida Stoliczka, 1871

**Superfamily** Arcoidea Lamarck, 1809

**Family** Arcidae Lamarck, 1809

**Subfamily** Anadarinae

**Genus** *Anadara*

*Anadara oblonga* (Philippi, 1849)

Pl.3 Figs. 1 (a,b)

**Distribution**: Range from Thailand to the Plilippines and Taiwan.

**Habitat**: Usually occurring intertidally and down to 10 m depth in mud and sand. Gulf of Thailand it was recorded very common from soft muddy or shell bottom at depth 5-20 m.

**Fossil records**: Late Miocene of Indonesia and Philippines; Pliocene of Indonesia, Taiwan and Japan; Quaternary of Indonesia, Thailand and Taiwan; Holocene of Thailand.

*Tegillarca granosa* (Linnaeus, 1758)

Pl.3 Figs. 2 (a,b)

**Distribution**: Ise Bay, Japan and southward to India.

**Habitat**: Embayment mud bottom in intertidal zone to 10 m deep.

**Genus** *Scapbarca*

*Scapbarca* sp.

Pl.3 Figs. 3 (a,b)

**Order** Mytiloida

**Family** Mytilidae (Rafinesque, 1815)

**Genus** *Mytilus*

Pl.3 Figs. 4 (a,b)

**Order** Pteriomorpha

**Family** Noetidae

*Didimacar tenebrica* (Reeve, 1844)

Pl.3 Figs. 5 (a,b)

**Distribution**: The species ranges from India to Southeast Asia, Queensland and northward to Japan and Chaina.

**Habitat**: It is an epifaunal element uauslly found intertidally and down to 20 m on rubble bottoms.

**Genus** *Striarca*

*Striarca lacteal*

Pl.3 Figs. 6 (a,b)

**Habitat**: attach to the su bstrate using a byssus.

**Subclass** Heterodonta

**Orde**r Carditoida

**Superfamily** Carditoidea

**Family** Carditidae

**Genus** *Carditella*

*Carditella (Carditellona)* pulebella Lynge, 1909

Pl.3 Figs. 7 (a,b)

**Distribution**: Gulf of Thailand and Japanese waters.

**Habitat**: Sandy, stony or shelly bottoms, occasionally in mud, at depth of from 2 to 54 m (Lynge, 1909; Hape, 1968)

**Fossil record**s: Pliocene of Indonesia and Taiwan.

**Order** Carditoida

**Superfamily** Crassatelloidea

**Family** Crassatellidae

**Subfamily** Crassatellinae

*Batbytormus radiates* (Sowerby,1825)

Pl.3 Figs. 8 (a,b,c,d)

**Distribution**: The species is reported to be common in the tropical Indo-Pacific, from Red Sea to Southeast Asian water. (Lynge,1909;Prashad,1932)

**Habitat**: It dwells in predominantly sandy infralittoral bottoms. Previous Thai records were from muddy, sandy and shelly substrate at depth from 3 to 54 m. (Lynge,1909;Tantanasiriwong,1979)

**Fossil records**: Lower Miocene of Myanmar; Middle Miocene of Myanmar and Indonesia; Upper Miocene to Pliocene of Indonesia and Philippines; Quaternary of Indonesia; Holocene of Thailand.

**Order** Veneroida

**Family** Mactridae

**Genus** *Mactra*

*Mactra* sp.

Pl.3 Figs. 9 (a,b)

**Distribution**: Endemic to southeastern and southwestern Australia (TAS, VIC, SA and WA). In Tasmania this species is restricted to the N coast and Bass Strait islands, where locally common.

**Habitat**: Lives subtidally in sand, especially in moderately exposed environments.

**Superfamily** Solenoidea

**Family** Solenidae

**Genus** *Solen*

*Solen* sp.

Pl.3 Figs. 10 (a,b)

**Superfamily** Tellinoidea

**Family** Tellinidae (Blainville, 1814)

**Subfamily** Macominae Olsson, 1961

**Genus** *Psammotreta* Dall,1900

**Subgenus** *Psammotreta (Tellinimactra)* Lamy,1918

*Psammotreta (Tellinimactra) edentula* (Spengler,1798)

Pl.3 Figs. 11 (a,b)

**Distribution**: Red Sea, Australia, China Sea, Java and Thailand.

**Habitat**: Mud and sand, mangroves and intertidal to 10 m.

**Fossil record**s: Holocene of Thailand.

**Family** *Semelidae*

*Semele carnicolor* (Hanley,1847)

Pl.3 Figs. 12 (a,b)

**Distribution**: Indo Pacific, from Red Sea to Indonesia and northward to Japan.

**Habitat**: It dwell in coarse sandy bottoms intertidally and down to 25 m depth. Former records in Thai waters were from coarse beach sands (Nieisen, 1976).

**Fossil record**s: Pliocene and Quaternary of Japan.

**Superfamily** Veneroidea

**Family** Veneridae

**Subfamily** Chioninae

**Genus** *Amomalocardia* Schumacher, 1817

*Anomalocardia (Anomalodiscus) squamosa* (Linnaeus,1758)

Pl.3 Figs. 13 (a,b)

**Distribution**: *Anomalocardia squamosa* ranges from Australia to Japan. According to Bernard et. al. (1993). Previous record in the Gulf of Thailand were from the strand of the mangrove at Koh Chang (Lynge, 1909).

**Habitat**: it is an intertidal element dwelling in mud.

**Fossil record**s: Late Miocene and Pliocene

**Genus** *Placamen*

*Placamen cholorotica* (Philippi,1849)

Pl.3 Figs. 14 (a,b)

**Distribution**: Taiwan and southward to Indian ocean. Previous records in the Gulf of Thailand were from strand off the mangrove forest, in very shallow water (Lynge, 1909).

**Habitat**: Sandy bottom in intertidal zone to 50 m deep.

**Fossil record**s: Middle and Upper Miocene of Indonesia; Pliocene of Indonesia, Philippines, Taiwan and Japan; Quaternary of Indonesia; Holocene of Thailand.

**Genus** *Paphia*

*Paphia (Papbia) undulate* (Born, 1778)

Pl.4 Figs. 1 (a,b)

**Distribution**: Widely distribution in the tropical Indo-Pacific, from the Red Sea to Australia and northward to Japan.

**Habitat**: Muddy substrate in the intertidal zone and down to 50 m (Kuroda et al., 1971;Bernard et al., 1993). On the west coast of Malaya and Thailand it occurs in muddy bottoms at and below low water mark of neap tides (Tantanasiriwong, 1979; Purchon & Purchon, 1981) In the Gulf of Thailand, it was recovered in very large numbers from muddy substrate 5-35 m deep (Lynge, 1909).

**Fossil record**s: Upper Miocene of Indonesia and Japan; Pliocene of Indonesia, Philippines, Taiwan and Japan; Quaternary of the Indo-Pacific area; Holocene of Thailand.

**Genus** *Dosinia*

*Dosinia sp.*

Pl.4 Figs. 2 (a,b)

Pl.4 Figs. 3 (a,b)

*Dosinia Scopoli*, 1777

Pl.4 Figs. 4 (a,b)

**Distribution**: India to Southeast Asia.

**Habitat**: Intertidal sands and rocks and mangroves on the west coast of Malaya (Morr&Purchon,1981). Previous record in the Gulf of Thailand were at Koh Chang, from strand off the mangrove forest (Lynge,1909).

**Fossil records**: Holocene Thailand.

**Genus**: *Donax*

*Donax sp.*

Pl.4 Figs. 5 (a,b)

**Genus** *Capsella*

*Capsella sp*

Pl.4 Figs. 6 (a,b)

**Genus** *Tellina* Linnaeus, 1758

*Tellina timorensis* (Lamarck, 1818

Pl.4 Figs. 7

**Distribution**: Indo-Pacific, Red Sea, Japan, Indonesia and Thailand.

**Habitat**: Sand in intertidal flat to 25 m.

**Fossil records**: Upper Miocene of Indonesia, Philippines and Japan; Pliocene and Quaternary of Indonesia; Holocene of Thailand.

**Genus** *Leptomya*

*Leptomya* sp.

Pl.4 Figs. 8 (a,b)

**Class** Scaphopoda

**Order** Dentaliida

**Family** Dentaliidae

**Genus** *Antalis*

*Antalis sp.*

Pl.4 Figs. 9

**Phylum** Echinodermata

**Subphylum** Echinozoa

**Class** Echinoidea

Pl.4 Figs. 10

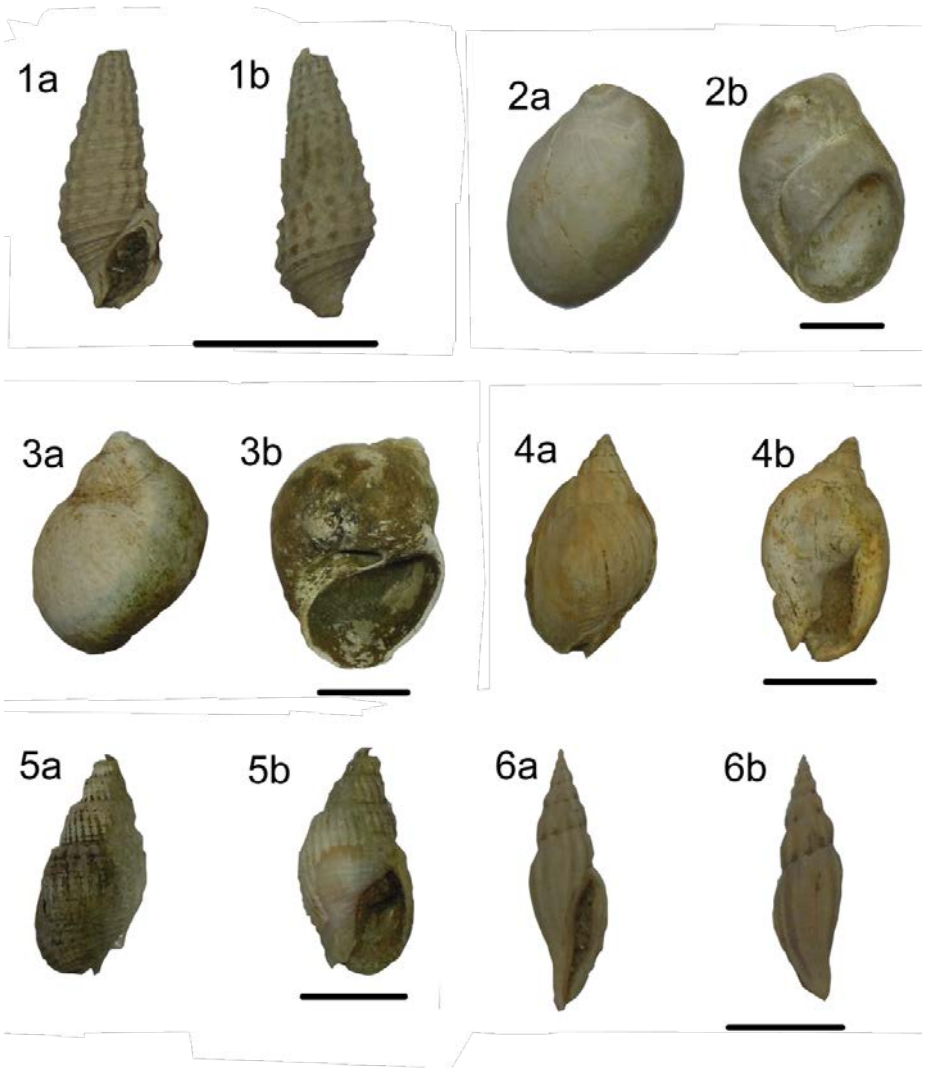


**Plate1:** Figs.1 (a,b) *Celypeomorus coralia* Figs. 2 (a,b) .*Polinices(Polinices) mammilla* Figs. 3 (a,b) *Natica trigina* Figs. 4 (a,b) *Nassarius pullus* Figs. 5 (a,b) *Nassarius siquijorensis* Figs. 6 (a,b) *Peristernia incarnate*, all scale bar are 1 cm.

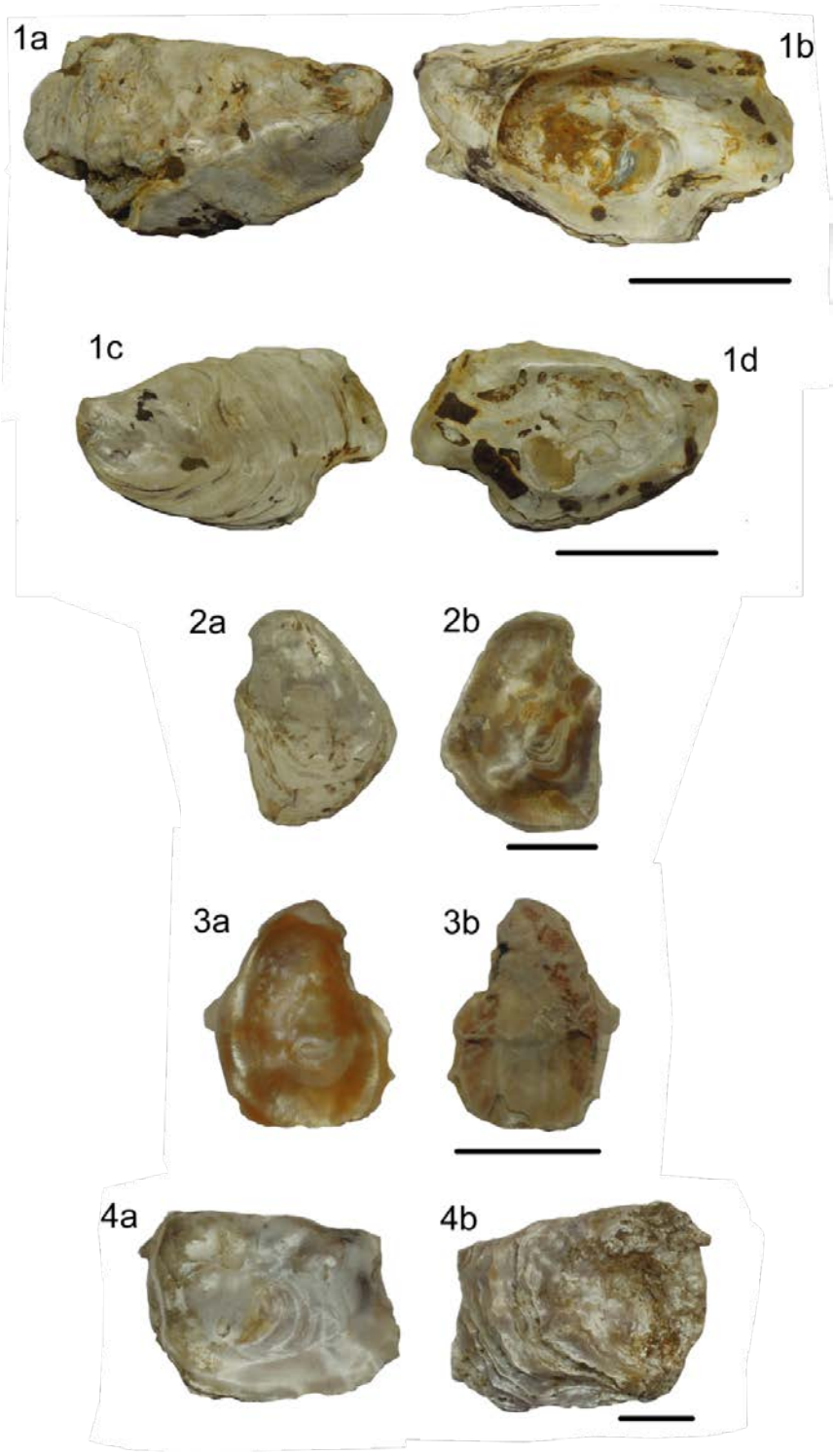


**Plate2:** Figs. 1 (a,b,c,d), scale bar 5 cm. Figs. 2 (a,b), scale bar 1 cm. Figs. 3 (a,b) ), scale bar 1 cm Figs. 4 (a,b) ), scale bar 1 cm Ostreidae.

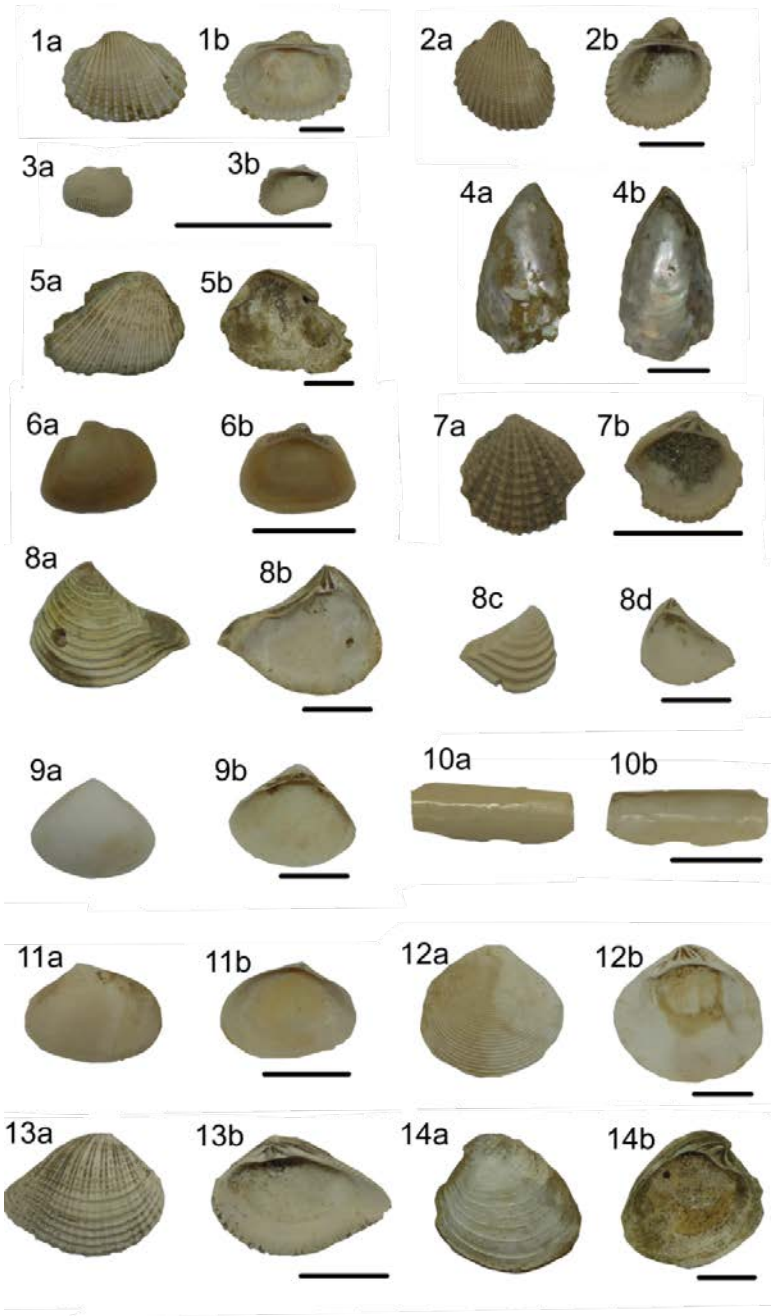


**Plate3:** Figs. 1 (a,b) *Anadara oblonga* Figs. 2 (a,b) *Tegillarca granosa* Figs. 3 (a,b) *Scapbarca* sp. Figs. 4 (a,b) *Mytilus* sp. Figs. 5 (a,b) *Didimacar tenebrica* Figs. 6 (a,b) *Striarca lacteal* Figs. 7 (a,b) *Carditella (Carditellona)* pulebella Figs. 8 (a,b,c,d) *Batbytormus radiates* Figs. 9 (a,b) *Mactra* sp. Figs. 10 (a,b) *Solen* sp. Figs. 11 (a,b) *Psammotreta (Tellinimactra) edentula* Figs. 12 (a,b) *Semele carnicolor* Figs. 13 (a,b) *Anomalocardia (Anomalodiscus) squamosa* Figs. 14 (a,b) *Placamen cholorotica***,** all scale bar are 1 cm.

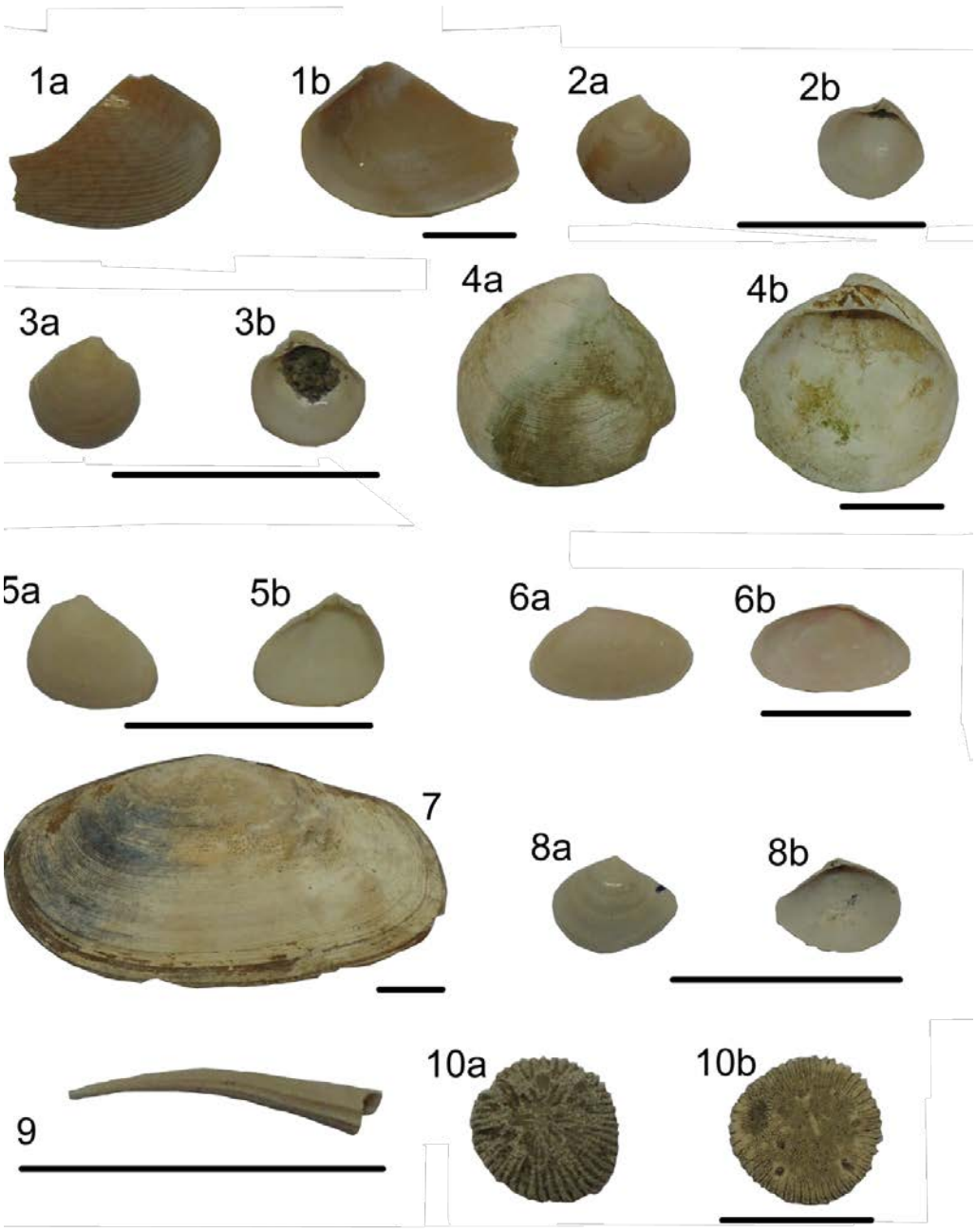


**Plate4:** Figs. 1 (a,b) *Paphia (Papbia) undulate* Figs. 2 (a,b) Figs. 3 (a,b) *Dosinia sp.* Figs. 4 (a,b) *Dosinia Scopoli* Figs. 5 (a,b) *Donax sp.* Figs. 6 (a,b) *Capsella sp* Figs. 7 *Tellina timorensis* Figs. 8 (a,b) *Leptomya* sp. Figs. 9 *Antalis sp.* Figs. 10 Echinoidea, all scale bar are 1 cm.

# CHAPTER IV

# DISCUSSIONS

This chapter provides the discussions of all results from field survey and laboratory analyzes leading to propose the model showing landforms evolution in the study area. Discussions start with the interpretation of paleo-shoreline boundary, the sedimentological characteristics from each of beach ridge plain, fossil evidence, age determination and the episodic evolution of coastal landforms based mostly on geomorphological, sedimentological basis and some results from age dating of beach ridges.

## 4.1 Boundary of paleo-shoreline from aerial photograph interpretation

Since 1980's, the works on landform evolution has been carried out extensively at the lower Central Plain of Thailand. The mid Holocene paleo-shoreline was proposed by many researchers. For example, Supajanya (1981, 1983) proposed the late Holocene shoreline based on aerial photograph interpretation in relation to the position of ancient settlements. This work revealed that the ancient settlement sites of the Dvaravati period are elevated between 3.5-4 meters above the present mean sea level. The use of aerial photograph interpretation from this work is one of excellent analog and proofed well that the more accuracy to delineate the boundary of paleo-shoreline can be carried out from aerial photograph.

In the study area, the tentative boundary of the westernmost paleo-shoreline can be estimated (Figure 4.1) and is located far approximately 5 kilometers inland from the present shoreline. It is evidenced from the occurrence of inner beach ridge plain. As mentioned in chapter 3, the beach ridge plains recognized in the study area were divided into 3 trends as inner beach ridges, middle beach ridges and outer beach ridges. All beach ridge plains own their

orientation parallel to the present shoreline, but they reflect the difference in paleo-longshore current direction. The orientation of beach ridges within the inner ridges plain revealed the longshore current direction was likely to the north. On the other hand, the middle and outer beach ridge plains were likely originated by southward longshore current direction due mainly to sand ridge branches out in the tail as part of sand spit.

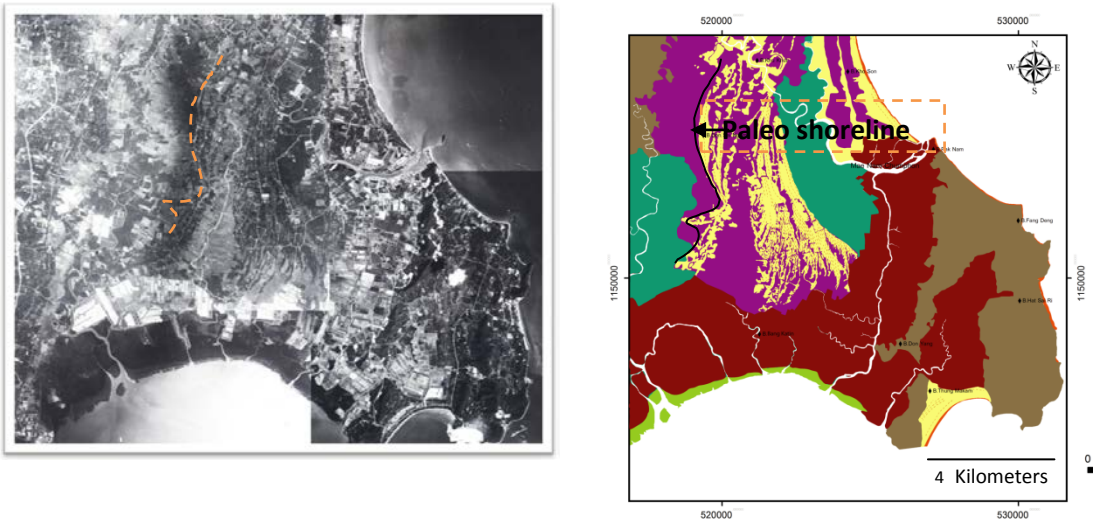


**Figure 4.1.** Coastal geomorphological map (right) interpreted from aerial photographs (left). The westernmost boundary of paleo-shoreline (dash line in left picture) recognized from aerial photograph.

### 4.2 Sedimentological characteristics from each of beach ridge plain

As mentioned in Chapter 3, some differences in statistic parameters can be detected from each of beach ridge plains. Grain size distribution is one of physical properties that reflect the different energy during the depositional processes. However, grain size distribution could not be used alone for sedimentary environment identification, but it has to be combined with the other lines of evidence (roundness, sphericity and heavy minerals, biogenic components) (Martins and Barboza, 2005). Skewness and kurtosis are also used for special purpose and usually are

diagnostic in the comparison of sediments from different sedimentary occurring in the same environment (Martins and Barboza, 2005).

In the study area, the so-called “old beach’’ is relatively inferred to have formed sometimes during the late Pleistocene. Old beaches usually show similar properties to the so-called “modern beach” (presumably formed in the Holocene). Sometimes, the orientation of beaches and coastal dune were overlapped. However, this study shows that the difference in grain size distributions of beach sediment is varied depending on both time and space. This may because the daily wave and tidal influence on sediment deposition on the beach, swash processes create an ever-changing foreshore sediment distribution (Martins and Barboza, 2005).

As shown in Figures 3.10-3.15 of Chapter 3, all 6 scatter plots of sand sample from inner beach ridge reveals widest distribution. Scatter plot of mean size versus standard deviation (sorting) shows narrow range of grain size (very fine to coarse sand) and show moderately to moderately well sorted. It indicates high energy environment of beach (Folk and Ward, 1957). Based on the plot of sorting versus skewness, some of sand sediments in outer ridge and inner ridge have showed extreme kurtosis value and good sorting that indicated neritic sediments. The result of skewness versus kurtosis scatter plot reveals half of all sediment samples are characterized by leptokurtic and positive skewed sediments. They indicated that sediments are transported near the source of the sand (Folk and Ward, 1957). Skewness and kurtosis were referred as the indicators of selective action of the transporting agent (Martin, 1964). Beach sands generally have negative skewness that is similar to those recognized from Pak Nam area.

Result of grain-size analysis indicated that beach sand is normal or negative skewness and leptokurtic as suggested by Martin (1964). Dune sand has positive skewness and mesokurtic, whereas, eolian flat sand has positive skewed and leptokurtic. The beach sand is more poorly sorted than the other types. Beach sands generally has negative skewness as same as beach sand at Pak Nam area.

In this study, skewness value is fine- to coarse skewed that indicates the environmental change between calm (stable current) and storm (variable current velocities and turbulence during deposition). Poorer sorting indicates variable current velocities and turbulence during deposition while good sorting indicates smooth and stable currents. Local shoaling in a shallow marine environment may produces the complex current flow patterns, eddying, and wave-generated turbulence leading to skewness of beach sands was found to be negatively skewed for the most part (Ameral and Pryor, 1997).

Most of beach sand composition from beach ridge is composed of quartz. Textures of sediment are sub-angular to angular. They can be classified as sub-mature texture stage as suggested by Folk (1951) and pointed relatively to short transportation for a considerable time and distance (Friedman, 1967).

**4.3 Fossil evidence**

Broken shell fragments in the present beach area indicate a relatively shallow, near shore environment as suggested by Valia and Cameron (1977). All fossil of gastropoda, bivalvia, scappophoda and echinoidea indicate former environment as mangrove and intertidal zone. This is a key for supporting that the occurrence of some key fauna can be used as the indicator of the former shoreline. In the past, sea water incurred landward far from Pak Nam Chumphon at approximately 9 kilometers from the present shoreline (as evidenced by intertidal fossils found at location number T3-PN2). Almost shell fossils were found at Pak Nam area that is comparatively the same type to those found in the Holocene Bangkok clay in the Lower Central Plain and Phetchaburi coastal area as mentioned in Robba et al. (2002).

## 4.4 Age determination

It is important to note here that the TL dating technique owns its limitation in various ways that may make up of the older number of the age from the expectation. From the results of age determination by TL dating mentioned in Chapter 3, the age ranging of beach ridge extended from 4,300 to 53,000 years. This also makes a limitation and complication to the interpretation in the history of beach ridge formation in this area. The wide range of TL age dating especially the old age dating may reflects the extensive reworking process and the repeat of deposition of beach sand. For example, some results show the age of beach ridge older than 30,000 years. These ages are likely impossible for beach formation because the global sea level during that time was recorded to much lower than the present mean sea level. Therefore, in this study, the average youngest number of dating from each of beach ridge plain is selected to avoid the age of reworking processes. As a result, the inner ridge dating determined that the formation of inner ridge plain is in average around 7,000 years which is corresponded well with the age of highstand from the literatures. Result of age dating can be contributed to model the landform evolution as shown in Figure 4.8.

## 4.5 Paleo-sea level changes

### 4.5.1 Paleo-sea level changes in Pleistocene epoch

Fleming et al. (1998) mentioned that the eustatic component of relative sea-level change in Pleistocene provides a measure of the amount of ice transferred between the continents and oceans during glacial cycles. This has been quantified for the period since the Last Glacial Maximum by correcting observed sea-level change for the glacio-hydro-isostatic contributions using realistic ice distribution and earth models. During the Last Glacial Maximum (LGM) the eustatic sea level was 125 $\pm$ 5 m lower than the present day as shown in Figure 4.2. Result of sea level change in Pleistocene epoch found in many areas along the world coast. However, it was difference in local scale.

In west Asia, sea-level of Persian Gulf in Pleistocene last glacial period was drop down more 140 below present mean sea level. Wood (2012) studied the coastline along the southern Arabian Gulf between Al Jubail, Kingdom of Saudi Arabia, and Dubai, UAE, and found that sea level appears to have risen at least 125 m in the last 18,000 years. Wood (2012) also revealed result of dating and topographic surveying of paleo-dunes (43–53 ka), paleo-marine terraces (17–30 ka), and paleo-marine shorelines (3.3–5.5 ka) as shown in Figure 4.3.

In Southeast Asia, Hanebuth et al. (2000) proposed a sea-level curve for the Sunda Shelf derived from shoreline facies. On the proximal part of the Sunda Shelf transect, the late-glacial transgression could be directly followed between a water depth of 70 and 126 m. Pedogenesis on the late Pleistocene land surface indicates a low sea-level stillstand in the LGM at 22 ka. This surface is overlaid by transgressive coastal sediment and marine sands then cover the transgressive sediments after a hiatus. Ages from *Rotalia* sp. from mud layer vary widely from 12.4 to 4.1 ka and indicate that these shelf sediments were reworked and mixed up to recent times as shown in Figure 4.4.

Sea level curve in Pleistocene epoch in Huon Peninsula, New Guinea from coral terraces shown mean eustatic sea level change (Pillans et al., 1998). During 12 Ma, sea-level began to fall and shown fluctuation. The sea-level was lowest than mean eustatic sea level at 120 meter below present mean sea level as shown in Figure 4.5.

From many researches regarding eustatic sea-level history in Pleistocene epoch (Fleming et al., 1998; Pillans et al., 1998; Hanebuth et al., 2000; Wood, 2012) mentioned above, the shoreline everywhere along the world coast was located in much lower level than the present sea level. In this regard, it can be referred that the shoreline at Pak Nam Chumphon area were also located far away offshore from the present shoreline. This also helps to conclude that result from TL dating in this study possibly represents the age of sediments that were possible reworked. As well, the result of TL age dating in the modern beach deposit from this area was around 7,000 years ago that also confirmed reworking process.

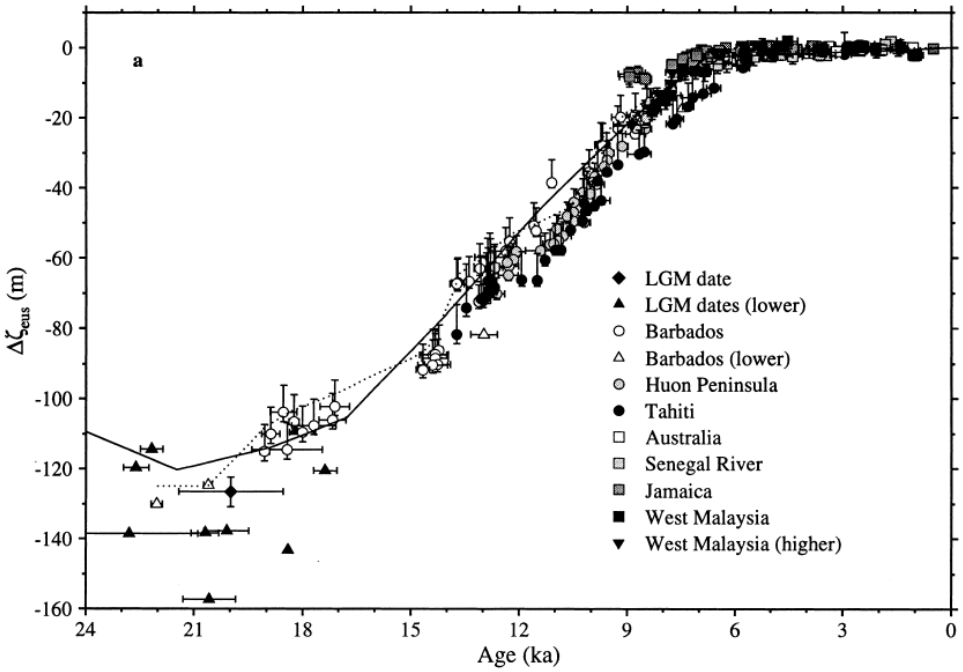


**Figure 4.2.** The estimated eustatic sea-level change from the Last Glacial Maximum to the present day from Fleming et al. (1998).

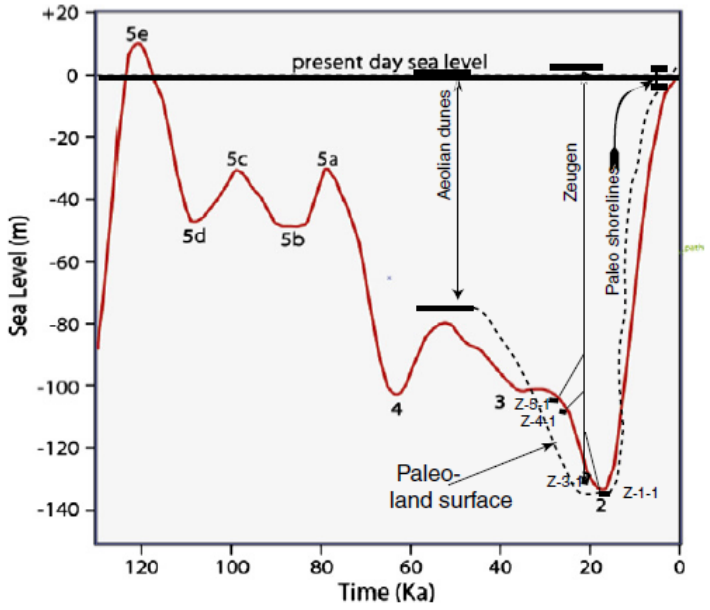


**Figure 4.3.** Land surface of the southern Arabian (Persian) Gulf elevation, for the last 53 ka, superimposed on sea level from Wood (2012).

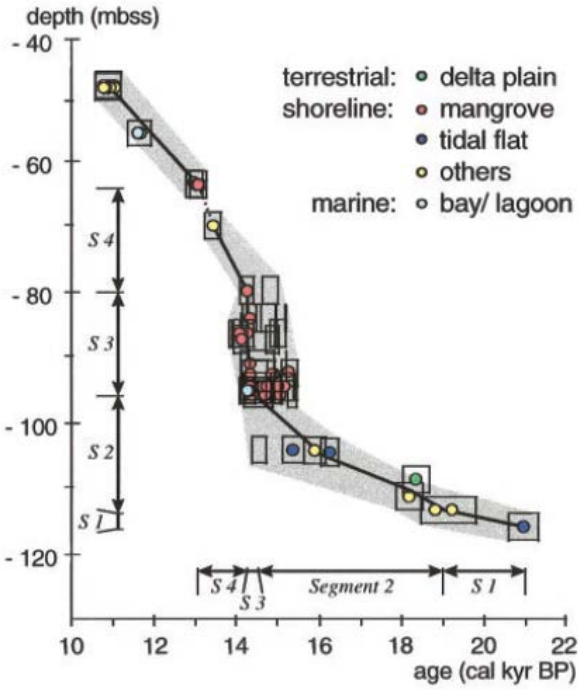


**Figure 4.4.** Sea-level curve for the Sunda Shelf derived from shoreline facies (Hanebuth et al., 2000).

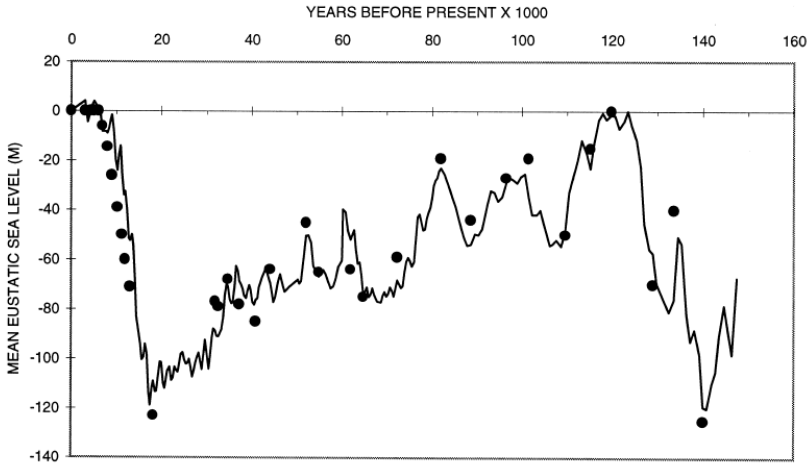


**Figure 4.5.** Sea-level changes for last 150 ka derived from isotope record using temperature and sea-level isotope from Huon Peninsula sea-level data (dots) (Pillans et al., 1998).

### 4.5.2 Paleo-sea level changes in Holocene epoch

In Southeast Asia, history of sea-level change during the Holocene were studied by many researchers, for example, the Strait of Malacca, Indonesia (Geyh and Kudrass, 1979), Malay–Thai Peninsula and Sunda Shelf (Hanebuth et al., 2000), and the Huon Peninsula, Papua New Guinea Chappell and Polach (1991). The discussion here will be focused only on the works from Thai-Malay peninsula. Tjia (1996) studied abrasion platforms, sea-level notches and oyster beds in Peninsula Malaysia and produced over 130 radiocarbon-dated indicators. The sea-level curve proposed by Tjia (1996) revealed the two Holocene highstands at 5000 and 2800 $^{14}$C yrs BP. However, Tjia (1996) mentioned that sea-level in Thailand was fluctuated at least three times from mid/late Holocene highstands at 6000, 4000 and 2700 $^{14}$C yrs BP. Scoffin and Le Tissier (1998) studied intertidal reef-flat corals (microatolls) for mid/late Holocene highstands at Phuket, Southern Thailand. The evidence there suggested a single Holocene highstand with a constant rate of RSL fall since 6000 cal yrs BP, and thus, contradicts conclusions drawn by Tjia (1996). However, it should be noted that Scoffin and Le Tissier's (1998) research was from only one site with eleven dated samples (Woodroff and Horton, 2005).

The first sea-level curve for Thailand that is referred for this study was proposed by Sinsakul et al. (1985) and integrated into a Holocene history of sea-level changes for the wider Thai–Malay Peninsula (Tjia, 1987) (Figure 4.2 from Choowong, 2011). The curve by Sinsakul et al (1985) shows two Holocene highstands at 5,000 and 2,800 years. In general, the sea-level curve for Thailand and Malaysia indicated three probable rebound phases during the Mid- to Late Holocene with highstands at 6, 4 and 2.7 ka (Sinsakul et al, 1985; Tjia, 1987).

A revised sea-level envelope for the Gulf of Thailand was proposed by Choowong et al. (2004) (Figure 4.3) which corresponded well with the sea-level curves subsequently constructed by Horton et al. (2005) for the Thai–Malay Peninsula. The curves show an upward trend of rising Holocene sea level to a Mid-Holocene highstand, and then a gradual fall of sea level to the

present. The average rate of sea-level rise from the Thai–Malay Peninsula was c. 5.5 mm/year, whereas the sea-level fall from the highstand was at about 1.1 mm/year, with no evidence of a second highstand (Horton et al. 2005; Choowong, 2011).

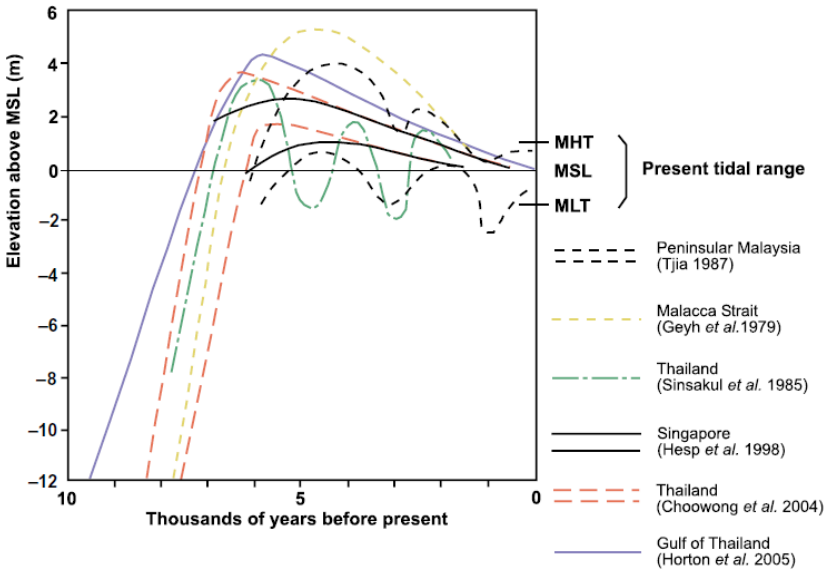


**Figure 4.6**. Sea-level curves from Thailand and neighboring countries. The curves show rapid transgression from the early Pleistocene to the mid-Holocene highstand, at about 3-4 m above present MSL. Fluctuations were reported locally from Thailand (Sinsakul et al., 1985) and Peninsular Malaysia (Tjia, 1987) during sea-level regression after the mid-Holocene highstand.

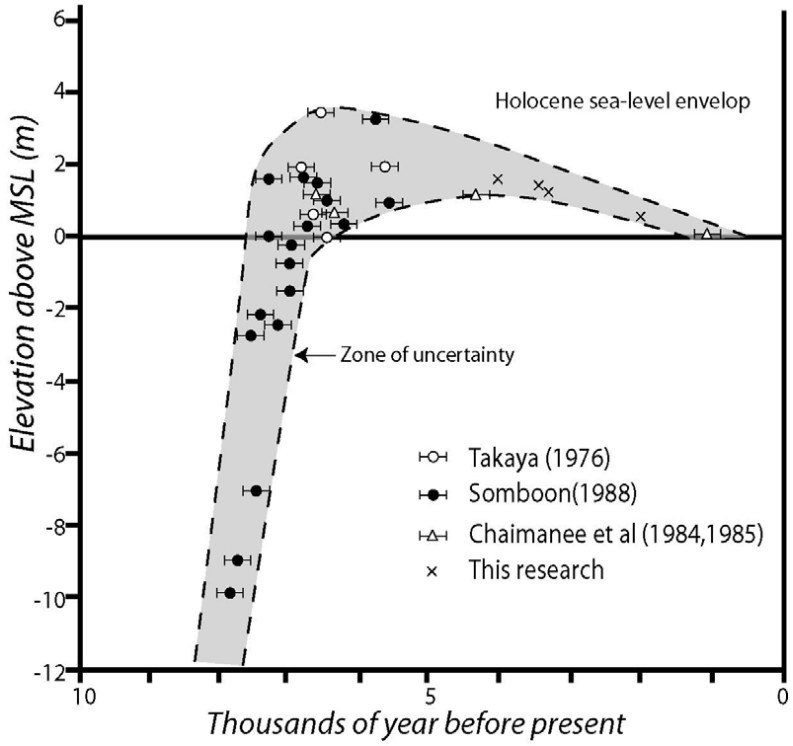


**Figure 4.7.** Holocene sea-level envelope for Thailand (Choowong et al., 2004).

Interpretation of former sea level is commonly helped to reconstruct a wide variety of environmental indicators including morphological and archaeological data and other lithostatigraphical change. But far the most widely used sea-level indicators in far-field locations are coral. There are many different types of coral, but only a few species are found in narrow elevation range. Other widely used sea-level indicators include geomorphological features, such as paleo-shoreline, notches, paleo-reef flats and beach deposit (Woodroff and Horton, 2005).

At Pak Nam Chumphon area, the interpretation of former sea level was done by using all paleo- and recent coastal geomorphology on coastal plain and the use of marine fossil. All geological evidences confirm that Pak Nam Chumphon area has been interacted from the influence of sea water. From the alignment of innermost beach ridges at approximate elevation 4-5 meter from mean sea level can be inferred the highest level of transgression in Pak Nam Chumphon area.

**4.6 Model of coastal geomorphological evolution**

It is important to note here that the model of coastal evolution in this section (Figure 4.8) was created based mostly from the occurrence of coastal beach ridges series. However, though the TL age dating has been made from this research, only a few results can be selected to help modeling the coastal evolution.

Based on the geological setting, this coastal plain is mapped as Quaternary alluvium sediments beneath the marine and brackish deposits (Thongpinyochai, 1996). As previous studies indicated that, in the last interglacial period in late Pleistocene epoch, sea level dropped down more 12 meters below the present mean sea level (Tjia, 1986; Choowong et al., 2004), therefore, this area was covered by alluvial and colluvial deposits mostly formed in terrestrial environment (Figure 4.8 top left). This also means that the paleo-shoreline during the late Pleistocene was located far away offshore from the present shoreline. Then, in the early-Holocene, sea level was raised rapidly by sudden melting down of ice mass leading to rapid eustatic sea level rise. In Thailand, the highstand is referred to have occurred in the middle-Holocene with the elevation of approximate 4 m above the present mean sea level (Supajanya, 1982; Thiramongkol, 1983; Choowong, 2002a, 2002b; Choowong et al., 2004). This rapid rising of sea level to about 4 m above the present MSL made up of the narrow transgressive beach ridges as seen in the area as the inner series of beach ridge plain (Figure 4.8 top right). The orientation in set of inner beach ridges also indicated the northward direction of paleo-longshore current. After the sea has reached highstand level and later started to fall, the middle and outer beach ridges plains were formed by the southward direction of longshore current (Figure 4.8 bottom left). The orientation and dimension of middle and outer beach ridge plains has indicated their gradual seaward progradation mostly in forms of sand spits. The outer beach ridge plain was slowly prograded probably due to the gradual regression. In the meantime, the estuary can be formed leading to the formation of tidal flat deposits, mangrove and mud flat. As seen in the present time, the modern

beach ridge plain in this study area was probably started to its formation since the late Holocene when the sea level is almost equal the present mean sea level (Figure 4.8 bottom right).

Tentative major paleo-longshore current made up of beach ridges plain at Pak Nam Chumphon area can be interpreted from the orientation of the coastal landform and helped to find the source of the sediments (Figure 4.9). The direction of paleo-longshore current for accumulation of sand in a different directions from this area included 1) the inner ridge designates paleo-longshore current drift from south to north, and 2) the middle and outer ridges showing paleo–longshore from north to south.

From the orientation of the beach ridges, the source of the sand sediments to form the inner ridge were probably carried a long way from the south to the north of alluvial or old beach sediment. Sediments to form the middle and outer beach ridges were probably transported from the old beach sediments or sediments from old estuary from the Chumphon River by channel from north to south. This can be confirmed by the result of sieve analysis that shows dissimilarity among inner, middle and outer beach ridges. Inner ridge sorting is characterized by very well to moderate. Middle and outer ridges are moderately well to moderate-sorted. Therefore, inner ridge shows better sorting than the middle and outer ridge. Then, it can be concluded that the environment was calm as also confirmed by the occurrence of large tidal flat deposit.

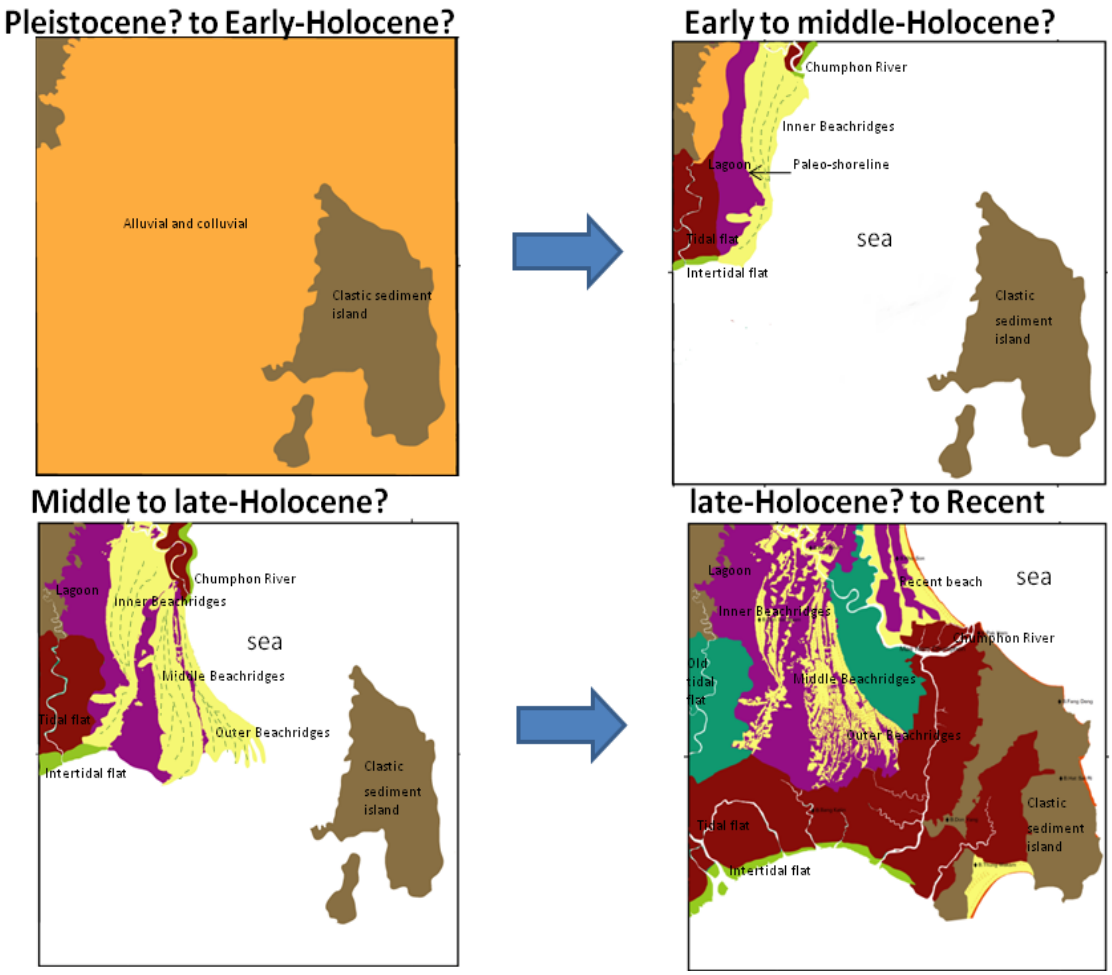


**Figure 4.8**. Model of coastal geomorphological evolution in Pak Nam Chumphon.

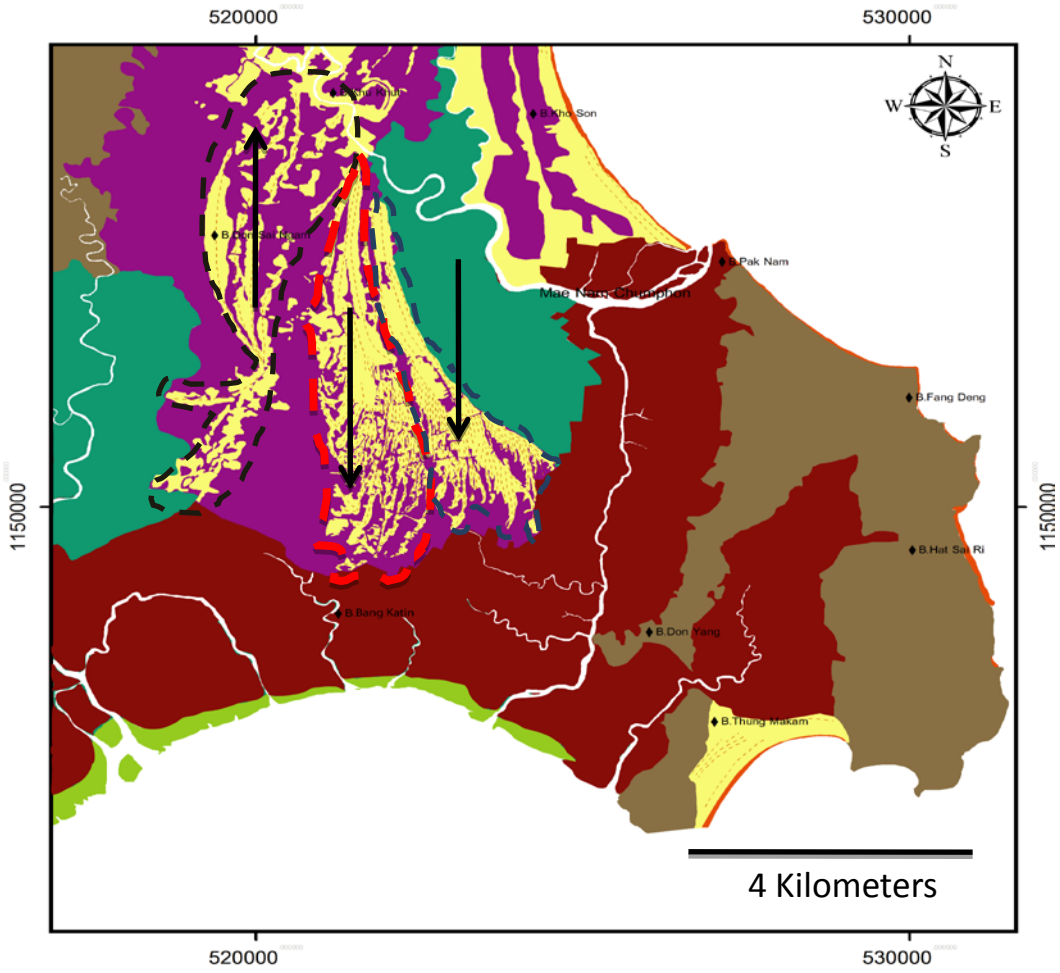


**Figure 4.9**. Tentative paleo-longshore currents at Pak Nam Chumphon.

# CHAPTER V

# CONCLUSION

This research is aimed at modeling the coastal evolution from Pak Nam Chumphon area located at the coastal zone in the Gulf of Thailand. Basically, the coastal geomorphological map was necessary the first step to be constructed based on the aerial photograph interpretation. Then as a result, the coastal landforms in this area can be classified into 7 units as old sandy beach, old lagoon, young sandy beach, old tidal flat, upland and mountain, intertidal flat ,tidal flat and it can be related with sea level change. In terms of depositional environment, the evidence of shell and peat fragments recognized from this area indicates their living position in the former tidal flat as previously studied by Sinsakul (1988). Broken shell fragments in the marginal part of beach area also indicate a relatively shallow, near shore environment as suggested by Valia and Cameron (1977). In this research, the episodic coastal evolution model was made from aerial photo interpretation and types of landforms with their trends of formation. Though, TL dating technique is applied to this study, the age dating of beach ridge from TL seems likely older than what they should be. It can be suggested that results of TL dating in this thesis reflect the reworking process of beach deposits. The conclusion in this chapter will be summarized as follows.

Beach ridge deposition characterizes from sediment layer from each landform from boreholes. Beach ridge is generally characterized by medium to fine sand. Only one location at T1-PN1 (inner most beach ridge) is dominated by mud underneath sand layer. Color of sediment is different in each bore hole. Sediment in swale (old lagoon) is common as sandy mud and mud, dark brown, brownish black, grey color and some location found peat fragments. Old tidal flat sediment is described by mud confined with sandy mud found small shell fossils. Recent beach sediment is brown and grey fine sand found some shell fragments.

Result of textural analysis from grain size distribution can be concluded as follows. In the inner ridge series, mean grain size is characterized by very fine to coarse sand, very poorly sorted to very well sorted, very fine skewed to very coarse skewed and very leptokurtic to platykurtic. Middle ridge series is represented by fine to medium sand , poorly sorted to very well sorted, fine skewed to very coarse skewed and very leptokurtic to leptokurtic. Outer ridge series is described by fine to medium sand, poorly sorted to moderately well sorted, fine skewed to coarse skewed and very mesokurtic to leptokurtic. Recent beach contains fine sand, moderately to moderately well sorted, symmetrical to very coarse skewed and very mesokurtic to very leptokurtic.

Average composition of old beach ridge and young beach ridge is mainly composed of quartz and minor of feldspar. All beach ridges (inner, middle and outer beach ridges) show similarity in composition of sand sediment, but in the inner ridge the minor compositions contain feldspar and ferromagnesian more than the middle and outer ridge. Roundness and sphericity of beach ridge sediment is dominated by particle compactness and bladedness. Average roundness of inner ridge series is sub angular. Angular-sub angular is characterized from roundness trend of middle beach ridge series. Likewise, the outer ridge series roundness trend is sub angular. High sphericity all of beach ridge sediments may come from the coastal area and the mountains in the western and northern area, that are composed of the Permo-carboniferous rocks and Permian rocks.

More than 33 Moluscan species (Gastropod: 6/Bivalvia: 26/Scaphopoda:1) were found from 6 locations in old lagoon of the study area. It was observed from T1-PN12; *Batbytormus radiates*. They were investigated from T2-PN10; *Dosinia sp., Leptomya sp., Donax sp.*, *Scapbarca sp., Solen sp*. and 2 Ostreidae, Scaphopoda can classified as *Antalis sp*. and 1 Echinoidea can't identify. They were investigated from T2-PN11; *Celypeomorus coralia, Anomalocardia (Anomalodiscus) squamosa,* Psammotreta (Tellinimactra) edentula, *Anadara (Potiarca) pilula*. They were investigated from T3-PN1; *Peristernia incarnate***,** *Striarca lacteal,*

*Paphia (Papbia) undulate.* They were investigated from T3-PN2; *Celypeomorus coralia, Anomalocardia (Anomalodiscus) squamosa, Carditella (Carditellona) pulebella.* They were investigated from T3-PN5; *Batbytormus radiates*, *Placamen cholorotica*, *Semele carnicolor*, *Dosinia sp., Mytilus sp.*, *Mactra sp., Anadara oblonga, Arca sp.*, *Celypeomorus coralia, Nassarius pullus, Nassarius siquijorensis, Polinices(Polinices) mammilla, Natica trigina.*

Fossils are of marine environment that can be indicated sandy infralittoral bottoms, intertidal, mangrove habitat when they live. This can be concluded that one of the study areas at T3-PN2 (Ban Thung Kha Noi) used to dominate by marine incursion as far as 9 km from recent coastline. In addition T3-PN1, T3-PN5, T2-PN11, T2-PN10 and T1-PN12 contain bivalve, gastropod, echinoidia, scaphopoda fossil too. These locations used to be effected by the transgression and the intertidal or mangrove environment.

Based on themoluminescence dating (TL dating) of beach ridge sands, the three beach ridge series in the study area are referred to have formed in the late Pleistocene to early Holocene. The wide range of TL age dating from this research may reflect the extensive reworking process and the repeat of deposition of beach sand. However, result of inner ridge dating determined that the formation of inner ridge plain is no older than 10,000 years.

## REFERENCES


Aitken, M.J. 1985. Thermoluminescence dating. London: Academic Press, cited in Pailoplee, S. 2004 . Thermolumonescence dating of Quarternary sediments using total bleach and regeneration method. Master's Thesis, Department of Geology, Faculty of Science, Chulalongkorn University.

Ameral E.J. and Pryor, W.A. 1997. Depositional Environment of the ST. Peter Sandstone Deduce by Textural Analysis. Jounal of Sedimentary Petrology. 47(1): 32-52.

Baruah J., Kotoky P. and Sarma J.N. 1997. Textural and geochemical study on river sediment: A case study on the Jhanji River, Assam. Journal of Indian Association Sedimentologists. 16: 195-206. cited in Kumar, G. , Ramamathan AL. and Rajkumar K. 2010. Textural characteristic of the surface sediments of a Tropical mangrove ecosystem Gilf of Kachchh, Gujarat, India. Journal of Indian Association Sedimentologists. 39(3): 415-422.

Bell, W.T. 1979. Attenuation factors for the absorbed radiation dose in quartz inclusions for thermoluminescence dating. Ancient TL 8: 2-13, cited in Pailoplee, S. 2004 . Thermolumonescence dating of Quarternary sediments using total bleach and regeneration method. Master's Thesis, Department of Geology, Faculty of Science, Chulalongkorn University.

Boggs, S. 1987. Principle of sedimentology and stratigraphy, Merrill Publ. Co.

Chaimanee, N. 2000. COASTAL EVOLUTION OF THE GREATER SURAT THANI CITY AREA , SOUTHERN THAILAND. Academic symposium , Geology division, Department of Mineral Resource 3-4 September 2000.

Choowong, M. 2010. Academic lectures and discussion on " U-Thong of civilization Suvarnabhumi " in Lecture notes and academic discussion about the " U-Thong of civilization Suvarnabhumi. at the Department of Fine Arts Regional Office 2 at Suphanburi. 1-15 p.

Choowong, M. 2002a. Isostatic models and Holocene relative changes in sea level from the coastal lowland area in the Gulf of Thailand. Journal of Scientific Reserch, Chulalongkorn University 27(1): 83-92.

Choowong, M. 2002b. The geomorphology and assessment of indicators of sea-level change to study coastal evolution from the gulf of Thailand. International Symposium on Geology of Thailand. pp. 208-220. Department of Mineral Resource, Bangkok, Thailand.

Choowong, M., Ugai, H., Charoentitirat, T., Charusiri, P., Daorerk, V., Songmuang, R. and Ladachart, R. 2004. Holocene Biostratigraphical Record in Coastal Deposit from Sam Roi Yod National Park, Prachuap Khiri Khan, Western Thailand. The Natural History Journal of Chulalongkorn University 4(2): 1-18.

Choowong, M. 2006. Lecture note Advance Geomorphology. Department of Geology, Faculty of Science, Chulalongkorn University. p.203.

Choowong, M., 2011. “Quaternary”, Book Series “Geology of Thailand”. In: Ridd, M.F., Barber, A.J., Crow, M.J. (Eds). Geological Society of London (Chapter 12), 335-349

Compton, R.R., 1962, Manual of field geology: New York, John Wiley and Sons, Inc., 378 p.

Compton,1962. Charts for Estimating Mineral Grain Percentage Composition of Rocks and Sediments [online] Available from: http://www.usouthal.

Department of Mineral resource. Geology of Thailand. On the occasion of the auspicious ceremony of King Bhumibol Adulyadej Celebrations 6 round Dec. 5, 1999 by the Department of Mineral Resources-Bangkok: Department of Mineral Resources. Ministry of Industry 2001, 556 pages; 30 cm

Detriche, S., Rodrigues, S., Macaire, J.J., Bonte, P., Breheret, J.G., Bakyono, J.P. and Juce, P. 2010. Caesium-137 in sandy sediment of the River Loire (France): Assessment of an alluvial island evolving over the last 50 years. Geomorphology 115: 11-22.

Dheeradilok, P. 1995. Quaternary Coastal Morphology and Deposition in Thailand . Quaternary International , 26 : 49-54.

Fleming, K., Johnston, P., Zwartz, D, Yokoyama, Y., Lambeck, K. and Chappell, J. 1998. Refining the eustatic sea-level curve since the Last Glacial Maximum using far-and intermediate-field sites Earth and Planetary Science Letters. 163 : 327–342.

Folk, R .L. 1951. Stage of textural matuarity in sedimentary rock. Journal of Sedimentary Petrology. 34 : 864-874. cited in Valia, H.S. and Cameron, B. 1977. Skewness as a Paleoenvironmental Indicator. Journal of Sedimentary Petrology. 47(2) :784-793.

Folk, R.L. and Ward, C.W. 1957. Brazos river bar: a study in the significance of grain size parameters. Journal of Sedimentary Petrology 27(1): 3-26.

Friedman, G. M. 1967. Dynamic process and statistical parameter compared for size frequency distribution of beach and river sand. Journal of Sediment Petrology 37(2):327-354.

Friedman, G. M. and Sander J.E. 1978. Principle of sedimentology: New York-Chichester-Brisbane-Toronto, John Wiley and Sons, 792 p.

Grove, S. A guide to the seashells and other marine mollusks of Tasmania. [online] Available from : http://www.molluscsoftasmania.net [2012, September 11]

Hanebuth,T., Stattegger, K. and Grootes, M.P.2000. Rapid Flooding of the Sunda Shelf: A Late-Glacial Sea-Level Record. SCIENCE. 288:1033-1035.

Huntley D.J. 1985. On the Zeroing of the Thermoluminesence of Sediments. Physics and Chemical of Minerals 12:122-127.

Huntley, D. J., and Prescott, J. R. 2001. Improved methodology and new thermoluminescence ages for the dune sequence in south-east South Australia. Quaternary Science Reviews 20: 57-69.

Huntley, D. J., Godfrey-Smith, D. I., and Thewalt, M. L.W. 1985. Optical dating of sediments. Nature, 313: 105-107.

Hesp, P.A., Hung C.C., Hilton M., Ming C.L. and Turner I.M. 1998. A first Tentative Holocene Sea-Level Curve for Singapore . Journal of Coastal reserch 14(1) : 308-314.

Intarat , T. 2010. Paleo-Coastal Line in Chon Buri Province. SWU Science Journal 26(1): 58-72.

International Fossil Shell Museum, FRANCE: Miocene, Serravalian, Screen 47: Arcoidea. [online] Available from : http://www.fossilshells.nl [2012, September 11]

Kalchgruber, R., Göksu, H. Y., Hochhäuser, E., and Wagner, G. A. 2002. Monitoring environmental dose rate using Risø TL/OSL readers with built-in sources: recommendations for users. Radiation Measurements 35: 585-590, cited in Pailoplee, S. 2004 . Thermolumonescence dating of Quarternary sediments using total bleach and regeneration method. Master's Thesis, Department of Geology, Faculty of Science, Chulalongkorn University.

Krumbein, W. C. 1941. Measurement and geological significance of shape and roundness of sediment particles. Journal of Sedimentary Petrology 11 : 64-72.

Larson, R., Morang, A. and Gorman, L. 1997. Monitoring the coastal environment; Part II; Sediment sampling and geotechnical methods. Journal of coastal research, 13(2); 308-330.

Martin, L.R., 1964. Significant of skewness and kurtosis in environmental interpretation, manuscript received November 19, 1964.

Martin, L. R. and Barboza, E. G. 2005. Sand-Gravel Marine Deposit and Grain-Size Properties, Gravel, 3: 59-70.

Munyikwa, K., Van Den Haute, P., Vandenberghe, D. and De Corte, F. 2000. The age and palaeoenvironmental significance of the Kalahari Sands in western Zimbabwe: a thermoluminescence reconnaissance study. Journal of African Earth Sciences 30(4): 941-956.

Natural History Museum Rotterdam – Noetiidae. [online] Available from : http://www.nmr-pics.nl/Noetiidae/album/.[2012, September 11]

National Center Of Excellence For Environmental And Hazardous Waste Management Chulalongkorn University. 2006. Report of Age determination of soil layer in Sri Sawat Fault and Three pagoda fault , Kanchanaburi province submit a report to Department of Mineral Resource. 169p.

National Musium Wales, Marine Bivalve Shells of the British Isles. [online] Available from : http://naturalhistory.museumwales.ac.uk/britishbivalves/browserecord.php?-recid=50. [2012, September 11]

Olivier Caro 1997-2012 ,SEASHELLS COLLECTION , DENTALIIDAE. [online] Available from : http://www.idscaro.net/sci/01_coll/plates/scapho/pl_dentaliidae_1.htm. [2012, September 12]

Pailoplee, S. 2004 . Thermolumonescence dating of Quarternary sediments using total bleach and regeneration method. Master's Thesis, Department of Geology, Faculty of Science, Chulalongkorn University.

Pettijohn, F.J. 1957. Sedimentary rocks. 2nd ed. New York: Harper & Bros. 718p.

Phantuwongraj, S. 2006 . Shoreline change after the 26 December 2004 Tsunami between Leam Prakarang-Khao Lak area, Changwat Phang-Nga, Thailand. Master's Thesis, Department of Geology, Faculty of Science, Chulalongkorn University.

Pillans, B., Chappell, J., Naish, T. R. 1998. A review of the Milankovitch climatic beat: template for Plio–Pleistocene sea-level changes and sequence stratigraphy. Sedimentary Geology 122:5–21.

Powers, M. C. 1953. A new roundness scale for sedimentary particle. Journal of Sedimentary 23: 117-119

Rabineau, M., Bern, S., Olivet, J. L., Aslanian, D., Guiillocheau, F. and Joseph, P. 2006. Paleo sea levels reconsidered from direct observation of Paleoshoreline position during Glacial Maxima (for the last 500,000 yr). Earth and Planetary Science Letters 252: 119-137.

Ray A.K. Tripathy S.C., Patra S. and Sarma V.V., 2006. Assesment of Godavari estuarine mangrove ecosystem through trace metal studies. Environment International. 32: 219-223. cited in Kumar, G., Ramamathan AL. and Rajkumar K. 2010. Textural characteristic

of the surface sediments of a Tropical mangrove ecosystem Gilf of Kachchh, Gujarat, India. Journal of Indian Association Sedimentologists. 39(3): 415-422.

Ridd, M.F., Barber A.J. and Crow, M.J. 2011.The Geology of Thailand. The Geological Society of London. 626p.

Robba, E., Geronimo, I. D., Chaimanee, N., Negri, M.P. and Sanfilippo, R. 2002. Holocene and Recent shallow soft-bottom mollusks from the northern Gulf of Thailand area: Scaphopoda, Gastropoda, additions to Bivalve, by Societa Italiana di Malacologia. Bolletino Malacologico 38(5-8): 49-132.

Royai Thai Survey Department.2000. Topographic map scale 1:50,000. Sheet 4829 IV series L7018, edition 1-RTSD. Bangkok: Royal Thai Survey Department.

Peter S. Roy. 1990. Offshore mineral exploration in the gulf of Thailand; Review of Quaternary Geology of the coast and offshore seabed in exploration area 2, by Marine Geologist, Geological Survey of NSW, Department of Mineral and Energy and Research Affiliate, Department of Geography, The University of Sydney, NSW 2006, Australia. Mission Report: February 4-28, 1990.

Rubey, W.W. 1933. The size distribution of heavy minerals within a water-laid sediment. Journal of Sedimentary Petrology. 3: 3-11. Cited in Thomas, D.S.G. Discrimination of depositional environments using sedimentary characteristics in the Mega Kalahari, central southern Africa. Inpress. 293-306.

Silapanth, P. 2005. Geoarcheology of Thungsetthi, Tambon Nayang, Amphoe Cha-Am, Changwat Phetchaburi. Master's Thesis, Department of Geology, Faculty of Science, Chulalongkorn University.

Silsakul, S., Sonsuk, M. and Hesting, P.J. 1985. Holocene sea level in Thailand: Evidence and basis for interpretation. Journal of Geology Society of Thailand 8:1-12.

Silsakul, S., Tantiyapirat, S., Chaimanee, N. and Aramprayoon, B., 2002, Academic report of The Changing coastal areas of the Gulf of Thailand. 1th Edition. Modern Film Center Company Ltd. Bangkok.

Simon, J.B. and Kenneth, P. 2001. Gradistat : A Grain Size Distribution and Statistics Package for the Analysis of Unconsolidated Sediments. Earth Surface Processes and Landforms 26: 1237-1248.

Supajanya, T. 1981. Delineation of the regression shorelines in the lower Chao Phraya Plain. Proceedings of the Seventeenth Session, Committee for Coordination of Joint Prospecting for Mineral Resources, 232-237, cited in Choowong, M. Basic Geomorphology. 500. 1. Teanwattana printing, 2010.

Supajanya, T. 1983. Tentative correlation of old shorelines around the Gulf of Thailand. First Symposium on Geomorphology and Quaternary Geology of Thailand, Bangkok, Thailand, October 1983,96-105, cited in cited in Choowong, M. Basic Geomorphology. 500. 1. Teanwattana printing, 2010.

Surakiatchai, P. 2005. Classification of gastropoda and bivalvia fossils from the KHao Sam Roi Yod National Park, Prachuap Khiri Khan Provimce, Thailand. Master's Thesis, Department of Geology, Faculty of Science, Chulalongkorn University.

Takashima, I., and Honda, S. 1989. Comparision between K-Ar and TL dating results of pyroclastic flow deposits in the Aizutajima area, Northeast Japan. Joural of Geological Society 95: 807-816, cited in Pailoplee, S. 2004 . Thermolumonescence dating of

Quarternary sediments using total bleach and regeneration method. Master's Thesis, Department of Geology, Faculty of Science, Chulalongkorn University.

Takashima, I. and Walanabe, K. 1994. Thermoluminescence age determination of lava flows/domes and collapsed materials at Unzen volcano, SW Japan. Bulletin of the Volcanological Society of Japan 39: 1-12, cited in Pailoplee, S. 2004 . Thermolumonescence dating of Quarternary sediments using total bleach and regeneration method. Master's Thesis, Department of Geology, Faculty of Science, Chulalongkorn University.

Thongpinyochai, A. 1996. Geology of Chumphon Province in Minerals Resources Regional Office 2 (Phuket) Report, Department of Mineral Resource, Ministry of Industry.

Valia, H.S. and Cameron, B. 1977. Skewness as a Paleoenvironmental Indicator. Journal of Sedimentary Petrology. 47(2): 784-793.

Vana, N. Applications of TL and OSL dating. Institute of Atomic and Subatomic Physics, Vianna Univesity of Technology [online] Available from : http://www.ati.ac.at/arch/css/files/Vana.pdf , September 2]

Vongvisessomjai, S. 2010. Effect of Global warming in Thailand. Songklanakarin J. Sci. Technol. 32(4): 431-444.

Walker, M. 1947. Quaternary dating methods. John Wiley and Sons Ltd, England, 304 P.

Wikipedia, the free encyclopedia, oyster. [online] Available from : http://en.wikipedia.org/wiki/Oyster#Habitat_and_behaviour [2012, September 11]

Wikipedia, Arca (genus). [online] Available from : http://en.wikipedia.org/wiki/Arca_ (genus). [2012, September 11]

Wikipedia, Donax. [online] Available from : http://en.wikipedia.org/wiki/Donax. [2012, September 12]

Wikipedia, Tusk shell . [online] Available from : http://en.wikipedia.org/wiki/Tusk_shell#Habitat_and_distribution. [2012, September 12]

Wintle, A. G. and Huntley, D. J. 1980. Thermoluminescence dating of ocean sediments. Canadian Journal of Earth Sciences 17: 348-360.

Wood, W.W., Bailey, R. M., Hampton, B. A., Kraemer T. F., Lu, Z., Clark D.W., James, R.H. and Al Ramadan, K. 2012. Rapid late Pleistocene/Holocene uplift and coastal evolution of the southern Arabian(Persian) Gulf. Quaternary Research 77: 215–220.

Woodroffe, S.A. and Horton, B.P. 2005. Holocene sea-level changes in the Indo-Pacific. Journal of Asian Earth Science. 25: 29-43.

Won-in, K. 2003. Quaternary geology of the Phrae basin, northern Thailand and application of thermoluminescence technique for quaternary chronology. Doctoral dissertation. Graduate School of Mining and Engineering, Akita University, Japan , cited in Pailoplee, S. 2004 . Thermolumonescence dating of Quarternary sediments using total bleach and regeneration method. Master's Thesis, Department of Geology, Faculty of Science, Chulalongkorn University.

# APPENDICES

# Appendix A

Data for Lithological of Bore Hole.

| Lithology | Layer contact | Thickness (cm) | Description |
|---|---|---|---|
| 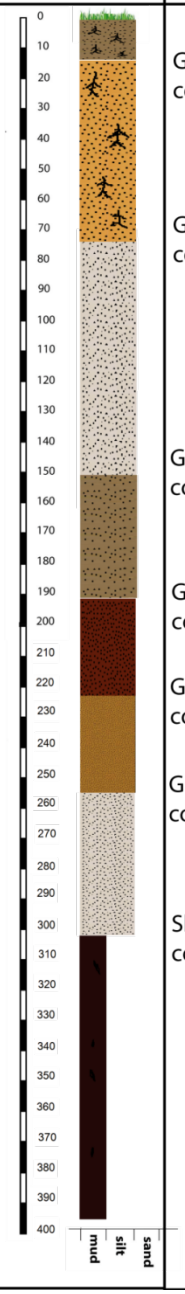 | Gradational contact | 13 | Organic sand ; fine sand; brownish black; rootlets. |
| | Gradational contact | 61 | Fine sand; brown; granules; rootlets. |
| | Gradational contact | 76 | Fine sand; light brown. |
| | Gradational contact | 40 | Fine sand; brown. |
| | Gradational contact | 33 | Fine sand; reddish brown. |
| | Gradational contact | 34 | Fine sand; brown. |
| | Sharp contact | 45 | Fine sand; light brown. |
| | | 95 | Mud; black; chacoal fragment. |



**Figure A.1** The lithological log of T1-PN1.

| Lithology | Layer contact | Thickness (cm) | Description |
|---|---|---|---|
| 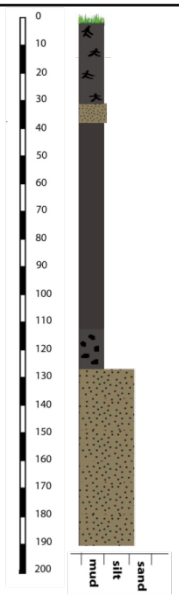 | Disturbe 50-60 cm. | 126 | Mud; brownish grey to grey; contaminated with sandy mud . in the bottom of layer found peat fragment. |
| | Gradational contact | 64 | Fine sand; grey. |



**FigureA.2** The lithological log of T1-PN2.

| Lithology | Layer contact | Thickness (cm) | Description |
|---|---|---|---|
| 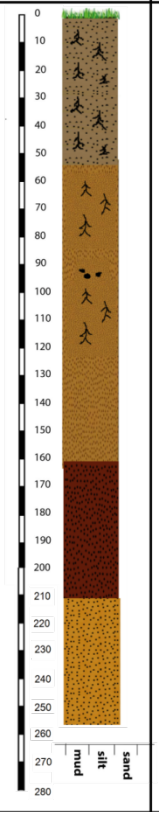 | | 53 | Organic sand ; fine sand; brown; rootlets. |
| | Gradational contact | | |
| | | 57 | Fine sand; brown; chacoal fragments; rootlets. |
| | Gradational contact | | |
| | | 50 | Fine sand; reddish brown. |
| | Gradational contact | | |
| | | 47 | Fine sand; brown. |



**Figure A.3** The lithological log of T1-PN3.

| Lithology | Layer contact | Thickness (cm) | Description |
|---|---|---|---|
| 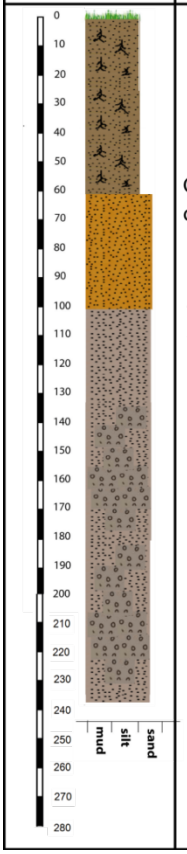 | Gradational contact | 60 | Organic sand ; fine sand; brown; rootlets. |
| | Gradational contact | 40 | Medium sand; yellowis brown; rootlets. |
| | | 138 | Mwdium sand; light brown. |



**Figure A.4** The lithological log of T1-PN6.

| Lithology | Layer contact | Thickness (cm) | Description |
|---|---|---|---|
| 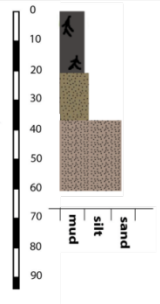 | Gradational contact | 38 | Mud; black; near contact found yellowish black shows oxidization of mud. In the bottom part exhibit sand confound with mud. |
| | | 22 | Fine sand; grey. |



**Figure A.5** The lithological log of T1-PN7.

| Lithology | Layer contact | Thickness (cm) | Description |
|---|---|---|---|
| 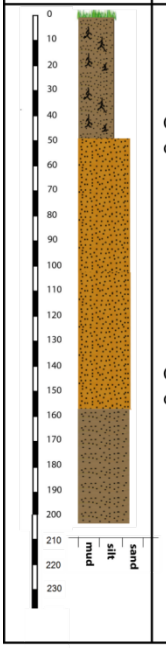 | | 50 | Organic sand ; fine sand; brownish black; rootlets. |
| | Gradational contact | | |
| | | 108 | Middle sand; yellowish brown. |
| | Gradational contact | | |
| | | 45 | Fine sand; light brown. |



**Figure A.6** The lithological log of T1-PN8.

| Lithology | Layer contact | Thickness (cm) | Description |
|---|---|---|---|
| 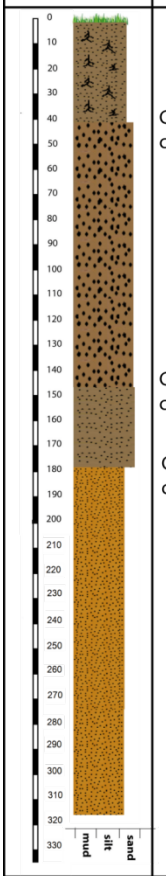 | | 40 | Organic sand ; fine sand; brown; rootlets. |
| | Gradational contact | | |
| | | 107 | Medium sand; yellowish brown. |
| | Gradational contact | | |
| | | 32 | Medium sand; light brown. |
| | Gradational contact | | |
| | | 126 | Fine sand; orangey brown. |



**Figure A.7** The lithological log of T1-PN9.

| Lithology | Layer contact | Thickness (cm) | Description |
|---|---|---|---|
| 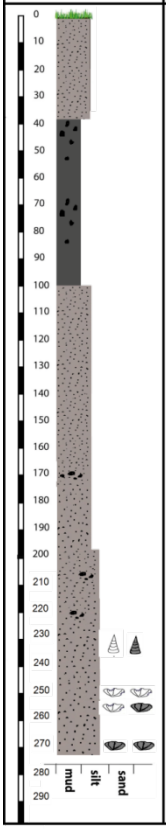 | | 38 | Muddy sand; greyish black with greenish grey mottle. |
| | Sharp contact | | |
| | | 62 | Mud; brownish black with peat fragment approximately 70%. |
| | Gradational contact | | |
| | | 100 | Muddy sand; brownish black with some peat fragment. |
| | | 70 | Sandy mud; brownish black to grey; with some peat fragment; shell fragment size 2-3 mm. and complete shell (bivalve and gastropod. |
| | Gradational contact | | |



**Figure A.8** The lithological log of T1-PN11.

| Lithology | Layer contact | Thickness (cm) | Description |
|---|---|---|---|
| 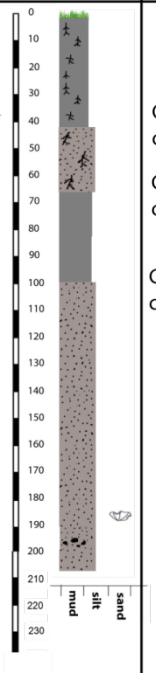 | | 13 | Mud ; greyish brown; rootlet. |
| | Gradational contact | | |
| | | 61 | Mud confound with medium sand; grey; roolets. |
| | Gradational contact | | |
| | | 76 | Mud ;grey with some brown mottle |
| | Gradational contact | | |
| | | 40 | Mud confound with fine sand; grey; bivalve and some peat fragment. |



**Figure A.9** The lithological log of T1-PN12.

| Lithology | Layer contact | Thickness (cm) | Description |
|---|---|---|---|
| 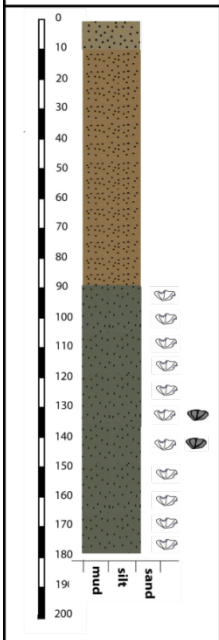 | Gradational contact | 10 | Fine sand; light brown. |
| | | 80 | Fine sand; brown. |
| | Gradational contact | | |
| | | 80 | Fine sand; grey to greenish gray with shell fragments. |



**Figure A.10** The lithological log of T1-PN13.

| Lithology | Layer contact | Thickness (cm) | Description |
|---|---|---|---|
| 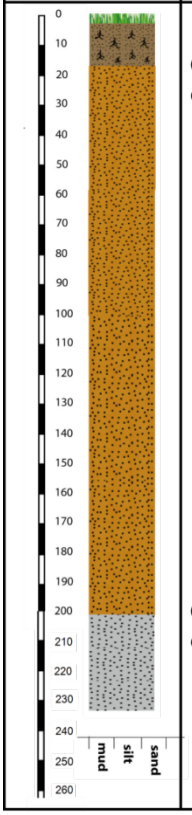 | Gradational contact | 18 | Medium sand; brown rootlets. |
| | | 182 | Medium sand; yellowish brown. |
| | Gradational contact | 33 | Medium sand; light brown. |



**Figure A.11** The lithological log of T1-PN14.

| Lithology | Layer contact | Thickness (cm) | Description |
|---|---|---|---|
| 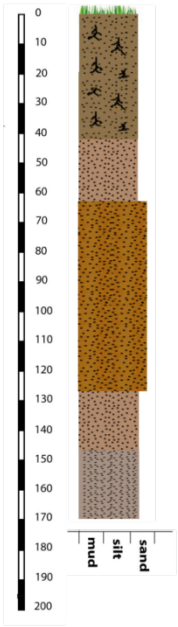 | | 40 | Organic sand; fine sand; dark brown; rootlets. |
| | Gradational contact | 23 | Fine sand; brown. |
| | Gradational contact | 60 | Medium sand; reddish brown to brown. |
| | Gradational contact | 20 | Fine sand; brown. |
| | Gradational contact | 22 | Fine sand; light brown; som shell fragments. |



**Figure A.12** The lithological log of T2-PN1.

| Lithology | Layer contact | Thickness (cm) | Description |
|---|---|---|---|
| 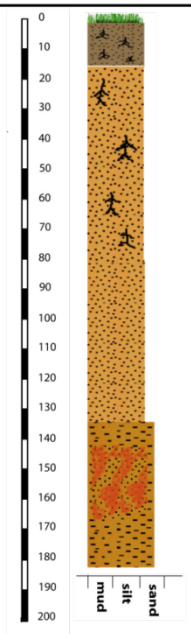 | Sharp contact | 18 | Organic sand; fine sand; brown ; rootlets. |
| | | 115 | Fine sand; yellowish brown ; some rootlets in upper part. |
| | Gradational contact | 50 | Coarse sand combine with mud and some gravel (gravel size less than 5 cm. ;approximately 50%); yellowish to reddish brown. |



**Figure A.13** The lithological log of T2-PN2.

| Lithology | Layer contact | Thickness (cm) | Description |
|---|---|---|---|
| 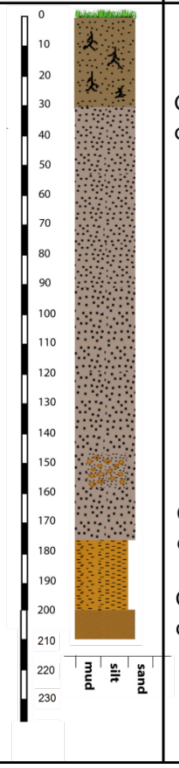 | | 30 | Fine sand; brown; rootlets. |
| | Gradational contact | | |
| | | 43 | Fine sand; light brown to light grey. |
| | Gradational contact | 22 | Very fine sand with some gravel ( 3%); yellowish brown. |
| | Gradational contact | 10 | Fine sand; brown. |



**Figure A.14** The lithological log of T2-PN3.

| Lithology | Layer contact | Thickness (cm) | Description |
|---|---|---|---|
| 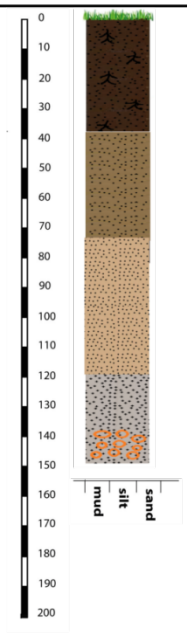 | | 37 | Organic sand; medium sand; dark brown ; rootlets. |
| | Gradational contact | | |
| | | 35 | Medium sand; brown. |
| | Gradational contact | | |
| | | 47 | Medium sand; light brown with som yellow mottle. |
| | Gradational contact | 28 | Medium sand; light grey with orangey brown mottle. |



**Figure A.15** The lithological log of T2-PN4.

| Lithology | Layer contact | Thickness (cm) | Description |
|---|---|---|---|
| 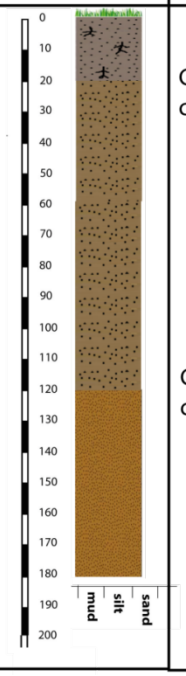 | Gradational contact | 20 | Organic sand ; medium sand sand; brownish black; rootlets. |
| | | 100 | Medium sand; brown. |
| | Gradational contact | | |
| | | 60 | Medium sand; yellowish brown. |



**Figure A.16** The lithological log of T2-PN5.

| Lithology | Layer contact | Thickness (cm) | Description |
|---|---|---|---|
| 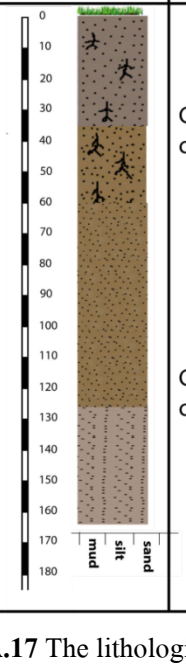 | | 37 | Organic sand ; medium sand; dark brown; rootlets. |
| | Gradational contact | | |
| | | 87 | Medium sand; brown. |
| | Gradational contact | | |
| | | 35 | Medium sand; dark brown. |



**Figure A.17** The lithological log of T2-PN6.

| Lithology | Layer contact | Thickness (cm) | Description |
|---|---|---|---|
| 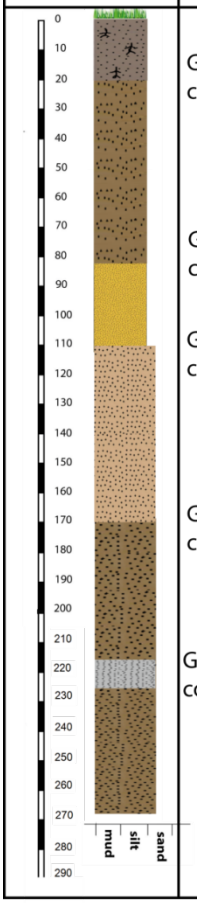 | Gradational contact | 20 | Organic sand ; fine sand; dark brown; rootlets. |
| | | 60 | Fine sand; brown. |
| | Gradational contact | | |
| | | 30 | Fine sand; yellowish brown. |
| | Gradational contact | | |
| | | 60 | Medium sand; light brown. |
| | Gradational contact | | |
| | | 48 | Medium sand; brown. |
| | Gradational contact | 10 | Medium sand; grey. |
| | | 40 | Medium sand; brown. |



**Figure A.18** The lithological log of T2-PN7.

| Lithology | Layer contact | Thickness (cm) | Description |
|---|---|---|---|
| 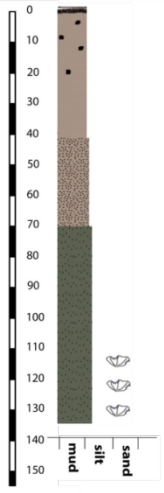 | | 40 | Mud; brown with some peat fragments. |
| | Gradational contact | 30 | Mud brown confound with very fine sand. |
| | Gradational contact | | |
| | | 80 | Fine sand con found with mud; grey to greenish gray with shell fragments. |



**Figure A.19** The lithological log of T2-PN8.

| Lithology | Layer contact | Thickness (cm) | Description |
|---|---|---|---|
| 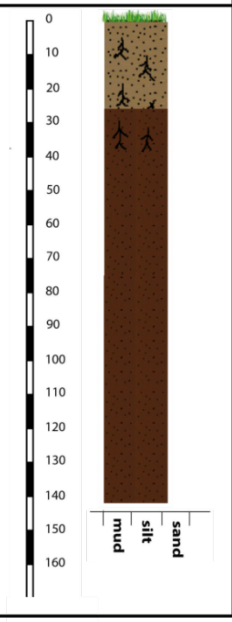 | Gradational contact | 38 | Organic sand; fine sand; dark brown ; rootlets. |
| | | 64 | Fine sand; brown. |



**Figure A.20** The lithological log of T2-PN9.

| Lithology | Layer contact | Thickness (cm) | Description |
|---|---|---|---|
| 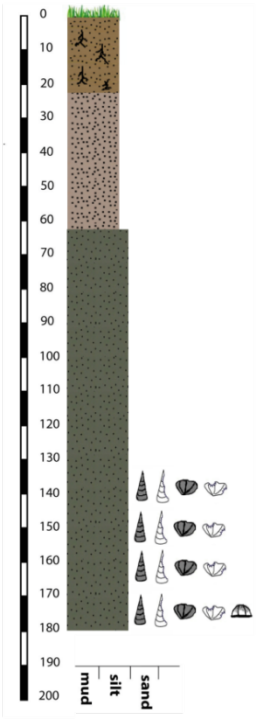 | Gradational contact | 20 | Medium to fine sand; brown with reddish brown mottle. |
| | Gradational contact | 40 | Medium to fine sand; grey to greenish grey. |
| | | 120 | Fine sand; greenish grey; found gastropods, gastropod fragments, bivalves, bivalve fragments, scaphopoda and echinoderm (sea urchin) at depth 140-180 cm. |



**Figure A.21** The lithological log of T2-PN10.

| Lithology | Layer contact | Thickness (cm) | Description |
|---|---|---|---|
| 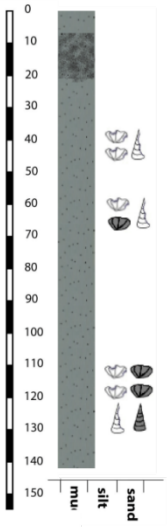 | | 140 | Fine sand confound with mud; grey; some gastropod and bivalve fragment and completed shell at depth 40 cm , 60-17cm and 110-130 cm. |



**Figure A.22** The lithological log of T3-PN2.

| Lithology | Layer contact | Thickness (cm) | Description |
|---|---|---|---|
| 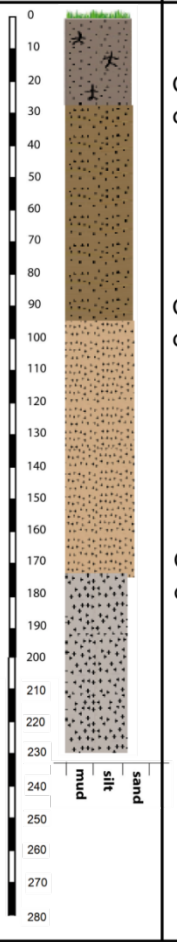 | Gradational contact | 30 | Organic sand ; medium sand; brown; rootlets. |
| | | 65 | Medium sand; brown. |
| | Gradational contact | | |
| | | 77 | Medium sand; light brown. |
| | Gradational contact | | |
| | | 55 | Fine sand; greyish brown. |



**Figure A.23** The lithological log of T3-PN3.

| Lithology | Layer contact | Thickness (cm) | Description |
|---|---|---|---|
| 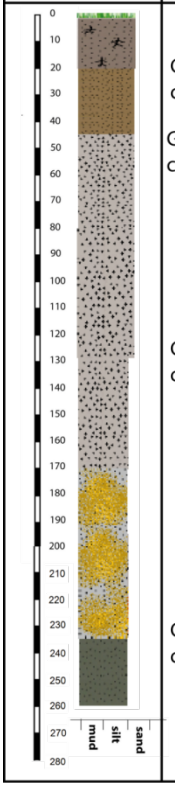 | | 20 | Organic sand ; Medium sand; dark brown; rootlets. |
| | Gradational contact | | |
| | | 24 | Medium sand; brown. |
| | Gradational contact | | |
| | | 85 | Medium sand; light brown. |
| | Gradational contact | | |
| | | 115 | Fine sand; greyish brown with yellowish brown mottle.. |
| | Gradational contact | | |
| | | 26 | Fine sand; brown. |



**Figure A.24** The lithological log of T3-PN4.

| Lithology | Layer contact | Thickness (cm) | Description |
|---|---|---|---|
| 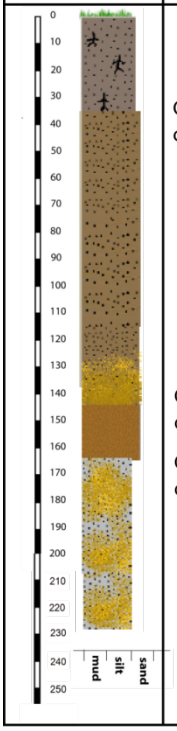 | | 35 | Organic sand ; fine sand; dark brown; rootlets. |
| | Gradational contact | | |
| | | 110 | Medium sand; brown. |
| | Gradational contact | | |
| | Gradational contact | 20 | Fine sand; yellowish brown to brown. |
| | | 60 | Fine sand; grey coat with yellowish brown. |



**Figure A.25** The lithological log of T3-PN5.

| Lithology | Layer contact | Thickness (cm) | Description |
|---|---|---|---|
| 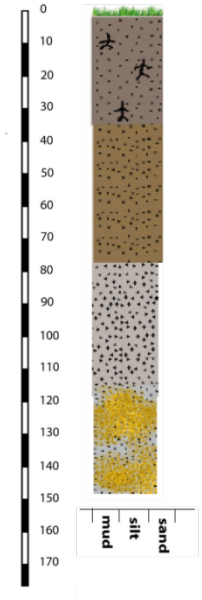 | | 35 | Medium sand; dark brown; rootlets. |
| | Gradational contact | | |
| | | 45 | Medium sand; light brown. |
| | Gradational contact | | |
| | | 70 | Fine sand; greyish brown coat with yellowish brown. |



**Figure A.26** The lithological log of T3-PN6.

| Lithology | Layer contact | Thickness (cm) | Description |
|---|---|---|---|
| 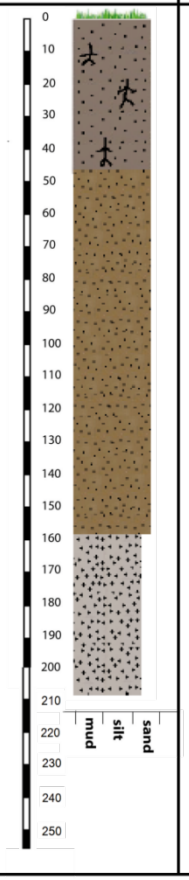 | | 47 | Organic sand ; medium sand; dark brown; rootlets. |
| | Gradational contact | | |
| | | 113 | Medium sand; brown. |
| | Gradational contact | | |
| | | 48 | Fine sand; light brown. |



**Figure A.27** The lithological log of T3-PN7.

| Lithology | Layer contact | Thickness (cm) | Description |
|---|---|---|---|
| 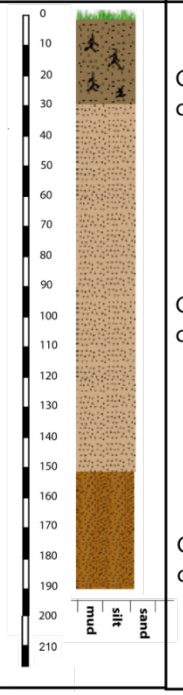 | Gradational contact | 30 | Fine sand; dark brown; rootlets. |
| | Gradational contact | 122 | Fine sand; brown to yellowish brown. |
| | Gradational contact | 38 | Fine sand; yellowish brown. |



**Figure A.28** The lithological log of T3-PN8.

| Lithology | Layer contact | Thickness (cm) | Description |
|---|---|---|---|
| 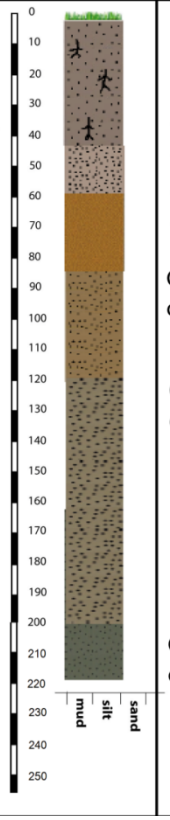 | | 42 | Organic sand ; fine sand; dark brown; rootlets. |
| | Gradational contact | 18 | Fine sand; light brown. |
| | Gradational contact | 25 | Medium sand; yellowish brown. |
| | Gradational contact | 37 | Fine sand; brown to yellowish brown. |
| | Gradational contact | 80 | Fine sand; brown. |
| | Gradational contact | 18 | Medium sand; greyish brown. |



**Figure A.29** The lithological log of T3-PN9.

# Appendix B

Composition and Physical Properties of Beach Ridge Sediments.

**Table B.1** Composition and Physical Properties of Beach Ridge Sediments of Transect 1.

| Sample number | Composition | | | | | | | | Sphericity | | Roundness | | | | | |
|---|---|---|---|---|---|---|---|---|---|---|---|---|---|---|---|---|
| | Quartz | Feldspar | Rock fragment | Mica | Skeleton debris | Ferromagnesian | Unknown | Other | Low | High | Very angular | angular | Sub-angular | Sub-round | Round | Well-rounded |
| T1-PN1-1 | 97.78 | 0.02 | 1 | 0 | 0 | 1.2 | 0 | 0 | | ✓ | | | | | | |
| T1-PN1-2 | 98.8 | 1 | 0 | 0 | 0 | 0.2 | 0 | 0 | | ✓ | | | | | | |
| T1-PN1-3 | 98.1 | 1.1 | 0 | 0 | 0 | 0.8 | 0 | 0 | | ✓ | | | | | | |
| T1-PN1-5 | 95.5 | 2.5 | 0 | 0 | 0 | 2 | 0 | 0 | | ✓ | | | | | | |
| T1-PN1-7 | 95 | 3 | 0 | 0 | 0 | 2 | 0 | 0 | | ✓ | | | | | | |
| T1-PN1-9 | 96 | 1.5 | 1.5 | 0 | 0 | 1 | 0 | 0 | | ✓ | | | | | | |
| T1-PN1-11 | 91.5 | 4 | 1.5 | 0 | 0 | 3 | 0 | 0 | | ✓ | | | | | | |
| T1-PN1-14 | 93 | 4.5 | 0.5 | 0 | 0 | 2 | 0 | 0 | | ✓ | | | | | | |
| Average | 95.71 | 2.2025 | 0.5625 | 0 | 0 | 1.525 | 0 | 0 | | ✓ | | | ✓ | | | |

| Sample number | Composition | | | | | | | | Sphericity | | Roundness | | | | | |
|---|---|---|---|---|---|---|---|---|---|---|---|---|---|---|---|---|
| | Quartz | Feldspar | Rock fragment | Mica | Skeleton debris | Ferromagnesian | Unknown | Other | Low | High | Very angular | angular | Sub-angular | Sub-round | Round | Well-rounded |
| T1-PN3-1 | 94.5 | 2.5 | 0 | 0 | 0 | 3 | 0 | 0 | | ✓ | | | | | | |
| T1-PN3-2 | 95.7 | 2 | 0 | 0.1 | 0 | 2.2 | 0 | 0 | | ✓ | | | | | | |
| T1-PN3-3 | 96.5 | 1.5 | 0 | 0 | 0 | 2 | 0 | 0 | | ✓ | | | | | | |
| T1-PN3-6 | 98.5 | 1 | 0 | 0 | 0 | 0.5 | 0 | 0 | | ✓ | | | | | | |
| T1-PN3-9 | 96.9 | 2.5 | 0 | 0.1 | 0 | 0.5 | 0 | 0 | | ✓ | | | | | | |
| T1-PN3-11 | 97.9 | 1.7 | 0 | 0.1 | 0 | 0.3 | 0 | 0 | | ✓ | | | | | | |
| Average | 96.667 | 1.86667 | 0 | 0.05 | 0 | 1.416666667 | 0 | 0 | | ✓ | | | ✓ | | | |

| Sample number | Composition | | | | | | | | Sphericity | | Roundness | | | | | |
|---|---|---|---|---|---|---|---|---|---|---|---|---|---|---|---|---|
| | Quartz | Feldspar | Rock fragment | Mica | Skeleton debris | Ferromagnesian | Unknown | Other | Low | High | Very angular | angular | Sub-angular | Sub-round | Round | Well-rounded |
| T1-PN5-1 | 99.3 | 0.2 | 0 | 0 | 0 | 0.5 | 0 | 0 | | ✓ | | | | | | |
| T1-PN5-4 | 98.3 | 1.5 | 0 | 0 | 0 | 0.2 | 0 | 0 | | ✓ | | | | | | |
| T1-PN5-6 | 98.75 | 1.2 | 0 | 0 | 0 | 0.05 | 0 | 0 | | ✓ | | | | | | |
| T1-PN5-8 | 98.6 | 1.3 | 0 | 0 | 0 | 0.1 | 0 | 0 | | ✓ | | | | | | |
| T1-PN5-11 | 98.3 | 1.5 | 0 | 0 | 0 | 0.2 | 0 | 0 | | ✓ | | | | | | |
| T1-PN5-13 | 95.35 | 4.5 | 0 | 0 | 0 | 0.15 | 0 | 0 | | ✓ | | | | | | |
| T1-PN5-15 | 97.4 | 2.5 | 0 | 0 | 0 | 0.1 | 0 | 0 | | ✓ | | | | | | |
| Average | 98 | 1.81429 | 0 | 0 | 0 | 0.185714286 | 0 | 0 | | ✓ | | | ✓ | | | |

| Sample number | Composition | | | | | | | | Sphericity | | Roundness | | | | | |
|---|---|---|---|---|---|---|---|---|---|---|---|---|---|---|---|---|
| | Quartz | Feldspar | Rock fragment | Mica | Skeleton debris | Ferromagnesian | Unknown | Other | Low | High | Very angular | angular | Sub-angular | Sub-round | Round | Well-rounded |
| T1-PN6-1 | 99.85 | 0.05 | 0 | 0 | 0 | 0.1 | 0 | 0 | | ✓ | | | | | | |
| T1-PN6-3 | 99.14 | 0.8 | 0 | 0 | 0 | 0.06 | 0 | 0 | | ✓ | | | | | | |
| T1-PN6-4 | 99.25 | 0.7 | 0 | 0 | 0 | 0.05 | 0 | 0 | | ✓ | | | | | | |
| T1-PN6-7 | 95 | 5 | 0 | 0 | 0 | 0 | 0 | 0 | | ✓ | | | | | | |
| Average | 98.31 | 1.6375 | 0 | 0 | 0 | 0.0525 | 0 | 0 | | ✓ | | | ✓ | | | |

| Sample number | Composition | | | | | | | | Sphericity | | Roundness | | | | | |
|---|---|---|---|---|---|---|---|---|---|---|---|---|---|---|---|---|
| | Quartz | Feldspar | Rock fragment | Mica | Skeleton debris | Ferromagnesian | Unknown | Other | Low | High | Very angular | angular | Sub-angular | Sub-round | Round | Well-rounded |
| T1-PN8-2 | 98.5 | 1.2 | 0 | 0 | 0 | 0.3 | 0 | 0 | | ✓ | | | | | | |
| T1-PN8-5 | 97.81 | 2 | 0.01 | 0 | 0 | 0.1 | 0 | 0 | | ✓ | | | | | | |
| T1-PN8-9 | 97.74 | 2.5 | 0 | 0.01 | 0 | 0 | 0 | 0 | | ✓ | | | | | | |
| Average | 98.017 | 1.9 | 0.0033 | 0.003 | 0 | 0.133333333 | 0 | 0 | | ✓ | | ✓ | ✓ | | | |

| Sample number | Composition | | | | | | | | Sphericity | | Roundness | | | | | |
|---|---|---|---|---|---|---|---|---|---|---|---|---|---|---|---|---|
| | Quartz | Feldspar | Rock fragment | Mica | Skeleton debris | Ferromagnesian | Unknown | Other | Low | High | Very angular | angular | Sub-angular | Sub-round | Round | Well-rounded |
| T1-PN9-1 | 96.8 | 0.9 | 0 | 0 | 0 | 2.3 | 0 | 0 | | ✓ | | | | | | |
| T1-PN9-4 | 97.3 | 1.8 | 0 | 0 | 0 | 0.9 | 0 | 0 | | ✓ | | | | | | |
| T1-PN9-8 | 93.72 | 6.2 | 0.06 | 0 | 0 | 0.02 | 0 | 0 | | ✓ | | | | | | |
| T1-PN9-10 | 95.92 | 3.1 | 0.9 | 0.01 | 0 | 0.07 | 0 | 0 | | ✓ | | | | | | |
| Average | 95.935 | 3 | 0.24 | 0.003 | 0 | 0.8225 | 0 | 0 | | ✓ | | ✓ | ✓ | | | |

| Sample number | Composition | | | | | | | | Sphericity | | Roundness | | | | | |
|---|---|---|---|---|---|---|---|---|---|---|---|---|---|---|---|---|
| | Quartz | Feldspar | Rock fragment | Mica | Skeleton debris | Ferromagnesian | Unknown | Other | Low | High | Very angular | angular | Sub-angular | Sub-round | Round | Well-rounded |
| T1-PN13-1 | 97.58 | 0.7 | 0 | 0.02 | 0.6 | 1.1 | 0 | 0 | | ✓ | | | | | | |
| T1-PN13-3 | 96.69 | 0.5 | 0 | 0.01 | 0.9 | 1.9 | 0 | 0 | | ✓ | | | | | | |
| T1-PN13-7 | 89.8 | 0.4 | 0 | 0.8 | 7 | 2 | 0 | 0 | | ✓ | | | | | | |
| Average | 94.69 | 0.53333 | 0 | 0.277 | 2.83333 | 1.666666667 | 0 | 0 | | ✓ | | ✓ | ✓ | | | |

| Sample number | Composition | | | | | | | | Sphericity | | Roundness | | | | | |
|---|---|---|---|---|---|---|---|---|---|---|---|---|---|---|---|---|
| | Quartz | Feldspar | Rock fragment | Mica | Skeleton debris | Ferromagnesian | Unknown | Other | Low | High | Very angular | angular | Sub-angular | Sub-round | Round | Well-rounded |
| T1-PN14-1 | 97.29 | 1.8 | 0.1 | 0.01 | 0 | 0.8 | 0 | 0 | | ✓ | | | | | | |
| T1-PN14-4 | 96.06 | 2.7 | 1.2 | 0.01 | 0 | 0.03 | 0 | 0 | | ✓ | | | | | | |
| T1-PN14-8 | 97.905 | 1.4 | 0.65 | 0 | 0 | 0.045 | 0 | 0 | | ✓ | | | | | | |
| T1-PN14-9 | 95.75 | 3.5 | 0.7 | 0 | 0 | 0.05 | 0 | 0 | | ✓ | | | | | | |
| T1-PN14-10 | 97.94 | 1.2 | 0.8 | 0.02 | 0 | 0.04 | 0 | 0 | | ✓ | | | | | | |
| T1-PN14-11 | 90.15 | 7.5 | 1.1 | 0.05 | 0 | 1.2 | 0 | 0 | | ✓ | | | | | | |
| Average | 95.849 | 3.01667 | 0.7583 | 0.015 | 0 | 0.360833333 | 0 | 0 | | ✓ | | ✓ | | | | |

**Table B.2** Composition and Physical Properties of Beach Ridge Sediments of Transect 2.

| Sample number | Composition | | | | | | | | Sphericity | | Roundness | | | | | |
|---|---|---|---|---|---|---|---|---|---|---|---|---|---|---|---|---|
| | Quartz | Feldspar | Rock fragment | Mica | Skeleton debris | Ferromagnesian | Unknown | Other | Low | High | Very angular | angular | Sub-angular | Sub-round | Round | Well-rounded |
| T2-PN1-1 | 98.46 | 0.04 | 0 | 0 | 0 | 1.5 | 0 | 0 | | ✓ | | | | | | |
| T2-PN1-3 | 99.09 | 0.8 | 0 | 0.01 | 0 | 0.1 | 0 | 0 | | ✓ | | | | | | |
| T2-PN1-5 | 98.52 | 1.4 | 0.01 | 0.01 | 0 | 0.06 | 0 | 0 | | ✓ | | | | | | |
| T2-PN1-7 | 98.12 | 1.75 | 0 | 0.04 | 0 | 0.09 | 0 | 0 | | ✓ | | | | | | |
| T2-PN1-8 | 94.07 | 5.8 | 0.08 | 0 | 0 | 0.05 | 0 | 0 | | ✓ | | | | | | |
| Average | 97.652 | 1.958 | 0.018 | 0.012 | 0 | 0.36 | 0 | 0 | | ✓ | | | ✓ | | | |

| Sample number | Composition | | | | | | | | Sphericity | | Roundness | | | | | |
|---|---|---|---|---|---|---|---|---|---|---|---|---|---|---|---|---|
| | Quartz | Feldspar | Rock fragment | Mica | Skeleton debris | Ferromagnesian | Unknown | Other | Low | High | Very angular | angular | Sub-angular | Sub-round | Round | Well-rounded |
| T2-PN2-1 | 99.05 | 0.8 | 0.05 | 0 | 0 | 0.1 | 0 | 0 | | ✓ | | | | | | |
| T2-PN2-3 | 98.76 | 1.1 | 0.09 | 0 | 0 | 0.04 | 0 | 0.01 | | ✓ | | | | | | |
| T2-PN2-6 | 99.4 | 0.5 | 0.04 | 0 | 0 | 0.06 | 0 | 0 | | ✓ | | | | | | |
| T2-PN2-7 | 97.61 | 1.1 | 0.09 | 0 | 0 | 1.2 | 0 | 0 | | ✓ | | | | | | |
| T2-PN2-8 | 94.1 | 0.9 | 3.3 | 0 | 0 | 1.7 | 0 | 0 | | ✓ | | | | | | |
| Average | 97.784 | 0.88 | 0.714 | 0 | 0 | 0.62 | 0 | 0.002 | | ✓ | | ✓ | | | | |

| Sample number | Composition | | | | | | | | Sphericity | | Roundness | | | | | |
|---|---|---|---|---|---|---|---|---|---|---|---|---|---|---|---|---|
| | Quartz | Feldspar | Rock fragment | Mica | Skeleton debris | Ferromagnesian | Unknown | Other | Low | High | Very angular | angular | Sub-angular | Sub-round | Round | Well-rounded |
| T2-PN3-1 | 98.03 | 0.03 | 0.04 | 0 | 0 | 1.9 | 0 | 0 | | ✓ | | | | | | |
| T2-PN3-3 | 97.73 | 0.05 | 0.02 | 0 | 0 | 2.2 | 0 | 0 | | ✓ | | | | | | |
| T2-PN3-5 | 99.06 | 0.02 | 0 | 0.02 | 0 | 0.9 | 0 | 0 | | ✓ | | | | | | |
| T2-PN3-7 | 99.375 | 0.015 | 0 | 0.01 | 0 | 0.6 | 0 | 0 | | ✓ | | | | | | |
| T2-PN3-8 | 99.91 | 0 | 0.02 | 0.03 | 0 | 0.04 | 0 | 0 | | ✓ | | | | | | |
| T2-PN3-9 | 97.87 | 0.07 | 0.9 | 0.06 | 0 | 1.1 | 0 | 0 | | ✓ | | | | | | |
| Average | 98.663 | 0.03083 | 0.1633 | 0.02 | 0 | 1.123333333 | 0 | 0 | | ✓ | | ✓ | | | | |

| Sample number | Composition | | | | | | | | Sphericity | | Roundness | | | | | |
|---|---|---|---|---|---|---|---|---|---|---|---|---|---|---|---|---|
| | Quartz | Feldspar | Rock fragment | Mica | Skeleton debris | Ferromagnesian | Unknown | Other | Low | High | Very angular | angular | Sub-angular | Sub-round | Round | Well-rounded |
| T2-PN4-1 | 97.91 | 0.07 | 0.01 | 0.01 | 0 | 2 | 0 | 0 | | ✓ | | | | | | |
| T2-PN4-2 | 99.81 | 0.08 | 0.07 | 0 | 0 | 0.04 | 0 | 0 | | ✓ | | | | | | |
| T2-PN4-4 | 99.91 | 0 | 0.04 | 0.02 | 0 | 0.03 | 0 | 0 | | ✓ | | | | | | |
| T2-PN4-5 | 99.95 | 0 | 0.04 | 0 | 0 | 0.01 | 0 | 0 | | ✓ | | | | | | |
| T2-PN4-6 | 99.95 | 0.01 | 0.02 | 0 | 0 | 0.02 | 0 | 0 | | ✓ | | | | | | |
| Average | 99.506 | 0.032 | 0.036 | 0.006 | 0 | 0.42 | 0 | 0 | | ✓ | | ✓ | | | | |

| Sample number | Composition | | | | | | | | Sphericity | | Roundness | | | | | |
|---|---|---|---|---|---|---|---|---|---|---|---|---|---|---|---|---|
| | Quartz | Feldspar | Rock fragment | Mica | Skeleton debris | Ferromagnesian | Unknown | Other | Low | High | Very angular | angular | Sub-angular | Sub-round | Round | Well-rounded |
| T2-PN5-1 | 99.85 | 0.02 | 0.07 | 0.01 | 0 | 0.05 | 0 | 0 | | ✓ | | | | | | |
| T2-PN5-4 | 99.9 | 0.04 | 0.05 | 0.01 | 0 | 0 | 0 | 0 | | ✓ | | | | | | |
| T2-PN5-7 | 99.93 | 0.01 | 0.03 | 0.02 | 0 | 0.01 | 0 | 0 | | ✓ | | | | | | |
| T2-PN5-8 | 98.29 | 0.03 | 1.6 | 0.02 | 0 | 0.06 | 0 | 0 | | ✓ | | | | | | |
| Average | 99.493 | 0.025 | 0.4375 | 0.015 | 0 | 0.03 | 0 | 0 | | ✓ | | ✓ | | | | |

| Sample number | Composition | | | | | | | | Sphericity | | Roundness | | | | | |
|---|---|---|---|---|---|---|---|---|---|---|---|---|---|---|---|---|
| | Quartz | Feldspar | Rock fragment | Mica | Skeleton debris | Ferromagnesian | Unknown | Other | Low | High | Very angular | angular | Sub-angular | Sub-round | Round | Well-rounded |
| T2-PN6-1 | 92.96 | 6.5 | 0.04 | 0 | 0 | 0.5 | 0 | 0 | | ✓ | | | | | | |
| T2-PN6-3 | 98.77 | 1.1 | 0.08 | 0 | 0 | 0.05 | 0 | 0 | | ✓ | | | | | | |
| T2-PN6-5 | 97.89 | 1.3 | 0.8 | 0 | 0 | 0.01 | 0 | 0 | | ✓ | | | | | | |
| T2-PN6-7 | 99.1 | 0.4 | 0.45 | 0.02 | 0 | 0.03 | 0 | 0 | | ✓ | | | | | | |
| Average | 97.18 | 2.325 | 0.3425 | 0.005 | 0 | 0.1475 | 0 | 0 | | ✓ | | | ✓ | | | |

| Sample number | Composition | | | | | | | | Sphericity | | Roundness | | | | | |
|---|---|---|---|---|---|---|---|---|---|---|---|---|---|---|---|---|
| | Quartz | Feldspar | Rock fragment | Mica | Skeleton debris | Ferromagnesian | Unknown | Other | Low | High | Very angular | angular | Sub-angular | Sub-round | Round | Well-rounded |
| T2-PN7-1 | 97.11 | 1.1 | 1.7 | 0.01 | 0 | 0.08 | 0 | 0 | | ✓ | | | | | | |
| T2-PN7-3 | 99.34 | 0.35 | 0.3 | 0 | 0 | 0.01 | 0 | 0 | | ✓ | | | | | | |
| T2-PN7-5 | 99.67 | 0.05 | 0.25 | 0 | 0 | 0.03 | 0 | 0 | | ✓ | | | | | | |
| T2-PN7-7 | 99.78 | 0.07 | 0.1 | 0 | 0 | 0.05 | 0 | 0 | | ✓ | | | | | | |
| T2-PN7-10 | 99.54 | 0.35 | 0.04 | 0.01 | 0 | 0.06 | 0 | 0 | | ✓ | | | | | | |
| T2-PN7-12 | 99.85 | 0.02 | 0.09 | 0.01 | 0 | 0.03 | 0 | 0 | | ✓ | | | | | | |
| Average | 99.215 | 0.32333 | 0.4133 | 0.005 | 0 | 0.043333333 | 0 | 0 | | ✓ | | | ✓ | | | |

| Sample number | Composition | | | | | | | | Sphericity | | Roundness | | | | | |
|---|---|---|---|---|---|---|---|---|---|---|---|---|---|---|---|---|
| | Quartz | Feldspar | Rock fragment | Mica | Skeleton debris | Ferromagnesian | Unknown | Other | Low | High | Very angular | angular | Sub-angular | Sub-round | Round | Well-rounded |
| T2-PN9-1 | 99.03 | 0.08 | 0.09 | 0 | 0 | 0.8 | 0 | 0 | | ✓ | | | | | | |
| T2-PN9-3 | 98.15 | 0.2 | 0.95 | 0 | 0 | 0.7 | 0 | 0 | | ✓ | | | | | | |
| T2-PN9-5 | 98.62 | 0.08 | 0.7 | 0 | 0 | 0.6 | 0 | 0 | | ✓ | | | | | | |
| Average | 98.6 | 0.12 | 0.58 | 0 | 0 | 0.7 | 0 | 0 | | ✓ | | | ✓ | | | |

**Table B.3** Composition and Physical Properties of Beach Ridge Sediments of Transect 3.

| Sample number | Composition | | | | | | | | Sphericity | | Roundness | | | | | |
|---|---|---|---|---|---|---|---|---|---|---|---|---|---|---|---|---|
| | Quartz | Feldspar | Rock fragment | Mica | Skeleton debris | Ferromagnesian | Unknown | Other | Low | High | Very angular | angular | Sub-angular | Sub-round | Round | Well-rounded |
| T3-PN3-1 | 99.25 | 0.2 | 0.3 | 0 | 0 | 0.25 | 0 | 0 | | ✓ | | | | | | |
| T3-PN3-4 | 99.02 | 0.9 | 0.08 | 0 | 0 | 0 | 0 | 0 | | ✓ | | | | | | |
| T3-PN3-6 | 99.91 | 0.03 | 0.06 | 0 | 0 | 0 | 0 | 0 | | ✓ | | | | | | |
| T3-PN3-7 | 99.87 | 0.02 | 0.1 | 0.01 | 0 | 0 | 0 | 0 | | ✓ | | | | | | |
| T3-PN3-9 | 99.76 | 0.08 | 0.15 | 0.01 | 0 | 0 | 0 | 0 | | ✓ | | | | | | |
| T3-PN3-11 | 99.85 | 0.03 | 0.1 | 0.01 | 0 | 0.01 | 0 | 0 | | ✓ | | | | | | |
| Average | 99.61 | 0.21 | 0.1317 | 0.005 | 0 | 0.043333333 | 0 | 0 | | ✓ | | | ✓ | | | |

| Sample number | Composition | | | | | | | | Sphericity | | Roundness | | | | | |
|---|---|---|---|---|---|---|---|---|---|---|---|---|---|---|---|---|
| | Quartz | Feldspar | Rock fragment | Mica | Skeleton debris | Ferromagnesian | Unknown | Other | Low | High | Very angular | angular | Sub-angular | Sub-round | Round | Well-rounded |
| T3-PN4-1 | 98.11 | 0.03 | 1.8 | 0 | 0 | 0.06 | 0 | 0 | | ✓ | | | | | | |
| T3-PN4-2 | 99.85 | 0.02 | 0.1 | 0 | 0 | 0.03 | 0 | 0 | | ✓ | | | | | | |
| T3-PN4-4 | 99.77 | 0.09 | 0.1 | 0.02 | 0 | 0.02 | 0 | 0 | | ✓ | | | | | | |
| T3-PN4-7 | 99.86 | 0.02 | 0.06 | 0.02 | 0 | 0.04 | 0 | 0 | | ✓ | | | | | | |
| T3-PN4-10 | 99.9 | 0.02 | 0.08 | 0 | 0 | 0 | 0 | 0 | | ✓ | | | | | | |
| T3-PN4-12 | 99.64 | 0.04 | 0.12 | 0.2 | 0 | 0 | 0 | 0 | | ✓ | | | | | | |
| Average | 99.522 | 0.03667 | 0.3767 | 0.04 | 0 | 0.025 | 0 | 0 | | ✓ | | ✓ | | | | |

| Sample number | Composition | | | | | | | | Sphericity | | Roundness | | | | | |
|---|---|---|---|---|---|---|---|---|---|---|---|---|---|---|---|---|
| | Quartz | Feldspar | Rock fragment | Mica | Skeleton debris | Ferromagnesian | Unknown | Other | Low | High | Very angular | angular | Sub-angular | Sub-round | Round | Well-rounded |
| T3-PN5-1 | 97.88 | 0.02 | 1.5 | 0 | 0 | 0.6 | 0 | 0 | | ✓ | | | | | | |
| T3-PN5-3 | 99.46 | 0.03 | 0.5 | 0 | 0 | 0.01 | 0 | 0 | | ✓ | | | | | | |
| T3-PN5-5 | 99.35 | 0.01 | 0.6 | 0 | 0 | 0.04 | 0 | 0 | | ✓ | | | | | | |
| T3-PN5-8 | 99.77 | 0.02 | 0.2 | 0 | 0 | 0.01 | 0 | 0 | | ✓ | | | | | | |
| T3-PN5-10 | 99.155 | 0.015 | 0.8 | 0 | 0 | 0.03 | 0 | 0 | | ✓ | | | | | | |
| Average | 99.123 | 0.019 | 0.72 | 0 | 0 | 0.138 | 0 | 0 | | ✓ | | ✓ | ✓ | | | |

| Sample number | Composition | | | | | | | | Sphericity | | Roundness | | | | | |
|---|---|---|---|---|---|---|---|---|---|---|---|---|---|---|---|---|
| | Quartz | Feldspar | Rock fragment | Mica | Skeleton debris | Ferromagnesian | Unknown | Other | Low | High | Very angular | angular | Sub-angular | Sub-round | Round | Well-rounded |
| T3-PN6-1 | 99.915 | 0.02 | 0.04 | 0.01 | 0 | 0.015 | 0 | 0 | | ✓ | | | | | | |
| T3-PN6-3 | 99.86 | 0.04 | 0.1 | 0 | 0 | 0 | 0 | 0 | | ✓ | | | | | | |
| T3-PN6-5 | 98.7 | 0 | 1.1 | 0 | 0 | 0.2 | 0 | 0 | | ✓ | | | | | | |
| T3-PN6-6 | 99.85 | 0 | 0.05 | 0.02 | 0 | 0.08 | 0 | 0 | | ✓ | | | | | | |
| T3-PN6-7 | 99.18 | 0 | 0.8 | 0 | 0 | 0.02 | 0 | 0 | | ✓ | | | | | | |
| T3-PN6-8 | 99 | 0.1 | 0.9 | 0 | 0 | 0 | 0 | 0 | | ✓ | | | | | | |
| Average | 99.418 | 0.02667 | 0.4983 | 0.005 | 0 | 0.0525 | 0 | 0 | | ✓ | | | ✓ | | | |

| Sample number | Composition | | | | | | | | Sphericity | | Roundness | | | | | |
|---|---|---|---|---|---|---|---|---|---|---|---|---|---|---|---|---|
| | Quartz | Feldspar | Rock fragment | Mica | Skeleton debris | Ferromagnesian | Unknown | Other | Low | High | Very angular | angular | Sub-angular | Sub-round | Round | Well-rounded |
| T3-PN7-1 | 99.88 | 0.02 | 0.04 | 0 | 0 | 0.06 | 0 | 0 | | ✓ | | | | | | |
| T3-PN7-6 | 99.95 | 0.01 | 0.04 | 0 | 0 | 0 | 0 | 0 | | ✓ | | | | | | |
| T3-PN7-9 | 99.85 | 0.01 | 0.1 | 0.04 | 0 | 0 | 0 | 0 | | ✓ | | | | | | |
| Average | 99.893 | 0.01333 | 0.06 | 0.013 | 0 | 0.02 | 0 | 0 | | ✓ | | ✓ | | | | |

| Sample number | Composition | | | | | | | | Sphericity | | Roundness | | | | | |
|---|---|---|---|---|---|---|---|---|---|---|---|---|---|---|---|---|
| | Quartz | Feldspar | Rock fragment | Mica | Skeleton debris | Ferromagnesian | Unknown | Other | Low | High | Very angular | angular | Sub-angular | Sub-round | Round | Well-rounded |
| T3-PN8-1 | 99.64 | 0.06 | 0.1 | 0 | 0 | 0.2 | 0 | 0 | | ✓ | | | | | | |
| T3-PN8-4 | 99.92 | 0 | 0.05 | 0 | 0 | 0.03 | 0 | 0 | | ✓ | | | | | | |
| T3-PN8-7 | 99.79 | 0.04 | 0.13 | 0.01 | 0 | 0.03 | 0 | 0 | | ✓ | | | | | | |
| T3-PN8-9 | 99.68 | 0.15 | 0 | 0 | 0 | 0.17 | 0 | 0 | | ✓ | | | | | | |
| Average | 99.758 | 0.0625 | 0.07 | 0.003 | 0 | 0.1075 | 0 | 0 | | ✓ | | | ✓ | | | |

| Sample number | Composition | | | | | | | | Sphericity | | Roundness | | | | | |
|---|---|---|---|---|---|---|---|---|---|---|---|---|---|---|---|---|
| | Quartz | Feldspar | Rock fragment | Mica | Skeleton debris | Ferromagnesian | Unknown | Other | Low | High | Very angular | angular | Sub-angular | Sub-round | Round | Well-rounded |
| T3-PN9-1 | 99.62 | 0.01 | 0.06 | 0 | 0 | 0.31 | 0 | 0 | | ✓ | | | | | | |
| T3-PN9-3 | 99.58 | 0.01 | 0.27 | 0 | 0 | 0.14 | 0 | 0 | | ✓ | | | | | | |
| T3-PN9-4 | 99.92 | 0.01 | 0.03 | 0 | 0 | 0.04 | 0 | 0 | | ✓ | | | | | | |
| T3-PN9-5 | 99.92 | 0.04 | 0.01 | 0.01 | 0 | 0.02 | 0 | 0 | | ✓ | | | | | | |
| T3-PN9-8 | 99.87 | 0.05 | 0.06 | 0.01 | 0 | 0.01 | 0 | 0 | | ✓ | | | | | | |
| T3-PN9-11 | 99.77 | 0.01 | 0.12 | 0 | 0 | 0.1 | 0 | 0 | | ✓ | | | | | | |
| Average | 99.78 | 0.02167 | 0.0917 | 0.003 | 0 | 0.103333333 | 0 | 0 | | ✓ | | | ✓ | | | |

# Appendix C

Result of Annual Dose Calculation for beach ridge sediments.

**Table C.1** Results of Annual Dose Calculation for beachridge sediments

| Sample no. | K2O (%) | K (%) | U (ppm) | Th (ppm) | AD (mGy/a) |
|---|---|---|---|---|---|
| T1-PN1 | 0.38 | 0.16 | 3.70 | 16.02 | 2.53 |
| T1-PN3 | 0.91 | 0.38 | 1.27 | 4.94 | 1.58 |
| T1-PN5 | 0.37 | 0.15 | 2.69 | 13.29 | 2.08 |
| T1-PN6 | 1.08 | 0.45 | 1.64 | 7.14 | 1.98 |
| T1-PN8 | 1.25 | 0.52 | 1.09 | 2.86 | 1.68 |
| T1-PN9 | 0.97 | 0.40 | 2.23 | 13.55 | 2.51 |
| T1-PN13 | 0.94 | 0.39 | 1.45 | 5.15 | 1.67 |
| T1-PN14 | 1.29 | 0.54 | 2.71 | 13.22 | 2.88 |
| T2-PN1 | 0.76 | 0.32 | 6.34 | 34.88 | 4.92 |
| T2-PN2 | 0.54 | 0.22 | 1.88 | 4.67 | 1.38 |
| T2-PN3 | 0.90 | 0.37 | 2.68 | 8.84 | 2.20 |
| T2-PN4 | 1.16 | 0.48 | 1.35 | 4.96 | 1.82 |
| T2-PN5 | 1.08 | 0.45 | 1.66 | 7.21 | 1.99 |
| T2-PN6 | 1.00 | 0.41 | 1.02 | 5.33 | 1.62 |
| T2-PN7 | 0.83 | 0.35 | 1.31 | 5.32 | 1.55 |
| T2-PN9 | 0.55 | 0.23 | 2.31 | 10.71 | 1.95 |
| T3-PN3 | 1.25 | 0.52 | 1.42 | 4.21 | 1.86 |
| T3-PN4 | 0.95 | 0.40 | 1.99 | 6.87 | 1.93 |
| T3-PN5 | 0.79 | 0.33 | 2.13 | 10.46 | 2.10 |
| T3-PN6 | 0.92 | 0.38 | 1.29 | 4.75 | 1.58 |
| T3-PN7 | 1.60 | 0.66 | 1.68 | 6.35 | 2.39 |
| T3-PN8 | 0.75 | 0.31 | 1.02 | 3.65 | 1.28 |
| T3-PN9 | 0.74 | 0.31 | 1.46 | 6.68 | 1.61 |

# Appendix D

Results of growth curve data for beach ridge sediments.

**Figure D.1** Results of growth curve data for beachridge sediments in Transection line 1.

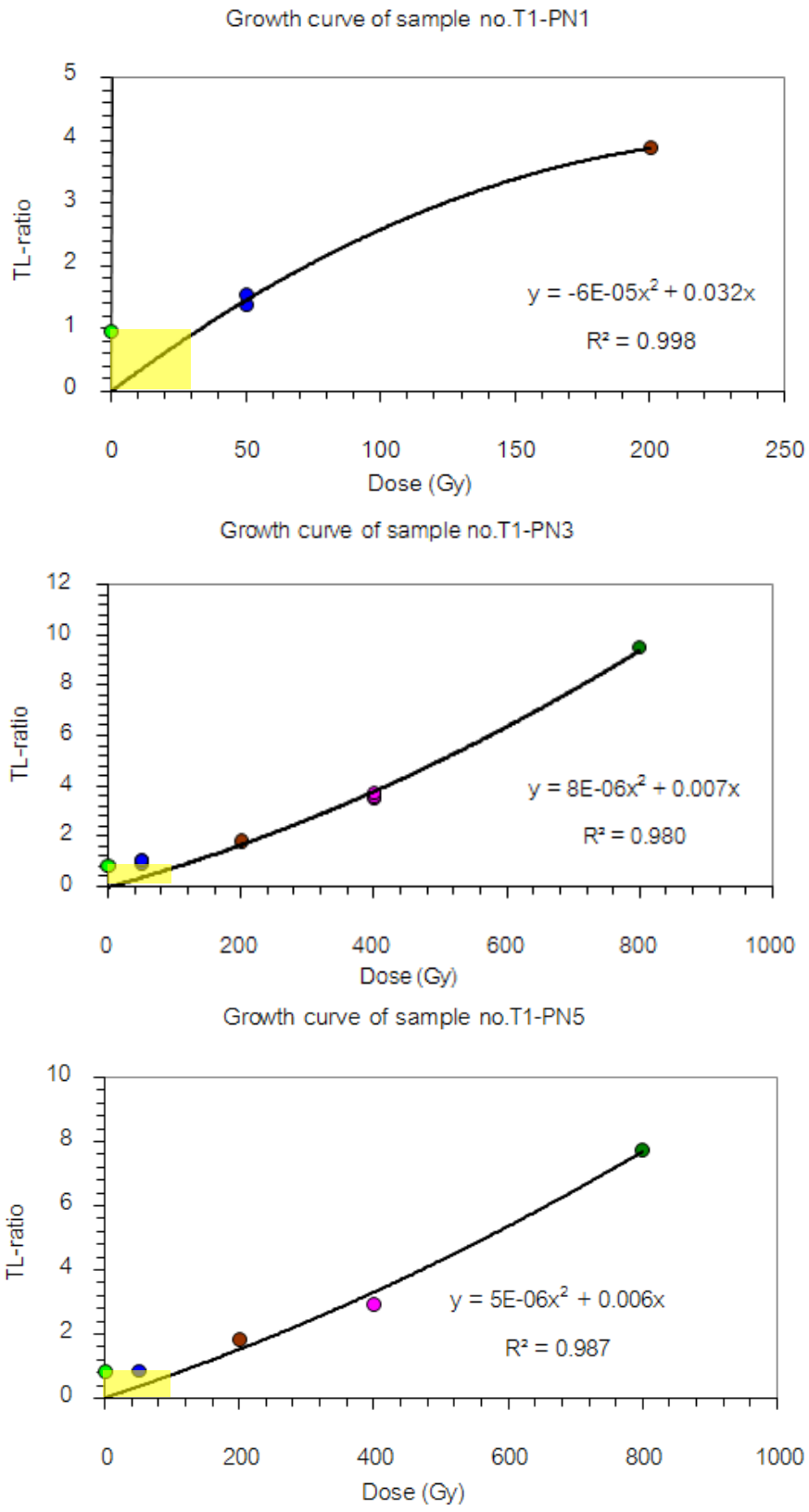

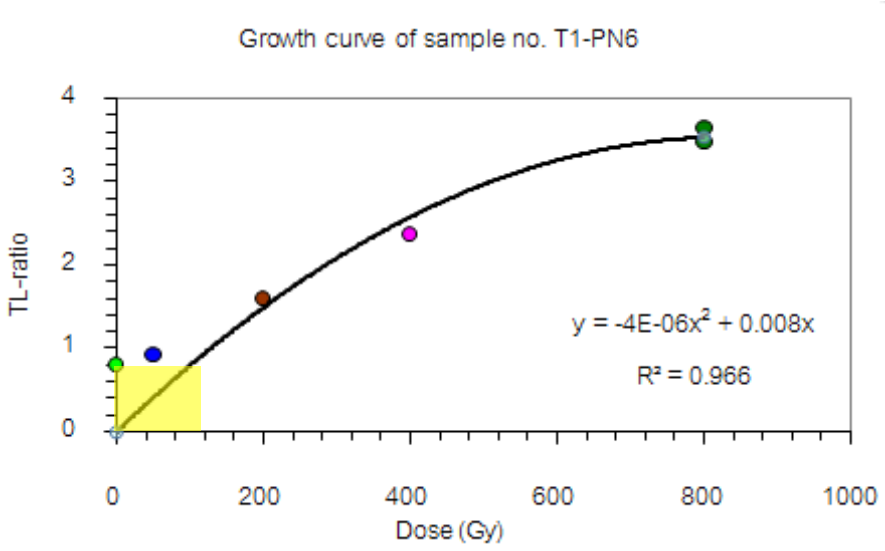
Growth curve of sample no. T1-PN6
TL-ratio
Dose (Gy)
y = -4E-06x² + 0.008x
R² = 0.966
0
1
2
3
4
0
200
400
600
800
1000

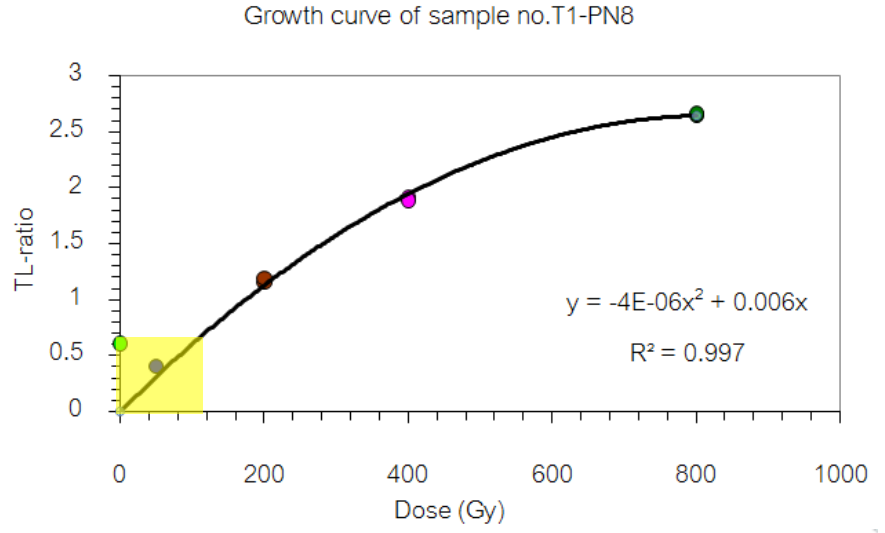
Growth curve of sample no.T1-PN8
TL-ratio
Dose (Gy)
y = -4E-06x² + 0.006x
R² = 0.997
0
0.5
1
1.5
2
2.5
3
0
200
400
600
800
1000

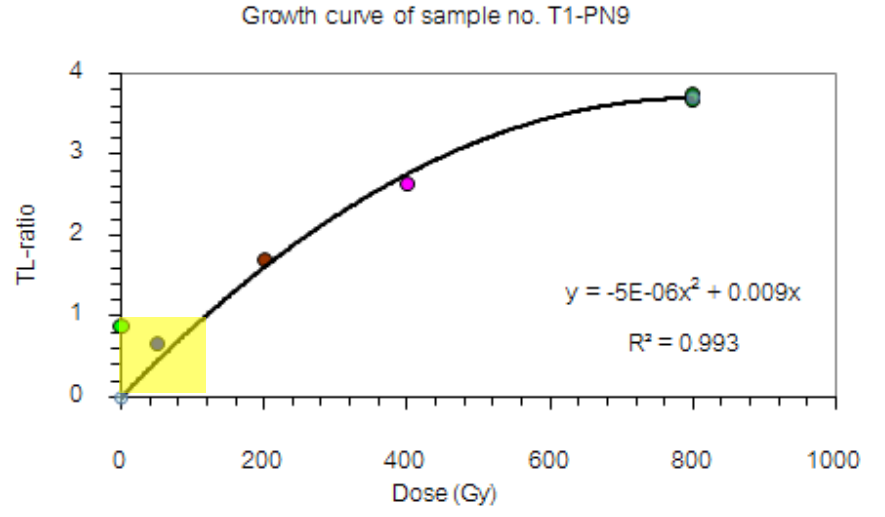
Growth curve of sample no. T1-PN9
TL-ratio
Dose (Gy)
y = -5E-06x² + 0.009x
R² = 0.993
0
1
2
3
4
0
200
400
600
800
1000

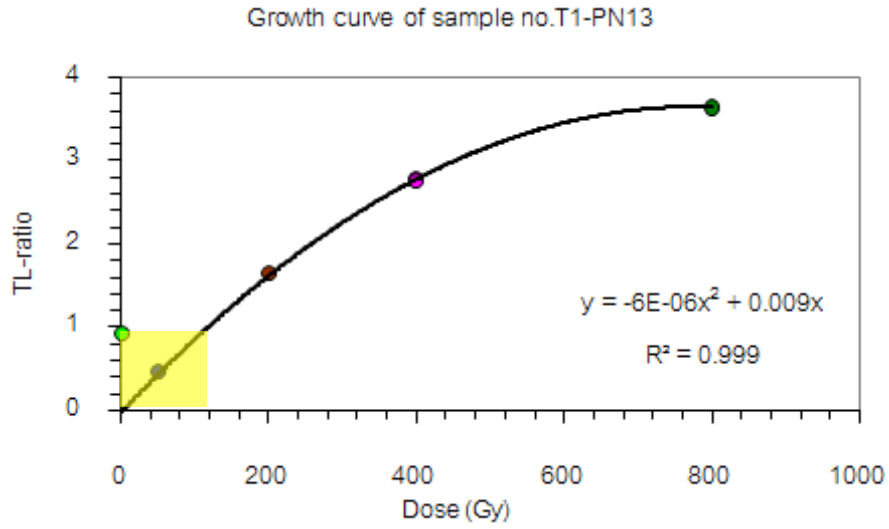
Growth curve of sample no.T1-PN13
TL-ratio
Dose (Gy)
y = -6E-06x² + 0.009x
R² = 0.999
0
1
2
3
4
0
200
400
600
800
1000

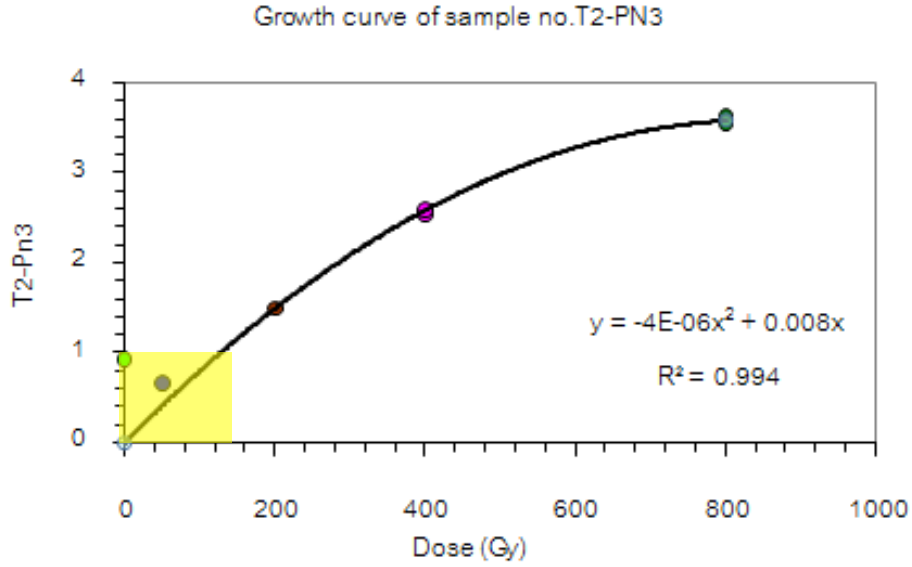
Growth curve of sample no.T2-PN3
T2-Pn3
Dose (Gy)
y = -4E-06x² + 0.008x
R² = 0.994
0
1
2
3
4
0
200
400
600
800
1000

**Figure D.2** Results of growth curve data for beachridge sediments in Transection line 2.

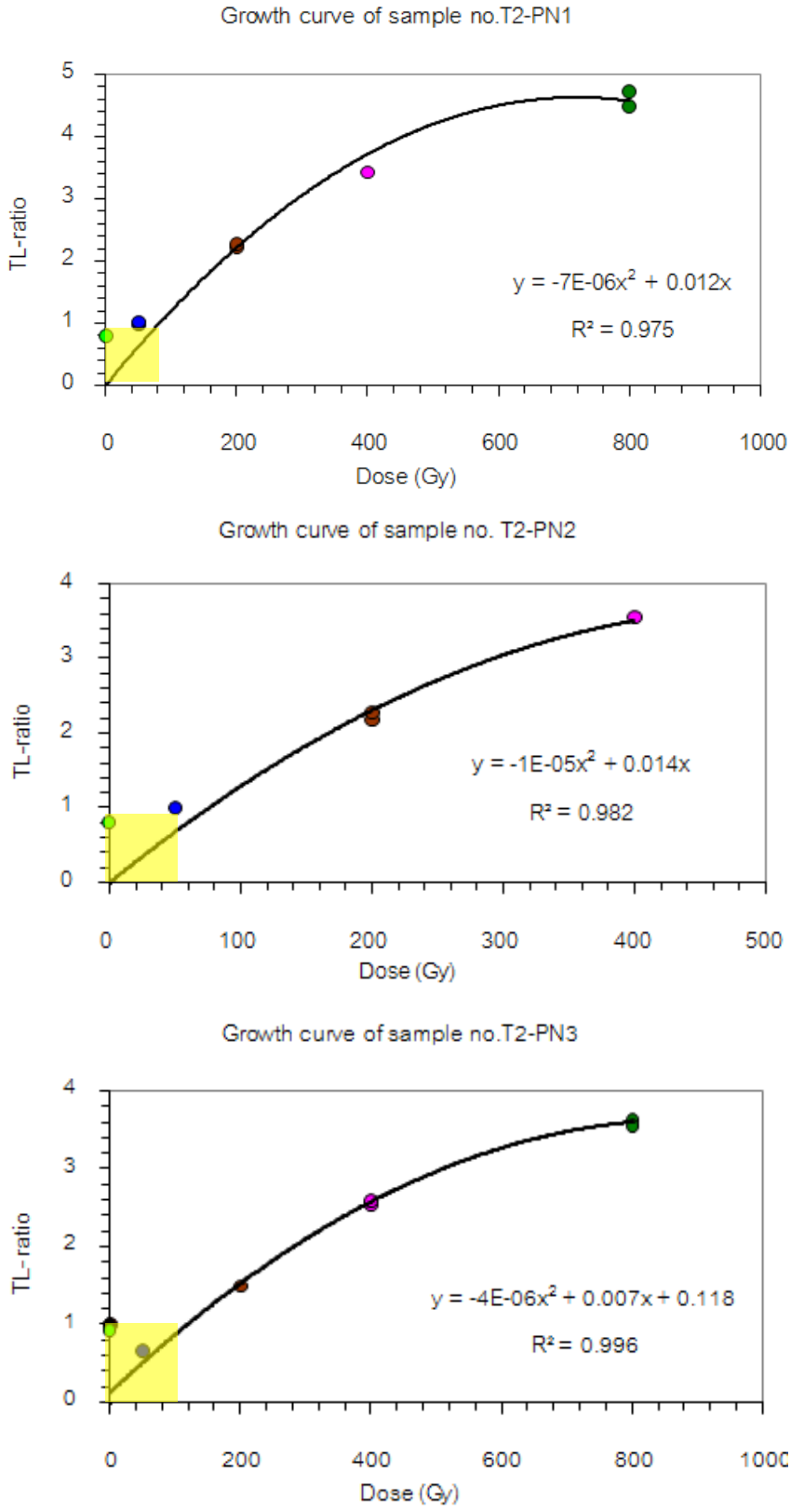

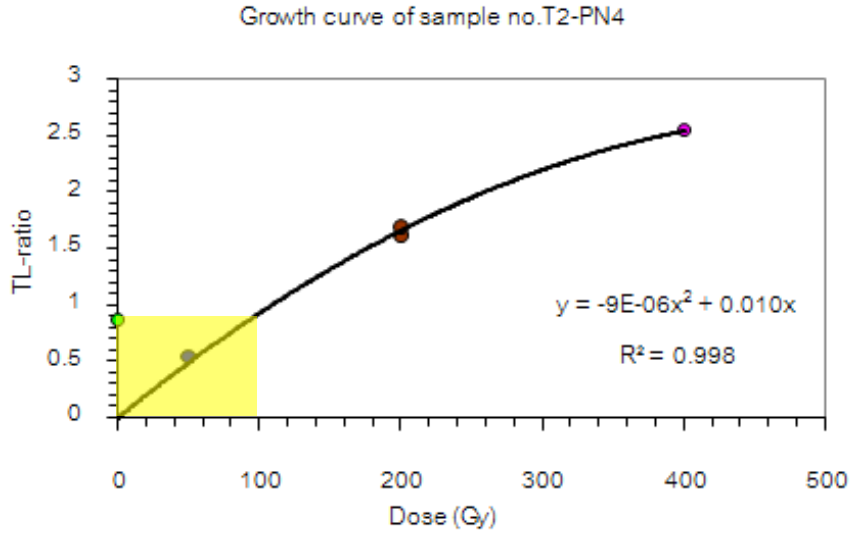
Growth curve of sample no.T2-PN4
TL-ratio
Dose (Gy)
y = -9E-06x² + 0.010x
R² = 0.998
0
0.5
1
1.5
2
2.5
3
0
100
200
300
400
500

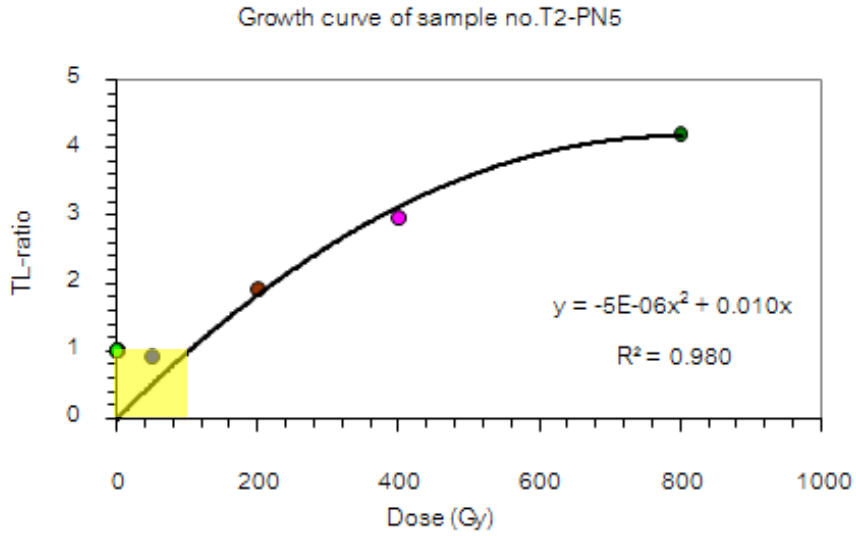
Growth curve of sample no.T2-PN5
TL-ratio
Dose (Gy)
y = -5E-06x² + 0.010x
R² = 0.980
0
1
2
3
4
5
0
200
400
600
800
1000

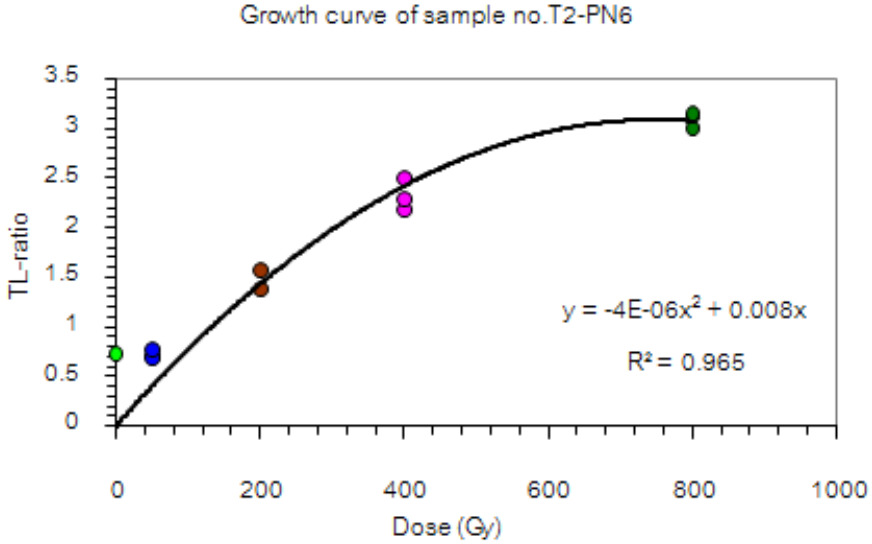
Growth curve of sample no.T2-PN6
TL-ratio
Dose (Gy)
y = -4E-06x² + 0.008x
R² = 0.965
0
0.5
1
1.5
2
2.5
3
3.5
0
200
400
600
800
1000

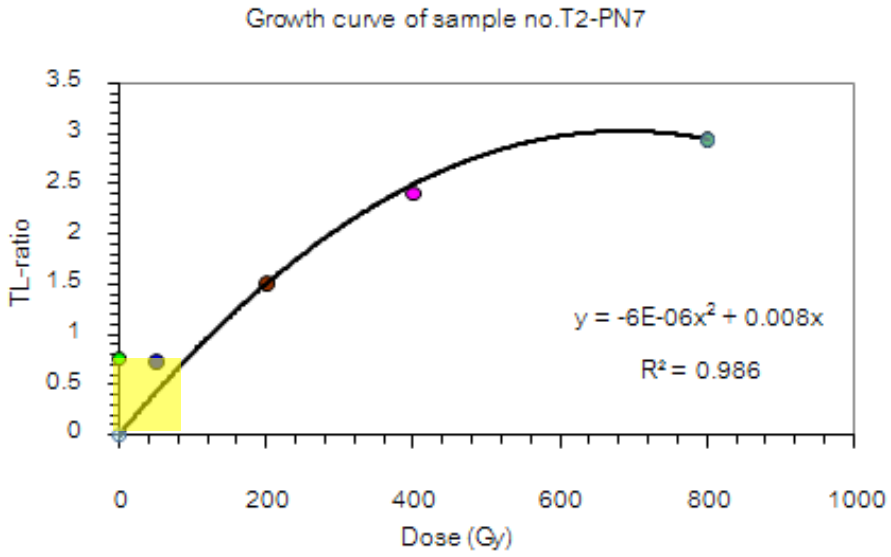
Growth curve of sample no.T2-PN7
TL-ratio
Dose (Gy)
y = -6E-06x² + 0.008x
R² = 0.986
0
0.5
1
1.5
2
2.5
3
3.5
0
200
400
600
800
1000

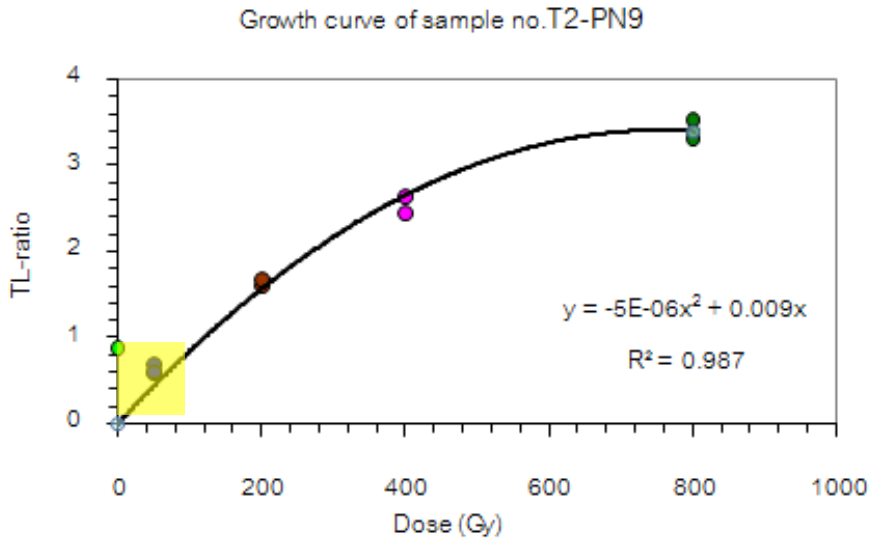
Growth curve of sample no.T2-PN9
TL-ratio
Dose (Gy)
y = -5E-06x² + 0.009x
R² = 0.987
0
1
2
3
4
0
200
400
600
800
1000

**Figure D.3** Results of growth curve data for beachridge sediments in Transection line 3.

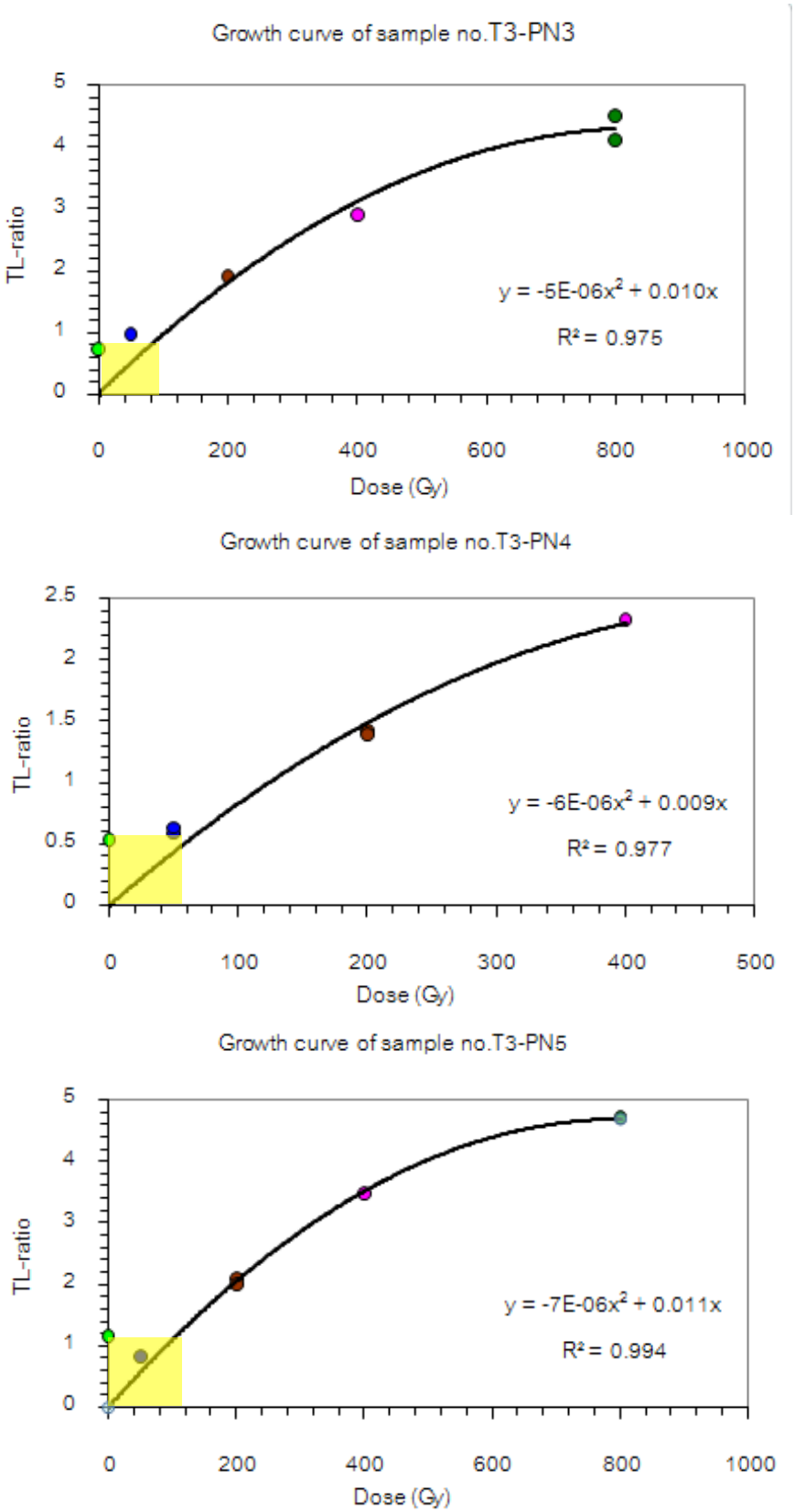

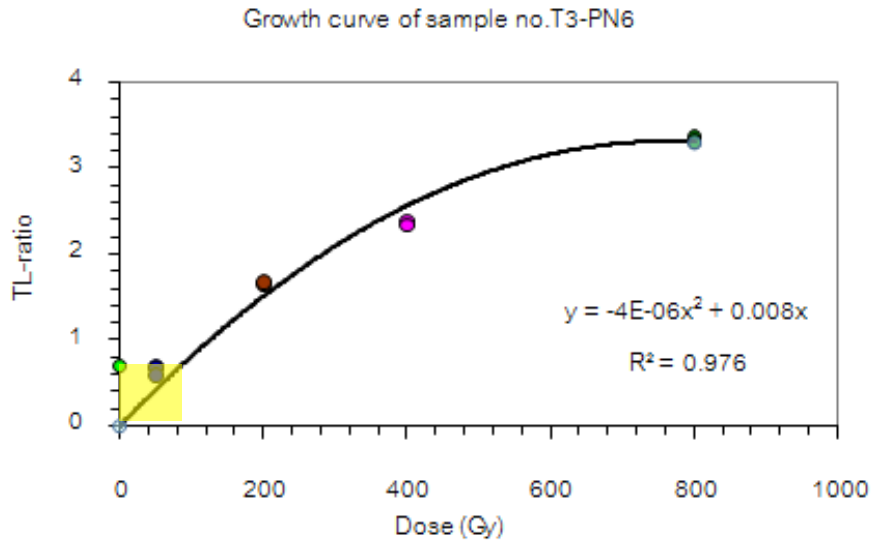
Growth curve of sample no.T3-PN6
TL-ratio
Dose (Gy)
y = -4E-06x² + 0.008x
R² = 0.976
0
1
2
3
4
0
200
400
600
800
1000

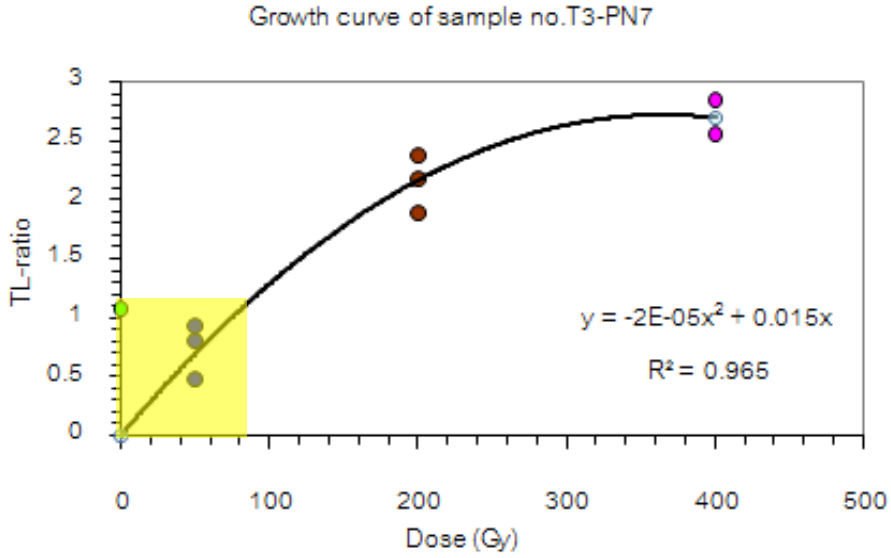
Growth curve of sample no.T3-PN7
TL-ratio
Dose (Gy)
y = -2E-05x² + 0.015x
R² = 0.965
0
0.5
1
1.5
2
2.5
3
0
100
200
300
400
500

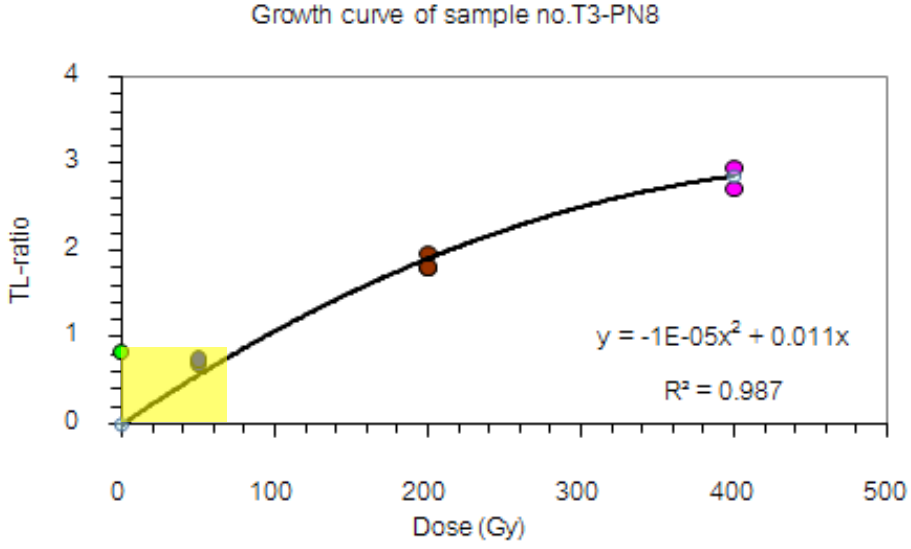
Growth curve of sample no.T3-PN8
TL-ratio
Dose (Gy)
y = -1E-05x² + 0.011x
R² = 0.987
0
1
2
3
4
0
100
200
300
400
500

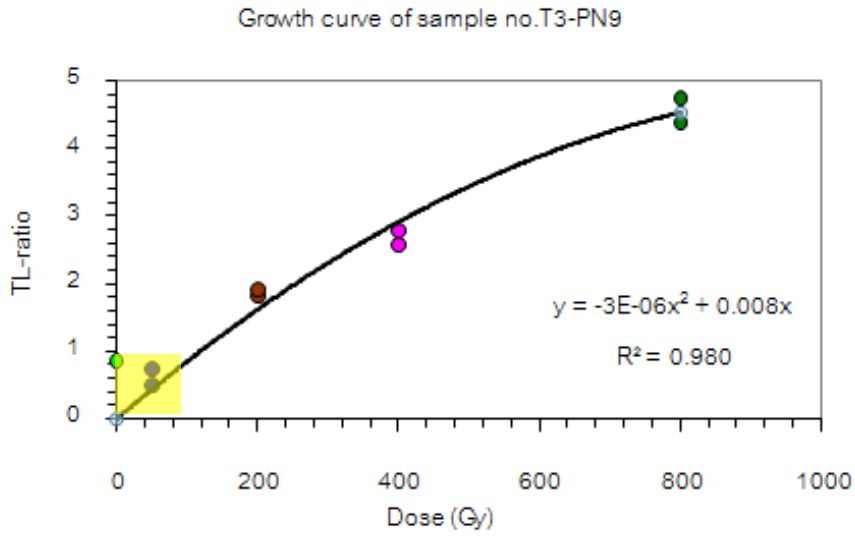
Growth curve of sample no.T3-PN9
TL-ratio
Dose (Gy)
y = -3E-06x² + 0.008x
R² = 0.980
0
1
2
3
4
5
0
200
400
600
800
1000

# BIOGRAPHY

Miss Parisa Nimnate was born in Kanchanaburi, Thailand on 26th November 1988. She completed high school from Thamuangrajbumrung School, Kanchanaburi in 2005. After that she was studying at Geoscience Program from and got the Sri Trang Thong Scholarship from Faculty of Science, Mahidol University. She graduated her Bachelor's Degree (B.Sc.) in 2009 focused the study of the relationship between natural gamma logging and ash content in the K coal seam at Mae Moh Mine, Lampang Province. After completed the B.Sc., she got scholarship from Human Resource Development in Science Project (Science Achievement Scholarship of Thailand, SAST) and continued to start her Master's Degree Program at Department of Geology, Faculty of Science , Chulalongkorn University. Her research has been focus on History of Sea-Level Change of Pak Nam Chumphon Area, Amphoe Muang, Changwat Chumphon and supported by 90th Year Chulalongkorn Scholarship. Some part of her research in the topic of Charateristic of former beach ridge plains from remote sensing data at Chumphon estuaries, southern of Thailand submitted in Bulletin of Earth Sciences of Thailand.